The coastal boundary layer: pattern, mechanism, and ecological effects of decreased alongshore transport

By

KERRY JEAN NICKOLS
B.A. (University of California, Berkeley) 2002

DISSERTATION

Submitted in partial satisfaction of the requirements for the degree of

DOCTOR OF PHILOSOPHY

in

Ecology

in the

OFFICE OF GRADUATE STUDIES

of the

UNIVERSITY OF CALIFORNIA

DAVIS

Approved:

_____

Brian Gaylord, Chair

_____

John L. Largier

_____

Louis W. Botsford

Committee in Charge

2012

ProQuest LLC.
789 East Eisenhower Parkway
P.O. Box 1346
Ann Arbor, MI 48106 - 1346

ABSTRACT

Dispersion of planktonic propagules connects shoreline populations of many marine species, and considerable effort has been directed at understanding this process. However, gaps in knowledge persist. In particular, relatively little information has been available regarding transport over the innermost portions of the continental shelf and its impacts on larval distributions and population connectivity. I quantified velocity in nearshore waters at 5 sites along the California coast and investigated characteristics relevant for dispersing larvae. Mean depth-averaged velocities increased with distance from shore at all sites. This repeated and consistent "coastal boundary layer" (CBL) pattern exhibits a logarithmic profile that resembles that associated with the "law of the wall" of smaller-scale turbulent boundary layers, despite differences in spatial dimension and governing physics. A tentative scaling of dominant terms in an alongshore momentum balance suggests nontrivial levels of lateral stress, but small cross-shore gradients in this quantity. Such a trend of near-constant lateral stress, when combined with simple representations of horizontal mixing (i.e., eddy viscosity) that increase approximately linearly with distance from shore, provides a possible explanation for the observed logarithmic velocity pattern. I incorporated these gradients in alongshore velocity and mixing into a 2-dimensional Lagrangian particle-tracking model to explore effects of the CBL on dispersal and self-retention for a variety of sites and life histories. Incorporating a CBL decreased mean dispersal distances up to 56% and was more profound for shorter pelagic larval durations (PLD) and gentler bathymetric slopes associated with broader CBLs. Most notable is that the presence of a CBL increased self-retention by as much as three orders of magnitude, which indicates that ignoring the

reduced velocities in the CBL may overestimate population connectivity. These model results were echoed by measurements of planktonic communities within the field. I measured cross-shore distributions of crustacean larvae within the CBL in northern California (between 250 and 1100 m from shore) and found high larval abundances within the CBL, peaking inshore of the 30 m isobath (1 km from shore). However, abundances decreased substantially in the inner portion of the CBL, and there were distinct larval communities between the nearshore and the rest of the CBL. These patterns persisted across sample dates, suggesting that the spatial structure of nearshore larval communities is robust to changes in physical conditions. High larval abundance within the CBL coupled with the potential of the CBL to reduce alongshore larval transport suggests that larvae may exhibit behaviors that interact with recirculating flow features to elevate local retention. Because of these consequences, CBLs should be considered in future models of coastal transport, as they appear to have large effects on population dynamics of marine species.

ACKNOWLEDGMENTS

I owe the completion of my Ph.D. to many people who have supported me throughout my career. I would not have achieved as much without the support and encouragement of my mentors, friends, and family. Additionally, I thank the Graduate Group in Ecology and the Bodega Marine Laboratory for fellowship support, as well as the National Science Foundation, California Environmental Quality Initiative, and California Sea Grant, who partially funded my research. Dan Reed and the Santa Barbara Coastal Long Term Ecological Research site also provided equipment and personnel for my research.

I would first like to recognize the people and experiences that brought me to the University of California, Davis. Zack Powell, Bernard Nietschmann, and Jim Hayward at the University of California, Berkeley, opened up a career path for me that I had never considered, and for that I am in their debt. I thank the Our World Underwater Scholarship Society for giving me the freedom to find my niche in the underwater world, and the opportunity to work with Hunter Lenihan, who provided my first encounter with the Acoustic Doppler Current Profiler that I have grown to love. I would like to thank Mark Steele for being my first mentor, giving me a taste of the research life, and offering advice and friendship, as well as Clare Wormald and Jameal Samhouri who, despite their best efforts, did not dissuade me from pursuing a Ph.D. and remain my champions.

I am very grateful for the interactions I have had with the faculty of UC Davis and the Bodega Marine Laboratory. My qualifying exam committee, Loo Botsford, Ted Grosholz, Alan Hastings, Jamie MacMahan (from the Naval Postgraduate School), and Steven Morgan, provided invaluable feedback on my research proposal and early

findings, as well as helped me frame my research in a broader context. I would like to thank Loo Botsford for his membership on my dissertation committee and for providing feedback on manuscripts and access to powerful computers when I became a modeler. Steven Morgan provided resources and advice for my third chapter and introduced me to the word of larval ecology. I thank Eric Sanford for his enthusiasm for research and teaching at BML, and for helping me become a better educator. I would like to thank Tessa Hill for serving as a female mentor and role model and cheering me on.

I am extremely grateful to the Bodega Marine Laboratory for resources to complete my research, as well as its wonderful community. I would like to thank everyone at the shop, particularly Steve Freeman, Philip Smith, and Brian Meyers, for help constructing equipment and assistance with the flume. Henry Fastenau, Jason Herum, and James Fitzgerald made sure my diving and boating operations were safe and well thought out. I thank everyone in the front office for assistance on a multitude of tasks. I thank Jackie Sones for her expertise in natural history and help in planning research on the reserve. Jennifer Fisher was a fantastic friend and resource for all things field, beer, and larval related. The community of graduate students, post-docs, etc. has been a joy to be a part of, and I thank them for their shenanigans, costumes, and support – in particular Rebecca Best, Jill Bible, Susanne Brander, Jarrett Byrnes, Hank Carson, Brian Cheng, Michelle Cooper, Cynthia Hays, Lisa Komoroske, Becca Kordas, Michèle LaVigne, Beth Lenz, Nature McGinn, Joe Newman, Karthik Ram, Megan Sheridan, Jenna Shinen, Amber Szoboszlai, and Dave Worth.

Members of the Largier lab played critical roles in my instrument deployments, including David Dann, Lauren Garske, Matt Robart, and especially Megan Sheridan. I

would also like to thank Chris Halle, Marcel Loosekoot, and Deedee Shideler for technical assistance and access to physical datasets as well as Silvia Piedracoba and Marisol García-Reyes for their support.

The Gaylord lab – Matt Ferner, Annaliese Hettinger, and Laura Jurgens – small but mighty, provided help with my research, moral support, and valuable life lessons.

I am very fortunate for the camaraderie and support provided by members of the Graduate Group in Ecology, particularly Michele Buckhorn and Liz Moffitt, and the 2005 GGE cohort, especially Jessica Blickley, Tobias Rohmer, and Kurt Vaughn, for their dark sparkle, amazing friendships, and adventures. I have also been bolstered by colleagues far and wide – Kate Hanson, Alison Haupt, Cheryl Logan, and Adrian Stier. I am grateful for their friendship, shared experiences, and all-out performances at WSN.

A few other colleagues from the Bodega Marine Laboratory warrant special attention. Ellie Fairbairn helped me keep perspective and lit my path to the desert. I thank Rachel Fontana for being a confidant and fellow mystic and matlabber. Seth Miller provided laughs, songs, and moral support, and fostered my love of larvae. I am in great debt to Will White for collaboration, friendship, support, and bourbon. I thank Tawny Mata for being my rock, especially over the last year of my dissertation. Without her support the lows would have been abyssal canyons, and I never would have soared so high (or eaten so well). Meow.

The pugs – David Bowie and Pixel – provided comic relief and snuggles.

I thank the flume for teaching me patience and the fact that not all research projects work, and matlab for reigniting my love of math.

Most importantly, I would like to thank my advisors, John Largier and Brian

Gaylord. I first met John when I interviewed for graduate school at a different institution, and although he wasn't accepting students, he sought me out and insisted we stay in touch and that I apply to UC Davis; for that I am forever grateful. John planted the seed of my dissertation in his Coastal Oceanography course, when I first learned of the coastal boundary layer. I thank John for his big-picture view and his interdisciplinary nature, as well as his dedication to his family and his kindness. I could not have asked for, or even dreamed of, a better mentor than Brian Gaylord. I am amazed by his intellect and breadth of knowledge and am inspired by his curiosity. I am thankful for his patience and guidance, and for reinstilling my passion for science. Together, my advisors believed in me when I didn't believe in myself, and they made me a rigorous scientist and a better person.

My parents, John and Lorna Nickols, are simply amazing and deserve Ph.D.'s in parenting. I am incredibly thankful for their love and encouragement. They have always supported me in everything I've done, from music to scuba and everything in between. They truly let me dive into life and always provided a safe place to surface.

Finally, I need to thank my fish friends. I feel so lucky to have spent hundreds of hours underwater, gaining access to a world few get to see. Watching marine life in their habitat initiated my interest in hydrodynamics and currents, and ultimately spawned this dissertation. Many years later I am still the girl who loves to be underwater and wants to save the ocean.

"Love dares you to change our way of caring about ourselves, this is our last dance… this is ourselves, under pressure." – David Bowie and Freddy Mercury

TABLE OF CONTENTS

LIST OF TABLES

LIST OF FIGURES

INTRODUCTION

The importance of nearshore waters to understanding coastal circulation, larval transport, and population connectivity

Larval transport is often referred to as the 'black box' of marine ecology (e.g., Menge et al. 2004), and is an especially challenging topic due to its interdisciplinary nature. Most marine organisms have a pelagic larval phase that develops in the water column before finding suitable habitat to settle. During this phase larvae are subject to ocean currents and disperse away from their natal site. As this is the primary dispersive phase of most coastal marine organisms, larval transport pathways determine the degree to which shoreline populations are connected; yet quantifying larval transport pathways and connectivity is a challenge due to the small size of larvae and the difficulty to track them (Levin 2006). Advances in our understanding of larval transport and connectivity has depended on studies of coastal populations and larval ecology, as well as physical oceanography. Over recent decades such interdisciplinary approaches have seen particular utility in concert with a reinvigorated interest in local retention of larvae.

Much of the seminal work in the field of ecology was conducted on rocky shore marine systems, where predation, competition, and disturbance were found to drive local population dynamics (Connell 1961, Paine 1966, Dayton 1971, Connell 1972). At the scale of a site, larval settlement was largely viewed as noise (Roughgarden 2006), but as the spatial scale of studies expanded it became clear that settlement varies in time and space (Caffey 1985) and that larval supply could play a significant role in shaping the distribution and abundance of organisms (Connell 1985). Although fisheries biologists long recognized the importance of fish stocks to recruits (Hjort 1914), what followed was a realization within the field of marine ecology that the larval stage of marine organisms plays an important role in population dynamics, therefore drawing attention to the transport pathways undertaken by larvae in the coastal ocean.

This led to a sea change in marine ecology, with more work focused on supply-side ecology (Lewin 1986, Underwood and Keough 2001) and the recognition that many marine systems function as metapopulations (Roughgarden and Iwasa 1986, Botsford et al. 1994). This focus spawns not only from a need to understand the fundamentals of marine population dynamics over local and regional scales, but also in response to the recognition that overfishing and habitat destruction can change connections between populations and have cascading effects beyond a local site (Sale et al. 2006). Mounting interest in metapopulations led to a boom in studies of oceanographic processes that may shape dispersal pathways and population connectivity (Roughgarden et al. 1988, Botsford et al. 1994, Wing et al. 1995b).

Coupled studies of larvae and physical processes revealed important effects of circulation features on larval supply. On the regional scale, wind-driven coastal upwelling can drive larvae offshore (Roughgarden et al. 1988), and subsequent reversals in winds and currents can move larvae back on shore (Wing et al. 1995a, Wing et al. 1995b). On meso-scales, larvae can be retained by topographically associated currents, such as island wakes (Swearer et al. 1999), headland wakes (Graham and Largier 1997, Roughan et al. 2005), and flows in embayments (Wolanski 1992). In addition to these retentive flows associated with particular conditions in time and space, there may be more ubiquitous mechanisms of retention. There is increasing evidence that self-recruitment of coastal populations is higher than previously thought, and that dispersal distances are often lower than expected based on an organisms' pelagic larval duration (Swearer et al. 2002, Palumbi 2004, Levin 2006, Shanks 2009). High self-recruitment has been reported across a variety of taxa (Shanks 2009) and in studies using a variety of

techniques, including tagging (Jones et al. 2009) natural tracers (Thorrold et al. 2007) and genetics (Hellberg et al. 2002, Weersing and Toonen 2009). In addition, emerging data suggest that regions within a few kilometers from shore often have the highest abundance of larvae (Borges et al. 2007, Morgan et al. 2009, Shanks and Shearman 2009), which implies that local physical processes may be important.

Despite the proximity to shore, the nearshore zone (between the surf zone and a few kilometers offshore, sometimes referred to as the inner shelf) has been relatively little explored, as it was historically seen as "too shallow for oceanographers with ships, too deep for coastal engineers without ships" (Smith 1995). Yet currents in this region may be crucial to the transport and delivery of larvae. Technological advances coupled with growing appreciation for this region have led to an increase in studies of biological and physical processes (e.g., Lentz et al. 1999, Kirincich et al. 2005, Tapia and Pineda 2007, Rilov et al. 2008, Lentz and Fewings 2012).

A relatively unexplored place to look for physical mechanisms of local retention is in the interaction of coastal flows with shoreline topography and bathymetry. As nearshore currents move adjacent to the shore, they 'feel' the bottom and side-walls of the coastline, and experience a reduction in velocity. This region of attenuated flow, which is mostly confined to waters of less than approximately 30 m depth, is sometimes termed the "coastal boundary layer" (CBL). The CBL was first described by Csanady (1972a, b) who deployed current meters perpendicular to shore in Lake Ontario, leading to the discovery of a nearshore boundary layer where currents adjusted to the presence of the shoreline. Cross-shore transects on the eastern coast of North America reported results similar to the limnetic studies: strong polarization of currents in the alongshore

direction, with velocities highly influenced by frictional forces (Pettigrew 1980, Lentz et al. 1999). These studies took place over large spatial extents (1-15 km offshore), due to the broad shelf in these regions, with little resolution nearest the shore, where most benthic marine organisms reside. Further measurements on the west coast of North America reported lower velocities in the inner shelf, as compared to further offshore, although there was generally only one instrument deployed within the inner shelf (Lentz and Winant 1986, Lentz 1994).

In addition to temperate systems, tropical systems also show evidence of a CBL. Wolanski (1992) described inhibited mixing between inshore and offshore waters on the Northeastern Australian coast, due to the presence of the CBL, and found that the CBL varied with the topographic nature of sites: headlands increased mixing, and therefore associated CBL's were not as temporally persistent as straight shallow coasts. This study also recognized the ecological impacts of the CBL, noting its role in trapping constituents, such as terrestrial runoff, sediment, and nutrients (Wolanski 1992).

From an ecological standpoint the CBL is an area of great interest as it is located near the land-sea interface, where most benthic marine organisms reside. The CBL geographically restricts and concentrates biological and biogeochemical activity within the narrow band of the coastal zone and trapping of CBL waters can enhance pelagic secondary production, such as zooplankton and larval fishes (Alongi and McKinnon 2005). The CBL can also impact predictions of dispersal (Largier 2003). The addition of attenuated nearshore velocity in dispersal models can lead to persistence for populations that were not persistent under a uniform flow field (Possingham and Roughgarden 1990). Results from a large-scale circulation model revealed that larvae that exited the region

within a few kilometers from shore and entered into increased current velocities offshore traveled much farther, showed increased spread in settlement distributions, and were largely unable to settle along the coast, as compared to larvae that stayed within the CBL region (Aiken et al. 2007). While these results indicate the potential importance of the CBL for dispersal, connectivity, and ecosystem dynamics, most modeling and empirical studies do not include the resolution needed to characterize the CBL. Most empirical studies of larval distributions have only sampled from one or two stations within the CBL (Morgan et al. 2009, Shanks and Shearman 2009), and circulation models, such as Regional Ocean Modeling Systems (ROMS) models are restricted to resolution of 500 m or greater (Cowen et al. 2006, Aiken et al. 2007, Watson et al. 2010). The absence of the nearshore brings about a potential disconnect in biophysical interpretations of larval transport, and we would benefit greatly from a general description of the CBL.

Recognizing the potential importance of the CBL for understanding population connectivity and the degree to which marine populations are open or closed, I explored how the CBL affects coastal circulation, larval transport, and population connectivity. In the subsequent chapters my aim is to paint a holistic picture of the CBL. I first provide a rigorous physical description of the CBL from current data from five sites in California. Velocity at all sites increased as a function of distance from shore, and largely followed a logarithmic form. I then propose mechanisms responsible for the logarithmic profile rooted in fluid dynamics and coastal oceanography. A likely candidate is lateral shear, which has largely been excluded from studies of inner shelf dynamics. This approach provides a means to estimate horizontal mixing through an eddy diffusivity term often used in larval transport models. The description of the CBL presented here provides a

generalized framework of coastal flow which may prove vital to designers of marine reserves who are intimately concerned with pathways of larval movement, as well as oceanographic modelers who must define mathematical boundary conditions used to constrain the edges of computational domains in circulation studies.

In the following chapter I explore the consequences of attenuated flow near the coast on larval dispersal pathways and settlement distributions. Incorporating the CBL into a particle-tracking model decreases predictions of dispersal distance and substantially increases self-retention, thus decreasing the scales of population connectivity and persistence. If the CBL is broadly characteristic of most coastlines, then much of our current understanding of connectivity, particularly the scales over which it occurs, is likely to be less than fully accurate, and assessing the physical mechanisms that facilitate retention is a major step forward in understanding population connectivity of marine organisms.

Finally, I provide a first exploration of the spatial and temporal structure of the larval community within the CBL, which reveals high larval abundance within the CBL and distinct spatial structure in larval communities across the CBL. Larval communities at the inner edge of the CBL are compositionally different from those just a few hundred meters offshore, and are consistently found in low abundance. Larvae have the potential to spend there entire pelagic duration within the CBL, lowering alongshore dispersal distances and increasing self-retention, yet the final hundred meters to the shoreline appears to be a different environment with its own set of challenges. This new knowledge of the CBL helps to open the ‘black box’ of marine ecology, although we still have much to learn about the very nearshore zone.

LITERATURE CITED

Aiken, C. M., S. A. Navarrete, M. I. Castillo, and J. C. Castilla. 2007. Along-shore larval dispersal kernels in a numerical ocean model of the central Chilean coast. Marine Ecology Progress Series **339**:13-24.

Alongi, D. and A. McKinnon. 2005. The cycling and fate of terrestrially-derived sediments and nutrients in the coastal zone of the Great Barrier Reef shelf. Marine Pollution Bulletin **51**:239-252.

Borges, R., R. Ben-Hamadou, M. A. Chicharo, P. Re, and E. J. Goncalves. 2007. Horizontal spatial and temporal distribution patterns of nearshore larval fish assemblages at a temperate rocky shore. Estuarine, Coastal and Shelf Science **71**:412-428.

Botsford, L., C. Moloney, A. Hastings, J. L. Largier, T. Powell, K. Higgins, and J. Quinn. 1994. The influence of spatially and temporally varying oceanographic conditions on meroplankton metapopulations. Deep-Sea Research II **41**:107-145.

Caffey, H. M. 1985. Spatial and temporal variation in settlement and recruitment of intertidal barnacles. Ecological Monographs **55**:313-332.

Connell, J. 1961. The influence of interspecific competition and other factors on the distribution of the barnacle *Chthamalus stellatus*. Ecology **42**:710-723.

Connell, J. 1972. Community interactions on marine rocky intertidal shores. Annual Review of Ecology and Systematics **3**:169-192.

Connell, J. 1985. The consequences of variation in initial settlement vs. post-settlement mortality in rocky intertidal communities. Journal of Experimental Marine Biology and Ecology **93**:11-45.

Cowen, R., C. Paris, and A. Srinivasan. 2006. Scaling of connectivity in marine populations. Science **311**:522-527.

Csanady, G. 1972a. The coastal boundary layer in Lake Ontario: Part II. The Summer-Fall regime. Journal of Physical Oceanography **2**:168-176.

Csanady, G. 1972b. The coastal boundaryl layer in Lake Ontario. Journal of Physical Oceanography **2**:41-53.

Dayton, P. 1971. Competition, disturbance, and community organization: The provision and subsequent utilization of space in a rocky intertidal community. Ecological Monographs **41**:351-389.

Graham, W. and J. Largier. 1997. Upwelling shadows as nearshore retention sites: The example of northern Monterey Bay. Continental Shelf Research **17**:509-532.

Hellberg, M., R. Burton, J. Neigel, and S. Palumbi. 2002. Genetic assessment of connectivity among marine populations. Bulletin Of Marine Science **70**:273-290.

Hjort, J. 1914. Fluctuations in the great fisheries of northern Europe reviewed in the light of biological research. Rapports, Conceil Permanent International pour l'Exploration de la Mer **20**:1-228.

Jones, G. P., G. R. Almany, G. R. Russ, P. F. Sale, R. S. Steneck, M. J. H. Oppen, and B. L. Willis. 2009. Larval retention and connectivity among populations of corals and reef fishes: history, advances and challenges. Coral Reefs **28**:307-325.

Kirincich, A., J. Barth, B. Grantham, B. Menge, and J. Lubchenco. 2005. Wind-driven inner-shelf circulation off central Oregon during summer. Journal of Geophysical Research-Oceans **110**:C10S03.

Largier, J. 2003. Considerations in estimating larval dispersal distances from oceanographic data. Ecological Applications **13**:S71-S89.

Lentz, S. 1994. Current dynamics over the northern California inner shelf. Journal of Physical Oceanography **24**:2461-2478.

Lentz, S., R. Guza, S. Elgar, F. Feddersen, and T. Herbers. 1999. Momentum balances on the North Carolina inner shelf. Journal of Geophysical Research-Oceans **104**:18205-18226.

Lentz, S. and C. Winant. 1986. Subinertial currents on the southern California shelf. Journal of Physical Oceanography **16**:1737-1750.

Lentz, S. J. and M. Fewings. 2012. The wind- and wave-driven inner-shelf circulation. Annual Review of Marine Science **4**:317-343.

Levin, L. 2006. Recent progress in understanding larval dispersal: new directions and digressions. Integrative and Comparative Biology **46**:282-297.

Lewin, R. 1986. Supply-side ecology. Science **234**:25-27.

Menge, B., C. Blanchette, P. Raimondi, T. Freidenburg, S. Gaines, J. Lubchenco, D. Lohse, G. Hudson, M. Foley, and J. Pamplin. 2004. Species interaction strength: Testing model predictions along an upwelling gradient. Ecological Monographs **74**:663-684.

Morgan, S. G., J. L. Fisher, S. H. Miller, S. T. McAfee, and J. L. Largier. 2009. Nearshore larval retention in a region of strong upwelling and recruitment limitation. Ecology **90**:3489-3502.

Paine, R. T. 1966. Food web complexity and species diversity. American Naturalist **100**:65-75.

Palumbi, S. R. 2004. Marine reserves and ocean neighborhoods: The spatial scale of marine populations and their management. Annual Review of Environment and Resources **29**:31-68.

Pettigrew, N. 1980. The dynamics and kinematics of the coastal boundary layer off Long Island. Massachusetts Institute of Technology and the Woods Hole Oceanographic Institution.

Possingham, H. and J. Roughgarden. 1990. Spatial population dynamics of a marine organism with a complex life cycle. Ecology **71**:973-985.

Rilov, G., S. E. Dudas, B. A. Menge, B. A. Grantham, J. Lubchenco, and D. R. Schiel. 2008. The surf zone: a semi-permeable barrier to onshore recruitment of invertebrate larvae? Journal of Experimental Marine Biology and Ecology **361**:59-74.

Roughan, M., A. Mace, J. Largier, S. Morgan, J. Fisher, and M. Carter. 2005. Subsurface recirculation and larval retention in the lee of a small headland: A variation on the upwelling shadow theme. Journal of Geophysical Research-Oceans **110**:C10027.

Roughgarden, J. 2006. Foreward. Pages xvii-xix *in* J. P. Kritzer and P. F. Sale, editors. Marine metapopulations. Academic Press, San Diego, CA.

Roughgarden, J., S. Gaines, and H. Possingham. 1988. Recruitment dynamics in complex life-cycles. Science **241**:1460-1466.

Roughgarden, J. and Y. Iwasa. 1986. Dynamics of a metapopulation with space-limited subpopulations. Theoretical Population Biology **29**:235-261.

Sale, P. F., I. Hanski, and J. P. Kritzer. 2006. The merging of metapopulation theory and marine ecology: Establishing the historical context. *in* J. P. Kritzer and P. F. Sale, editors. Marine Metapopulations. Academic Press, San Diego, CA.

Shanks, A. L. 2009. Pelagic larval duration and dispersal distance revisited. Biological Bulletin **216**:373-385.

Shanks, A. L. and R. K. Shearman. 2009. Paradigm lost? Cross-shelf distributions of intertidal invertebrate larvae are unaffected by upwelling or downwelling. Marine Ecology Progress Series **385**:189-204.

Smith, R. L. 1995. The physical processes of coastal ocean upwelling systems. *in* C. P. Summerhayes, editor. Upwelling in the ocean: Modern processes and ancient records. John Wiley, Hoboken, N.J.

Swearer, S., J. Caselle, D. Lea, and R. Warner. 1999. Larval retention and recruitment in an island population of a coral-reef fish. Nature **402**:799-802.

Swearer, S., J. S. Shima, M. Hellberg, S. Thorrold, G. Jones, D. Robertson, S. Morgan, K. Selkoe, G. Ruiz, and R. Warner. 2002. Evidence of self-recruitment in demersal marine populations. Bulletin of Marine Science **70**:251-271.

Tapia, F. J. and J. Pineda. 2007. Stage-specific distribution of barnacle larvae in nearshore waters: potential for limited dispersal and high mortality rates. Marine Ecology Progress Series **342**:177-190.

Thorrold, S., D. C. Zacherl, and L. A. Levin. 2007. Population connectivity and larval dispersal using geochemical signatures in calcified structures. Oceanography **20**:80-89.

Underwood, A. J. and M. J. Keough. 2001. Supply-side ecology: the nature and consequences of variations in recruitment of intertidal organisms. *in* M. D. Bertness, S. D. Gaines, and M. E. Hay, editors. Marine community ecology. Sinauer, Sunderland, Massachusetts, USA.

Watson, J., S. Mitarai, D. Siegel, J. Caselle, C. Dong, and J. McWilliams. 2010. Realized and potential larval connectivity in the Southern California Bight. Marine Ecology Progress Series **401**:31-48.

Weersing, K. and R. Toonen. 2009. Population genetics, larval dispersal, and connectivity in marine systems. Marine Ecology Progress Series **393**:1-12.

Wing, S., L. Botsford, J. Largier, and L. Morgan. 1995a. Spatial structure of relaxation events and crab settlement in the northern California upwelling system. Marine Ecology Progress Series **128**:199-211.

Wing, S., J. Largier, L. Botsford, and J. Quinn. 1995b. Settlement and transport of benthic invertebrates in an intermittent upwelling region. Limnology and Oceanography **40**:316-329.

Wolanski, E. 1992. Hydrodynamics of mangrove swamps and their coastal waters Hydrobiologia **247**:141-161.

CHAPTER 1

The coastal boundary layer: Predictable current structure decreases alongshore transport and alters scales of dispersal[*]

[*] Co-authors Brian Gaylord and John L. Largier

ABSTRACT

Dispersion of planktonic propagules connects shoreline populations of many marine species, and considerable effort has been directed at understanding this process. However, gaps in knowledge persist. In particular, relatively little information has been available regarding transport over the innermost portions of the continental shelf. We quantified velocity in nearshore waters at 5 sites along the California coast and investigated flow characteristics relevant for larvae and algal spores released into the water column from nearshore habitats. Mean depth-averaged alongshore velocities increased with distance from shore at all sites. This repeated and consistent "coastal boundary layer" (CBL) pattern exhibits a logarithmic profile that resembles that associated with the "law of the wall" of smaller-scale turbulent boundary layers, despite differences in spatial dimension and governing physics. A tentative scaling of dominant terms in an alongshore momentum balance suggests nontrivial levels of lateral stress, but small cross-shore gradients in this quantity. Such a trend of near-constant lateral stress, when combined with simple representations of horizontal mixing (i.e., eddy viscosity parameterizations) that increase approximately linearly with distance from shore, provides a possible explanation for the observed logarithmic velocity pattern. Incorporating these gradients in alongshore velocity and cross-shore mixing into a 2-dimensional particle-tracking simulation decreases mean alongshore transport of larvae and increases the variance in dispersal distance. Although modeled settlement is also reduced, the CBL is predicted to dramatically increase self-replenishment.

INTRODUCTION

The coastal zone operates as a physical and biological intermediary between shoreline environments and waters offshore. It is within this region where most algal spores and larvae of benthic invertebrates and fish start and end their lives, where nutrients are delivered to ecologically and economically important benthic ecosystems, and where the bulk of anthropogenic inputs originate. Yet the oceanography of this region – especially the area beyond the surf zone but within a few kilometers of shore – is relatively poorly described. The resultant knowledge gap hinders progress in understanding flow-driven movement of organisms and other waterborne constituents, and inhibits research on associated population and community processes (Largier 2002).

The subject of propagule dispersal, including the transport of larval fish and invertebrates as well as algal spores, has attracted the attention of marine scientists for decades. As early as the middle of the last century, biologists recognized the role of larval delivery in driving patterns of population variability (Thorson 1946). The concept of supply-side ecology (Lewin 1986) yielded greater appreciation for the influence of oceanographic processes on larval recruitment and overall population dynamics (Gaines et al. 1985, Roughgarden et al. 1988). Ensuing work addressed the capacity for ocean currents to contribute to the establishment of species range limits and biogeographic pattern (Cowen 1985, Gaylord and Gaines 2000). Research on the degree to which populations are self-seeding continues (Caley et al. 1996, Levin 2006), with considerable effort directed at quantifying population connectivity via oceanographic transport (Siegel et al. 2003, 2008, Paris et al. 2007).

In recent years impetus has developed for understanding localized physical processes that affect transport close to shore. Rationale for this interest derives from increasing evidence that self-recruitment of coastal populations is higher than previously thought, and that dispersal distances are often lower than expected based on an organisms' pelagic larval duration (Swearer et al. 2002, Palumbi 2004, Levin 2006, Shanks 2009). High self-recruitment has been reported across a variety of taxa (Shanks 2009) and in studies using a variety of techniques, including tagging (Jones et al., 2009) natural tracers (Thorrold et al. 2007) and genetics (Hellberg et al. 2002, Weersing and Toonen 2009). In addition, emerging data suggest that regions within a few kilometers from shore often have the highest abundance of larvae (Borges et al. 2007, Morgan et al. 2009, Shanks and Shearman 2009). It is also recognized that dispersal in taxa like canopy forming kelps, whose released spores remain viable in the water column for only a few days, is driven largely by nearshore flows (Gaylord et al. 2002, 2006). In some cases, explicit oceanographic mechanisms for the local retention of propagules have been identified, and these mechanisms are believed to enhance the return of larvae and spores to their natal site (e.g. island wakes, Swearer et al. 1999; headland wakes, Graham and Largier 1997; embayments and other features, Wolanski 1992). Even in systems where agents of retention have not been conclusively demonstrated (Jones et al. 2005, Becker et al. 2007), the potential for reduced scales of dispersal is receiving greater consideration. While biological interactions with the physical environment can be particularly relevant in nearshore environments (Sponaugle et al. 2002), especially as larvae can be active players within the water column (Leis 2006, Morgan and Fisher 2010), background features of the nearshore physical environment remain largely unresolved. Acquisition of

information regarding the coastal physical environment therefore represents an important next step towards understanding propagule transport and population connectivity, and may help shed light on observations of high self-recruitment and low dispersal distances across marine populations (Cowen and Sponaugle 2009).

Foreshadowed by work on island and headland wakes, an obvious, yet relatively unexplored place to look for physical mechanisms of reduced scales of dispersal is in the interaction of coastal flows with shoreline topography and bathymetry. As coastal currents transit along the continental shelf, frictional forces slow transport, producing a "coastal boundary layer" (CBL), a feature first described in the Great Lakes (Csanady 1972). Although not always termed a CBL, this decreased alongshore transport has since been quantified along sections of the east coast of the United States (Churchill 1985, Lentz et al. 1999) and along coasts of Australia (Wolanski 1992), as well as along the California margin (Hamilton et al. 2006). However, most measurements in this latter region have been confined to areas beyond the 30 m isobath (Lentz and Winant 1986, Lentz 1994), missing inshore waters that may be critical for the dispersal of larvae and algal spores released along the shoreline or in nearshore waters.

Zones of flow attenuation associated with the coastal boundary layer, while originating ultimately from increased bottom drag, are likely to be also influenced by bathymetry, shoreline topography, development of lateral shear, wave breaking and wave-current interactions, stratification and buoyancy flows, as well as the interplay of surface and bottom boundary layers which overlap in shallow water. Many of the above fluid dynamic processes are themselves the subject of study by the physical oceanographic community. Ongoing work includes refining estimates of nearshore

mixing and dispersion (Clarke et al. 2007, Drake and Edwards 2009, Ohlmann and Mitarai 2010), dissecting how winds and waves drive inner-shelf circulation (Fewings et al. 2008, Lentz and Fewings 2012), and quantifying drift and rip dynamics within the surf zone (Spydell et al. 2009, MacMahan et al. 2010). The complexity of this region is substantial, however, and progress towards a general understanding of coastal transport remains challenging. Even in highly resolved circulation models used to estimate patterns of larval connectivity (e.g., Mitarai et al. 2009) the finest scales of physical forcing are often not incorporated. Regional Ocean Modeling System (ROMS) analyses, for example, employ cells that are typically 600 m or more on a side and do not completely reach the shoreline (e.g., Rasmussen et al. 2009, Watson et al. 2010). However, there is a recognized need for understanding these finer-scale processes and developing methods to include them in models (Gawarkiewicz et al. 2007, Pineda et al. 2007, Werner et al. 2007). Individual-based models allow integration of circulation models, such as ROMS, and biological models that include larval behavior, allowing exploration of biophysical interactions (Paris et al. 2007). However these models still operate under the same spatial constraints as circulation models and only apply to the particular region and species modeled (Cowen and Sponaugle 2009). Widely employed experimental techniques, such as high-frequency radar mapping of surface currents, likewise extend to within only 1-2 kilometers of shore (Paduan and Rosenfeld 1996, Kaplan and Largier 2006). These spatial constraints significantly diminish the ability of scientists to predict dispersal patterns in taxa for which adult habitat is along the shoreline. Considerable advantages could therefore accrue from simple but robust parameterization schemes suitable for describing transport in the immediate vicinity of the coast.

Here we investigate general characteristics of nearshore currents and their potential to affect dispersal of propagules and other suspended materials. We focus on CBLs at multiple sites along the California coast, spanning a wide range of shoreline topographies and bathymetry. We describe a remarkably repeatable pattern in current velocity, discuss and discard several possible causes for this pattern that do not appear to hold, then present a first-order scaling analysis that points to a set of driving mechanisms consistent with observations. Lastly, we explore some implications of the CBL for propagule dispersal and marine population connectivity.

METHODS

Physical setting

Inner shelf currents were characterized at five sites along the California coast, spanning a range of bathymetric slopes and degree of shoreline sinuosity (Fig. 1.1; Table 1.1), as well as offshore oceanographic conditions. Two sites were located within the Southern California Bight: Huntington Beach (33°37’36”N, 117°59’13”W) is an open-coast site characterized by a gently sloping sandy beach and wide shelf (Hamilton et al. 2006), and Mohawk (34°23’29”N, 119°43’39”W) is a low-lying reef surrounded by sand within the Santa Barbara Channel (Gaylord et al. 2007). Within the Southern California Bight upwelling is weak and intermittent (Winant and Dorman 1997), and inner shelf circulation in the Santa Barbara Channel is influenced by meso-scale eddies (Bassin et al. 2005). Three other sites are located farther north. Hopkins (36°37’19”N, 121°53’55”W) is a rocky reef in southern Monterey Bay, surrounded by sand with the steepest slope and the most complex shoreline of the five sites, and with Cabrillo Point located a few

hundred meters to the west. Pajaro (36°51’37”N, 121°49’21”) is a gently sloping, straight sandy beach situated 1 km north of a river of the same name within Monterey Bay and 6.5 km north of the mouth of Monterey Canyon. Terrace Point (36°56’36”N, 122°4’50”W) is a rocky bench on the open coast, surrounded by sand, and with small coves and minor headlands nearby. Upwelling influences the region surrounding Monterey Bay, although the local topographies of each sites modulates the response. Terrace Point is located within an upwelling shadow, and Hopkins experiences topographic blockage from a minor headland. Inner shelf circulation within the Bay is largely driven by wind stress and an alongshore pressure gradient (Drake et al. 2005). Mohawk, Hopkins, and Terrace Point have neighboring kelp forests. At all sites depth increases roughly linearly with distance offshore.

Current velocity measurements

Water velocity was measured at each site using a transect of four to five bottom-mounted acoustic Doppler current profilers (ADCPs; RD Instruments 600 kHz, 1200 kHz; Nortek AWAC 1000 KHz) deployed in a cross-shore transect spanning 5-35 m depths and extending 190-5790 m from shore, depending on the bathymetric slope. The innermost instrument on each transect was placed no less than 100-200 m beyond the surf zone, to exclude any significant effects due to wave-driven currents. All measurements were made in late spring or summer (Table 1.1). Deployments varied in duration from one week to three months. For sites near kelp forests, ADCPs were typically located hundreds of meters away from the kelp beds, and all reef structures and even isolated

kelp individuals were always >10 m from the instruments. Measurements at Huntington Beach were obtained as part of a prior study (Nobel and Xu 2004, Hamilton et al. 2006).

The ADCPs collected 1-3 minute bursts of 0.75 Hz velocity data every two or three minutes in vertical bins that typically extended from ~1.5 m above the bottom to ~1.5 m below the surface. Exceptions included an instrument at Pajaro and two at Hopkins, which reached within 2.5 m of the surface, and the two deepest (25 and 35 m) instruments at Huntington Beach, which due to the distinct sampling goals of the prior study, reached to within only 4 and 8 m of the surface. Instruments deployed in ≤ 15 m water depth recorded in 0.5 m vertical bins, except for the 10 and 15 m stations at Huntington Beach, which recorded in 1 m bins. ADCPs deployed in water depth > 15 m recorded in 1 m vertical bins, except for the ADCP in 20 m at Mohawk, which recorded in 0.5 m bins, and two ADCPs at Hopkins (23 and 25 m depths) and the 35 m station at Huntington Beach, which recorded in 2 m bins. These differences in sampling protocol optimized tradeoffs in ADCP performance among vertical resolution, temporal resolution, depth range, and velocity estimate variance. For shallower deployments, small vertical bins were necessary to resolve finer vertical velocity structure, whereas for deeper deployments where spatial gradients were gentler, larger bins increased the vertical extent of measurements and reduced noise. These differences have limited bearing on interpretations of this study, which are based on depth- and time-averaged velocities.

To quantify general patterns of CBL circulation, following data collection the raw-velocity time series were depth-averaged and rotated onto their principal axes, which were determined from the low-pass filtered time series with a 33-h cutoff to remove

dominant tidal motions (Rosenfeld 1983). In all cases, the major principal axis aligned roughly parallel to shore, defining the orientation of alongshore velocity (*U*; see Table 1.2 for list of symbols). These depth-averaged velocities from each site were then further averaged over weekly durations to provide a focal data relevant for considering transport of many algal spores or larvae with relatively short pelagic larval durations. In these more detailed analyses, core statistics were determined over the first week at each site for which complete records were available at all stations (Table 1.1). At Mohawk the velocity record was 6 d long and velocities were averaged over the deployment duration. We recognize that CBL circulation may impact transport of larvae on longer time scales, but at shorter pelagic larval durations we expect these effects to be maximal.

RESULTS

Field observations

Depth-averaged currents were polarized in the alongshore direction at all stations, causing flows to be oriented predominantly parallel to the coast (Fig. 1.2; Table 1.3). Alongshore velocity magnitudes generally exceeded cross-shore magnitudes by a factor of ten, a pattern seen elsewhere in nearshore velocity records (e.g., Gaylord et al. 2007). Most importantly, weekly averaged alongshore current speeds were consistently weaker at shallower stations nearer the coast (Fig. 1.3; Table 1.3). Amongst our five sites velocity at the offshore edge of the measurements ranged from 0.01625 m s^{-1} at Huntington Beach to 0.0427 m s^{-1} at Hopkins, and inshore velocities ranged from 0.0012 m s^{-1} at Hopkins to 0.0332 m s^{-1} at Huntington Beach (Fig. 1.3-1.4; Table 1.3). Despite

the variability in velocity magnitudes amongst sites, the trend of weaker current speeds at shallower stations closer to the coast held across sites.

The increase in alongshore depth-averaged velocity with distance from shore closely followed a logarithmic pattern in most cases (Fig. 1.4). Logarithmic profiles at Mohawk, Terrace Point, and Huntington Beach fit the depth- and time-averaged field data strikingly well (Fig. 1.4A, D, E). At Hopkins, the logarithmic model did not hold, but the general trend of increasing velocity with distance was reproduced (Fig. 1.4C). At Pajaro, the velocity gradient was relatively poorly defined due to how data points were clustered; however a logarithmic relationship between velocity and distance from shore fit better than a linear relationship (Fig. 1.4B; $r^2 = 0.85$ versus 0.74).

The coastal boundary layer profile

A logarithmic pattern to the CBL is reminiscent of turbulent velocity profiles in smaller scale fluid dynamic boundary layers governed by the universal "law of the wall" (Schlicting 1979). In this model, velocities parallel to a boundary increase logarithmically with distance from that boundary according to:

$$\frac{u(z)}{u_*} = \frac{1}{\kappa}\ln\left(\frac{z}{z_0}\right) \tag{1.1}$$

where velocity (u) is normalized by the friction velocity ($u_* = \sqrt{\frac{\tau_0}{\rho}}$, where τ_0 is the wall shear stress), z is the distance from the wall normalized by a roughness parameter (z_0), and κ is von Karman's constant, traditionally set to 0.4.

The parameters underlying the law of the wall do not apply in any direct fashion to the CBL where different physical processes are active and scales of motion are orders

of magnitude larger. On the other hand, the law of the wall formulation provides a convenient mathematical shorthand for representing CBL structure. Using Eq. 1.1 as an analogy, cross-shore profiles of alongshore, depth-averaged velocity can be plotted for each site as a function of distance from shore (y) according to the expression:

$$\frac{U(y)}{U_{*CBL}} = \frac{1}{\kappa}\ln\left(\frac{y}{y_0}\right) \tag{1.2}$$

where U is the depth- and time-averaged alongshore component of velocity, and U_{*CBL} and y_0 represent CBL-scale friction velocity and roughness parameters, respectively. These latter two parameters can be calculated for each site from the slope (m) and intercept (b) of the linear regression of depth- and time-averaged alongshore velocity (U) plotted against the natural logarithm of distance from shore (y):

$$\begin{aligned} U_{*CBL} &= \kappa m \\ y_0 &= e^{\left(\frac{-b}{m}\right)} \end{aligned} \tag{1.3}$$

Normalizing the velocity and distance data by site-specific U_{*CBL} and y_0 values respectively, and assembling these data across sites, reveals a remarkably consistent trend. Plots of alongshore velocity, U, versus the natural logarithm of distance from shore, y, from all sites collapse to a single, straight line (Fig. 1.5). This apparently general relationship holds in spite of appreciable bathymetric and topographic differences among sites.

Across the five sites, values of U_{*CBL} ranged from 0.014 m s^{-1} to 0.037 m s^{-1}, and values of y_0 ranged from 150 m to 510 m. As might be expected, these CBL parameter values differed in character from friction velocities and roughness heights measured in small-scale benthic boundary layers. For example, values of U_{*CBL} were 17-35% of the velocity farthest from shore (taken as the free-stream velocity) whereas values of u_*

measured in benthic boundary layers are typically only 5-10% of the free-stream velocity (Grant and Madsen 1986, Denny 1988). These differences suggest that a greater relative "wall" drag is imposed by the complex and shoaling boundary in the CBL. In addition, values of y_0 were 2-4 orders of magnitude larger than roughness lengths characterizing benthic boundary layers, consistent with the larger scales of the CBL and the topographic irregularity of the shoreline, as well as the cross-shore scale of the wave-dominated surf zone.

Consistency of the CBL profile through time

A logarithmic trend to the CBL was particularly apparent during periods of slowly-varying (i.e., quasi-steady) alongshore flow. By contrast, this pattern degenerated periodically during current reversals or marked changes in the large-scale flow (Fig. 1.6A-C). Considering a sequence of one-week averaging periods shifted forward in one-day steps, a logarithmic pattern was present during all 14 of the averaging periods at Terrace Point (Fig. 1.6C), during 65% of the 80 averaging periods at Huntington Beach (Fig. 1.6A), and during 60% of the 13 averaging periods at Hopkins (Fig. 1.6B). The temporal consistency of the CBL pattern could not be determined at Mohawk and Pajaro due to shorter records or data gaps.

Although the logarithmic pattern persisted for weeks at a site, values of U_{*CBL} and y_0 at each site were not constant through time. Variation in these parameters was most pronounced at Huntington Beach (Fig. 1.6D, G), partly due to the diversity of flow conditions encountered over the longer deployment, as well as more pronounced reversals in the large-scale flow. However, at times when flow was quasi-steady (e.g.,

days 52-62), U_{*CBL} and y_0 at Huntington Beach exhibited reduced variance, with values similar to those at Hopkins and Terrace Point (U_{*CBL} from 0.010-0.030 m s^{-1}; y_0 from 50-500 m; Fig. 1.6D-I).

DISCUSSION

Bottom drag

The above observations demonstrate that depth-averaged alongshore currents near the coast exhibit a repeatable pattern analogous to the "law of the wall" of small-scale boundary layers. The general trend of slower velocities nearer the shore is itself not surprising, emerging as an accompaniment to the increased importance of bottom drag in a shallower water column. On the other hand, the geometry of the CBL differs significantly from that characterizing a 1-D wall-bounded flow, making the logarithmic relationship of Fig. 1.5 less than intuitive. Below we demonstrate that while bottom friction likely contributes to the logarithmic pattern, it does not by itself explain this feature of the CBL.

One clear deviation from the 1-D case is that the seabed within the CBL slopes upward to the shore such that a clear coastal "wall" cannot be identified. Instead, friction is manifested through a distributed drag imposed over a region of finite cross-shore extent. Within this region, bottom drag establishes a vertically oriented bottom boundary layer at each cross-shore position that can be described by Eq. 1.1 (e.g., Grant and Madsen 1986, Eckman 1990, Gaylord et al. 2006). Because this bottom boundary layer encompasses more of the water column in shallower depths, depth-averaged velocities

are reduced closer to shore. Estimates of depth-averaged velocities, U_{calc}, at given distances from shore, y, can be found by integrating Eq. 1.1 and dividing the result by the total water column depth, h:

$$U_{calc}(y) = \frac{1}{h}\int_{z_0}^{h} \frac{u_*}{\kappa} \ln\left(\frac{z}{z_0}\right) dz \tag{1.4}$$

where $h = y\tan\alpha$ and α is the bathymetric slope. Completing this mathematical operation yields (see Appendix A1):

$$U_{calc}(y) = \frac{u_*}{\kappa}\left[\ln\left(\frac{y\tan\alpha}{z_0}\right) - 1\right] + \frac{u_* z_0}{\kappa y \tan\alpha} \tag{1.5}$$

In coastal waters where $y >> z_0$ this expression approaches a logarithmic form in the y-dimension, indicating that a logarithmic bottom boundary layer (i.e. in the z-direction) acting over a linearly sloping seabed can indeed produce a near-logarithmic cross-shore profile in depth-averaged alongshore flow. Critically, however, values of bottom roughness (z_0) that would be required to reproduce the observed CBL gradient ($U_{calc}[y]$) are too large to be physically reasonable. For example, at Mohawk, a value of z_0 = 3.0 m would be required to fit Eq. 1.5 to the field data. Such roughness levels exceed typical values of z_0 by over an order of magnitude, even when considering events of high bottom stress and accounting for wave-current interaction (Wiberg et al. 1994). Conducting the opposite analysis reveals an analogous mismatch. Predicting a CBL from Eq. 1.5 using values of bottom stresses and roughness heights reasonable for benthic boundary layers (z_0 = 0.1 and u_* = 5% of free-stream velocity = 0.0063 m s^{-1} for Mohawk) yields profiles with unrealistically weak velocity gradients (Fig. 1.7A). Similar or greater discrepancies were found for all sites.

We can also go further. Implicit to Eqs. 1.1, 1.4, and 1.5 is the assumption that vertical mixing can be approximated by a linear "eddy viscosity" (Grant and Madsen 1986), defined as $K_z = \kappa u_* z$, where K_z is related to bottom shear stress (τ_0) and the vertical velocity gradient by:

$$\tau_0 = \rho K_z \frac{du}{dz} \tag{1.6}$$

An alternative form for eddy viscosity that is often employed in marine systems is (Eckman 1990, Gaylord et al. 2006):

$$K_z = \kappa u_* z \exp\left(\frac{-2z}{h}\right) \tag{1.7}$$

Integrating Eq. 1.6 numerically using this latter form for K_z, together with reasonable values for τ_0 (0.1 Pa) and z_0 (0.1 m), again reveals that bottom stress alone cannot explain the observed CBL profile (Fig. 1.7B). Regardless of the model of vertical mixing, and for all sites, the cross-shore CBL velocity gradients predicted solely by bottom boundary layer effects are much weaker than that those observed in the field.

Contributions from other stresses

Bottom drag is of course only one of several factors influencing the balance of alongshore momentum in the coastal zone. A more complete evaluation of forcing terms would include bottom, lateral, and surface stresses, acceleration, an alongshore pressure gradient, as well as buoyancy, rotational, and wave-driven effects. Characterizing the CBL with this level of detail is beyond the scope of the present study, as the requisite data are not available. However, we can focus on those terms that should be most important to the alongshore momentum balance in the CBL.

The conceptual model of the CBL is a well-mixed, quasi-steady, alongshore-uniform sheared flow within order of a kilometer from shore, remote from major topographic features and their associated flow disruptions. Rotational, buoyancy, and acceleration terms are assumed negligible. Wave effects are also neglected given that wave-driven components of alongshore movement outside the surf zone are typically much smaller than those attributed to wind and alongshore pressure gradients (Lentz and Fewings 2012). The CBL is bounded some distance offshore by a "free stream" alongshore flow forced by an alongshore pressure gradient and surface wind stress. Within the CBL, currents are subject to the drag of the coast and bottom. Additional momentum transfer occurs through lateral mixing across the sheared alongshore flow. This representation of the CBL, as well as its logarithmic form, are not expected to hold in or very near the surf zone where wave forcing is significant; indeed, one may interpret y_0 as the width of the nearshore zone excluded from this simplified momentum balance.

Within the logarithmic region of the CBL, the steady alongshore momentum balance can be modeled as the sum of the alongshore pressure gradient, surface wind stress, bottom stress, and lateral stress divergence, terms which have been shown to be important to the momentum balance over the inner shelf (Lentz et al. 1999, Kirincich and Barth 2009, Lentz and Fewings 2012):

$$\frac{1}{\rho}\frac{\partial P}{\partial x} + \frac{\tau_s}{\rho h} + \frac{\tau_b}{\rho h} + \frac{\partial \overline{u'v'}}{\partial y} = 0 \qquad (1.8)$$

where $\frac{\partial P}{\partial x}$ is the alongshore pressure gradient, τ_s is the surface wind stress, and τ_b is the bottom stress. The final term of Eq. 1.8 is the depth-averaged lateral stress divergence and represents the gradient of cross-shore exchange of alongshore momentum, where

lateral stress is the average product of alongshore and cross-shore velocity fluctuations (*u'* and *v'* respectively). Although the divergence term is rarely measured and therefore difficult to parameterize, it can be estimated from the other terms in the momentum balance:

$$-\frac{\partial \overline{u'v'}}{\partial y} = \frac{1}{\rho}\frac{\partial P}{\partial x} + \frac{\tau_s}{\rho y \tan\alpha} + \frac{\tau_b}{\rho y \tan\alpha} \tag{1.9}$$

where the quantity $y\tan\alpha$ has now replaced h to account for the sloping seabed and to convert depth to distance from shore. In practice, the lateral stress divergence is often sufficiently small as to be omitted from the alongshore momentum balance (e.g., Lentz and Winant 1986). It is important to note, however, that while the divergence may be small and thereby imply a near-constant lateral stress, this stress could potentially be large. The existence of a finite lateral stress may contribute substantially to the establishment of observed patterns of velocity within the CBL, much as it does in traditional boundary layers where $\tau_0 \neq 0$.

Reconciling the logarithmic profile

The momentum balance described by Eqs. 1.8 and 1.9 is more complex than that underlying a standard, 1-D logarithmic boundary layer. Yet, the CBL appears to adhere surprisingly well to the logarithmic functional form. Although the origins of this correspondence are not clear, and cannot fully be evaluated given data limitations, we offer a tentative analysis as a preliminary exploration of CBL structure.

Two linked factors are responsible for the logarithmic character of 1-D turbulent boundary layers: constant cross-shore transfer of alongshore momentum (i.e., constant lateral stress) and a lateral mixing profile, or eddy viscosity, that increases linearly with

distance from the boundary. Neither of these features is likely to hold exactly in the CBL case. On the other hand, it is possible that the complicated form of Eq. 1.9 reduces – at least approximately – to a simpler relationship once values for various terms are incorporated into the momentum balance.

To begin to evaluate this possibility, we conduct a rough evaluation of Eq. 1.9 across a range of distances from shore, *y*. Because it is not possible to accurately quantify the full suite of forcing terms at all locations at all of our sites, we focus on an exemplar site (Terrace Point) where we have the best data. We acknowledge that this is a site-specific analysis, which reduces the generality of any conclusions, but use it as an illustration. We expect common underlying dynamics due to the shared pattern. We assume an alongshore pressure gradient and wind stress that are constant with distance from shore. Based on published descriptions of nearshore dynamics off the coast of California (Hickey et al. 2003), we employ a value of 1×10^{-4} Pa m^{-1} for a weeklong average pressure gradient, and estimate alongshore surface wind stress from wind data collected just onshore of the ADCP transect at Terrace Point using a quadratic drag law:

$$\tau_s = 1.3 C_D u_w^{\,2} \tag{1.10}$$

where C_D is a neutral drag coefficient (Large and Pond 1981), and u_w is the velocity of the alongshore component of the wind. Eq. 1.10 yields a weeklong average wind stress of 1.42×10^{-2} Pa. Bottom stress is estimated from the equation:

$$\tau_b(y) = \rho r c U \tag{1.11}$$

where r is a linear drag coefficient ($= 5 \times 10^{-4}$; Lentz and Winant 1986) , and cU is an estimate of the average bottom velocity, computed by multiplying the depth-averaged

current velocity by the slope, c, of the linear regression between depth-averaged and bottom velocities (c = 0.2 for Terrace Point).

Of particular interest is whether lateral stress in the CBL is approximately constant across its width, as in a traditional logarithmic boundary layer, or whether it increases or decreases toward the shore. Recognizing that $-\rho\overline{u'v'}$ defines the lateral stress, τ_{lat}, Eq. 1.9 can be integrated to yield (see Appendix B1):

$$\tau_{lat}(y) = \frac{\partial P}{\partial x} y + \frac{\tau_s \ln y}{\tan\alpha} + \frac{\rho r c U_{*CBL}}{2\kappa \tan\alpha}\left[\ln\left(\frac{y}{y_0}\right)\right]^2 + D \qquad (1.12)$$

where D is an integration constant estimable from data of previous studies. Drifter deployments in northern California (Davis 1985) indicate that $\rho\overline{u'v'}$ declines toward the coast, reaching a value of 4 Pa at 1600 m from shore. Kirincich and Barth (2009) present a stress divergence value of $0.1\text{x}10^{-5}$ m s^{-2} at a distance of 1000 m over a weeklong period, suggesting a lateral stress of order 1 Pa. We therefore develop an order of magnitude estimate of D by solving Eq. 1.12 with lateral stress set to 1 Pa at a distance of y_0 = 225 m from shore, yielding D of -3.11.

With D and thus the complete expression of Eq. 1.12 in hand, we can then examine the shape of the lateral stress profile as a function of distance from shore. Over most of the domain spanned by the logarithmic portion of the CBL, the lateral stress is essentially constant, varying by less than a factor of 1.4 over the outer 80% of the boundary layer (Fig. 1.8, left axis). Or to represent this constancy in a different way, within this region values of the lateral stress profile vary by a factor between 0.8 and 1.5. These bounds also apply across a substantial range of forcing intensities, such that the lateral stress profile remains equivalently flat for all decreased pressure gradients as well

as for pressure gradients increased by over 350%. Lateral stress profiles also remain flat for wind stress adjustments as large as +35% or –15%, or for changes to the bottom drag coefficient as substantial as +280% or –40%. Importantly, the lateral stress across this spectrum of forcing intensities is never the smallest of the terms within Eq. 1.12.

Estimates of horizontal eddy viscosity

In the traditional derivation of a logarithmic boundary layer, a uniform lateral stress is accompanied by a linear eddy viscosity. Although limitations of the eddy viscosity concept for representing mixing are well known, it is a commonly used and convenient construct for describing horizontal dispersion of larvae or other biological particles (Jackson and Strathmann 1981, Gaines et al. 2003, Largier 2003). We therefore rely on it here for our rudimentary scaling analysis of the CBL, and proceed to explore whether it approximates a linear dependence on distance from shore.

Building on our evaluation of the lateral stress, we note the definitional expression (analogous to Eq. 1.6) that relates lateral stress, eddy viscosity and the CBL velocity gradient:

$$\tau_{lat} = \rho K_y \frac{dU}{dy} \tag{1.13}$$

From our field data, we know that velocities increase according to the logarithmic form described by Eq. 1.2, whose derivative is:

$$\frac{dU}{dy} = \frac{U_{*CBL}}{\kappa} \frac{1}{y} \tag{1.14}$$

The latter expression can be inserted into Eq. 1.13. The combination of Eqs. 1.13-1.14 can in turn be merged with Eq. 1.12 to produce an explicit expression for the eddy viscosity profile in the CBL:

$$K_y(y) = \frac{\kappa}{\rho U_{*CBL}} y\left[\frac{\partial P}{\partial x} y + \frac{\tau_s}{\tan\alpha}\ln y + \frac{\rho r U_{*CBL} c}{2\kappa \tan\alpha}(\ln\frac{y}{y_0})^2 + D\right] \qquad (1.15)$$

Although the dependence of K_y on distance from shore is not immediately apparent by inspection, a plot of Eq. 1.15 using the forcing parameters identified for Terrace Point indicates that K_y follows a roughly linear trajectory (Fig. 1.8, right axis). This trend is also robust to variation in forcing. Conducting the same sensitivity analysis employed for the lateral stress (i.e., pressure gradient increased by +350%, wind stress altered +35% or –15%, and drag coefficient changed +280% or –40%) reveals only modest deviations from linear. Indeed, least squares parameter fits of the simple expression $K_y(y) = ay^d$ to plots of Eq. 1.15 indicate relatively constrained values of a and d, with d in particular ranging between 0.8 and 1.4. Such a nearly linearly increasing profile of horizontal eddy viscosity is also consistent with previous empirical estimates. For example, drifter studies off the coast of Northern California within 60 km from shore suggest d ~ 1 (Davis 1985) and dye studies from various regions suggest $1 < d < 1.5$ (d = 1.33, Stommel 1949; d = 1.1, Okubo 1971).

In addition to the slopes, values of K_y computed from Eq. 1.15 (Fig. 1.8) are also within the range of measured K_y from other studies. Off north-central California, Lagrangian surface drifter tracks within 60 km from shore suggest $K_y \sim 16$ m^2 s^{-1} when interpolated to 2 km from shore using a linear model for eddy viscosity (Davis 1985). List et al. (1990) report values of 10-20 m^2 s^{-1} at a distance of 2.6 km from shore off

southern California from drogue and current meter data. Drake and Edwards (2009) showed a close correspondence between model simulations of particle diffusion and measured float dispersion when using a linear model for K_y that yielded a value of 60 m^2 s^{-1} at 2 km from shore. At a distance of 2 km from shore, our analysis gives a K_y of 83 m^2 s^{-1}, which is modestly larger than, but of the same order of magnitude as, the empirical measurements.

Implications of the CBL for dispersal

The well-defined structure of the CBL – including both its logarithmic velocity gradient and near-linear eddy viscosity profile – may substantially alter predicted dispersal distributions for larvae, algal spores, and/or other commodities suspended in the water column. We illustrate such potential consequences through the use of a 2-dimensional random-walk dispersal model (White et al. 2010b). We track simulated larvae considering three model cases. The base case represents the absence of a CBL, as in contemporary ecological models, by employing a spatially invariant alongshore velocity and a spatially invariant horizontal eddy viscosity (U = 0.075 m s^{-1}, K_y = 40 m^2 s^{-1}). The second case retains the same invariant eddy viscosity, but introduces weaker nearshore velocities represented by a logarithmic velocity profile typical of a CBL, using U_{*CBL} and y_0 parameters from Terrace Point. These parameters result in a velocity of 0.075 m s^{-1} at the outer edge of the CBL (y = 1100 m). The final case combines the logarithmic CBL profile from Terrace Point with reduced mixing nearshore, represented by the eddy viscosity profile from this site ($K_y = 5.92 \times 10^{-3} y^{1.26}$, which reaches 40 m^2 s^{-1} at the edge of the CBL). We assume that diffusion of larvae and spores operates akin to

diffusion of momentum, and therefore use our values of eddy viscosity to represent eddy diffusivity, a quantity more properly identified with mixing of water-borne material.

In conducting these simulations, larvae were released at a distance y_0 = 225 m from shore, to model a shallow subtidal organism spawning near the outside edge of the surf zone. Most marine species are developmentally unable to settle for some time after release, during a period typically termed a "precompetency window." After passing through this window, they usually enter a "competency window" of similar duration (Jackson and Strathmann 1981), during which they can settle if they encounter suitable habitat. Simulations were conducted with precompetency and competency windows set to 5 d to mimic species with pelagic larval durations of ~ 1 week, such as the red abalone of the west coast of North America, *Haliotis rufescens* (Haaker et al. 2001). Settling larvae were counted as those that returned to within 225 m from shore during the competency window. While we recognize that behavioral capabilities (e.g., vertical positioning or horizontal swimming) can play a major role in the dispersal of some larvae (Leis 2006, Shanks and Shearman 2009, Morgan and Fisher 2010), the goal of this model was to illustrate the potential impacts of velocity gradients alone on dispersal outcomes, and we treat larvae as passive particles.

Results of the simulations indicate strong potential effects of the CBL on larval dispersal. The incorporation of a logarithmic velocity profile and spatially variable eddy diffusivity decreased predicted mean transport by 10%, from 40 km to 36 km (Fig. 1.9). Inclusion of the logarithmic velocity profile and spatially variable eddy diffusivity also caused a 10% increase in the standard deviation of transport distance. Kurtosis additionally increased. These effects arose because slowed nearshore velocities reduce

net displacement, while slowed mixing across the velocity gradient broadens the alongshore distribution through enhanced shear dispersion. During the precompetency window, larvae were advected downstream from the release point. At the end of the precompetency window when larvae began to settle, without a CBL their initial distribution was narrow, with little spread around the mean displacement. When a velocity gradient was included, larvae were advected at different rates downstream depending on their cross-shore position, leading to a distribution of competent larvae with more spread than that resulting without a CBL. Adding a diffusivity gradient further increased the spread of the kernel because lower diffusivities near the coast required more time steps for larvae to settle than that required with higher constant diffusivity.

Perhaps even more important are predicted effects of the CBL on settlement and self-replenishment, the latter defined as the proportion of settling propagules returning to within 10 km of the source site. Incorporating a CBL velocity gradient and a linearly increasing eddy diffusivity resulted in an 18% decrease in settlement and a 1000% increase in self-replenishment. These effects arose because as diffusivities decrease closer to shore, horizontal mixing motions become smaller and the return to suitable habitat takes longer, which makes it more difficult for larvae to be mixed back toward shoreline habitat. In addition, a small diffusivity near the shore results in some larvae remaining very close to their site of origin (see distances of -10 to 10 km in Fig. 1.9).

Slower flows near the coast, and the resultant decrease in alongshore transport, likely add to a suite of physical processes affecting dispersal and recruitment. Although other mechanisms for the local return of dispersers have been invoked previously (as in the case of headland or island wakes), most are location- or time-specific (e.g., Wing et

al. 1995, Graham and Largier 1997, Swearer et al. 1999). By contrast, the CBL structure described here appears pervasive, deriving from unavoidable velocity shear near the coast. Implications of transport effects of the CBL may also be non-trivial, given their strong effects on the degree to which populations could self-seed. Indeed, they may result in substantially tighter coupling between local production and recruitment than has often been thought (Caley et al. 1996), even in the absence of other identifiable agents of retention, such as topographic features. Such retentive features may also have synergistic effects with the CBL, further reducing flow and potentially increasing coupling between production and recruitment. For example, Hopkins, located at the southern end of Monterey Bay, has a complex topography and low offshore velocities. The CBL acts to further reduce velocities adjacent to the shoreline, and may increase local retention. Although larval behavior has routinely been invoked as a key element in increasing return of larvae to their sites of origin, a potentially equally important factor could be the retention of organisms in slower flows in the inner portion of the CBL. Nearshore flow rates have already been shown empirically to affect recruitment rates of coastal marine invertebrates, with higher recruitment arising in cases of long residence times of water masses (Gaines and Bertness 1992). The present study reiterates the well-recognized connection between coastal processes and population dynamics of shoreline organisms.

The interaction of larval behavior and the lower velocities within the CBL may promote limited dispersal in marine populations. The results of the dispersal model should be interpreted with caution, as the treatment of larvae as passive particles is an oversimplification. However, the model predictions could be interpreted as conservative, as larval behavior, in addition to promoting the return of larvae to the coastal

environment, may play a major role in avoiding dispersal (Marliave 1986). For example, fish and invertebrate larvae that remain nearshore throughout development, as evidenced by the presence of larvae across stages, have been found in greatest concentrations near the bottom, in low flow environments (Borges et al. 2007, Morgan et al. 2009, Morgan and Fisher 2010). The combination of larvae maintaining position in lower flows near the bottom and the presence of lower velocities within the CBL may enhance the ability of larvae to avoid dispersal. This mechanism may explain observations of limited dispersal across a variety of taxa, even in regions that are thought to be strongly advective, such as the west coast of North America (e.g., Morgan et al. 2009, Shanks and Shearman 2009). Because limited dispersal has been observed in a variety of systems and taxa, using a variety of techniques (Palumbi 2004, Thorrold et al. 2007, Shanks 2009), a feature such as the CBL that applies over a range of settings and conditions may be an important contributor to this pattern.

Application of the CBL to circulation studies

Most circulation-resolving dispersal models do not account for small-scale spatial variations in velocity and mixing near to the coast, even though these variations may be of first-order importance for populations that spawn and recruit along the shoreline or in the nearshore habitats. However, incorporating more realistic nearshore flow properties in models for dispersal and population dynamics, even in simple advection-diffusion approaches, can change predictions appreciably (Aiken et al. 2007, White et al. 2010a, 2010b). In addition, existing numerical circulation models use a variety of boundary conditions (e.g., no-slip or free slip; Aiken et al. 2007, Mitarai et al. 2009). The CBL

pattern described here may provide more explicit rationale for certain choices. It may also facilitate interpolation of remote sensing data to shore (e.g., high-frequency radar maps of surface currents), closing an important information gap in existing dispersal models that are increasingly used to estimate population connectivity.

The results presented here derived from a 2-dimensional approach to understanding nearshore transport, and represent a first step at describing the general flow structure within the CBL. Future models of the CBL, particularly those which incorporate larval behavior, should consider the potential effects of vertical current profiles within the CBL, although these models would be location and species specific.

Further considerations for the CBL

Our studies of coastal velocity profiles were all conducted during the summer season, however we expect that the effects of the CBL apply across seasons. The frictional effect of the CBL responds to offshore forcing: while offshore velocities may change in response to season (e.g., the strength of the offshore California Current), velocities further inshore will still be under the influence of friction. For example, we captured a variety of offshore conditions, particularly in the longer record at Huntington Beach, which included changes in the direction of shelf-scale flow and still observed a CBL.

The level of nearshore flow attenuation described here may be a conservative estimate in certain circumstances, due to the potential for coastal currents to interact with more pronounced frictional elements like elevated reefs or dense vegetation. All our instruments were deliberately placed away from such elements, but their effects can be large. For example, alongshore velocities within kelp forests may be as low as 50% of

speeds outside (Jackson and Winant 1983, Gaylord et al. 2007, 2012, Rosman et al. 2007). Seagrass beds and mangroves are likely to have similar effects (e.g. Fonseca et al. 1982). Even in the absence of such additional flow attenuation, coastal boundary layers have clear potential to reduce alongshore transport of larvae, spores, and other suspended materials. Although these and other complexities of the coastal ocean do not lend themselves to simultaneously simple and complete representations, the straightforward parameterizations identified here are an important first step and provide a useful construct for conceptualizing and predicting consequences of nearshore velocity structure.

ACKNOWLEDGMENTS

We thank D. Reed, C. Nelson, S. Harrer, K. Aquilino, D. Dann, L. Garske, A. Hettinger, S. Miller, M. Sheridan, W. Dowd, M. Boller, M. Foley, and B. Mahoney for field assistance. J.W. White assisted with the particle-tracking model, and S.G. Monismith, C.A. Edwards, M. Fewings, and S.J. Lentz provided helpful feedback. This work was funded by NSF grants OCE-927255 and OCE-1065990, and by the University of California Marine Council Coastal Environmental Quality Initiative grants 04-T-CEQI-08-0048 and 07-T-CEQI-10-0060. K.J. Nickols was supported by a Bodega Marine Laboratory Graduate Student Fellowship, a Jastro Shields Research Scholarship, and funds from the University of California at Davis Graduate Group in Ecology. A subset of data was provided by the Partnership for Interdisciplinary Studies of Coastal Oceans and the Orange County Sanitation District.

LITERATURE CITED

Aiken, C. M., S. A. Navarrete, M. I. Castillo, and J. C. Castilla. 2007. Along-shore larval dispersal kernels in a numerical ocean model of the central Chilean coast. Marine Ecology Progress Series **339**:13-24.

Bassin, C. J., L. Washburn, M. A. Brzezinski, and E. E. McPhee. 2005. Sub-mesoscale coastal eddies observed by high frequency radar: A new mechanism for delivering nutrients to kelp forests in the Southern California Bight. Geophysical Research Letters **32**:L12604.

Becker, B. J., L. A. Levin, F. J. Fodrie, and P. A. McMillan. 2007. Complex larval connectivity patterns among marine invertebrate populations. Proceedings of the National Academy of Sciences (USA) **104**:3267-3272.

Borges, R., R. Ben-Hamadou, M. A. Chicharo, P. Re, and E. J. Goncalves. 2007. Horizontal spatial and temporal distribution patterns of nearshore larval fish assemblages at a temperate rocky shore. Estuarine, Coastal and Shelf Science **71**:412-428.

Caley, M. J., M. H. Carr, M. A. Hixon, T. P. Hughes, G. P. Jones, and B. A. Menge. 1996. Recruitment and the local dynamics of open marine populations. Annual Review of Ecology and Systematics **27**:477-500.

Churchill, J. H. 1985. Properties of flow within the coastal boundary layer off Long Island, New York. Journal of Physical Oceanography **15**:898-916.

Clarke, L. B., D. Ackerman, and J. L. Largier. 2007. Dye dispersion in the surf zone:

Measurements and simple models. Continental Shelf Research **27**:650-669.

Cowen, R. K. 1985. Large-scale pattern of recruitment by the labrid, *Semicossyphus pulcher*: Causes and implications. Journal of Marine Research **43**:719-742.

Cowen, R. K. and S. Sponaugle. 2009. Larval dispersal and marine population connectivity. Annual Review of Marine Science **1**:443-466.

Csanady, G. T. 1972. The coastal boundary layer in Lake Ontario: Part II. The Summer-Fall regime. Journal of Physical Oceanography **2**:168-176.

Davis, R. E. 1985. Drifter observations of coastal surface currents during CODE: The statistical and dynamical views. Journal of Geophysical Research-Oceans **90**:4756-4772.

Denny, M. W. 1988. Biology and the mechanics of the wave-swept environment. Princeton University Press, Princeton, NJ.

Drake, P. T. and C. Edwards. 2009. A linear diffusivity model of near-surface, cross-shore particle dispersion from a numerical simulation of central California's coastal ocean. Journal of Marine Research **67**:385-409.

Drake, P. T., M. A. McManus, and C. D. Storlazzi. 2005. Local wind forcing of the Monterey Bay area inner shelf. Continental Shelf Research **25**:397-417.

Eckman, J. E. 1990. A model of passive settlement by planktonic larvae onto bottoms of differing roughness. Limnology and Oceanography **35**:887-901.

Fewings, M., S. J. Lentz, and J. Fredericks. 2008. Observations of cross-shelf flow driven

by cross-shelf winds on the inner continental shelf. Journal of Physical Oceanography **38**:2358-2378.

Fonseca, M. S., J. S. Fisher, J. C. Zieman, and G. W. Thayer. 1982. Influence of the seagrass *Zostera marina* L., on current flow. Estuarine, Coastal and Shelf Science **15**:351-364.

Gaines, S. D. and M. D. Bertness. 1992. Dispersal of juveniles and variable recruitment in sessile marine species. Nature **360**:579-580.

Gaines, S. D., S. Brown, and J. Roughgarden. 1985. Spatial variation in larval concentrations as a cause of spatial variation in settlement for the barnacle, *Balanus glandula*. Oecologia **67**:267-272.

Gaines, S. D., B. Gaylord, and J. L. Largier. 2003. Avoiding current oversights in marine reserve design. Ecological Applications **13**:S32-S46.

Gawarkiewicz, G., S. G. Monismith, and J. L. Largier. 2007. Observing larval transport processes affecting population connectivity: progress and challenges. Oceanography **20**:40-53.

Gaylord, B. and S. D. Gaines. 2000. Temperature or transport? Range limits in marine species mediated solely by flow. American Naturalist **155**:769-789.

Gaylord, B., K. J. Nickols, and L. Jurgens. 2012. Roles of transport and mixing processes in kelp forest ecology. Journal of Experimental Biology **215**:997-1007.

Gaylord, B., D. Reed, P. T. Raimondi, and L. Washburn. 2006. Macroalgal spore dispersal in coastal environments: mechanistic insights revealed by theory and

experiment. Ecological Monographs **76**:481-502.

Gaylord, B., D. Reed, P. T. Raimondi, L. Washburn, and S. McLean. 2002. A physically based model of macroalgal spore dispersal in the wave and current-dominated nearshore. Ecology **83**:1239-1251.

Gaylord, B., J. H. Rosman, D. C. Reed, J. R. Koseff, J. Fram, S. MacIntyre, K. Arkema, C. McDonald, M. A. Brzezinski, J. L. Largier, S. G. Monismith, P. T. Raimondi, and B. Mardian. 2007. Spatial patterns of flow and their modification within and around a giant kelp forest. Limnology and Oceanography **52**:1838-1852.

Graham, W. M. and J. L. Largier. 1997. Upwelling shadows as nearshore retention sites: The example of northern Monterey Bay. Continental Shelf Research **17**:509-532.

Grant, W. D. and O. S. Madsen. 1986. The continental-shelf bottom boundary layer. Annual Review of Fluid Mechanics **18**:265-305.

Haaker, P., K. Karpov, L. Rogers-Bennett, I. Taniguchi, C. S. Friedman, and M. J. Tegner. 2001. Abalone. Pages 89-97 *in* W.S. Leet, C.M. Dewees, R. Klingbeil, E.J. Larson, editors. California's living marine resources: A status report. California Department of Fish and Game, Sacramento, CA.

Hamilton, P., M. A. Noble, J. L. Largier, L. K. Rosenfeld, and G. Robertson. 2006. Cross-shelf subtidal variability in San Pedro Bay during summer, 2001. Continental Shelf Research **26**:681-702.

Hellberg, M., R. Burton, J. Neigel, and S. Palumbi. 2002. Genetic assessment of connectivity among marine populations. Bulletin Of Marine Science **70**:273-290.

Hickey, B. M., E. L. Dobbins, and S. E. Allen. 2003. Local and remote forcing of currents and temperature in the central Southern California Bight. Journal of Geophyscal Research **108**:3081-3106.

Jackson, G. A. and R. R. Strathmann. 1981. Larval mortality from offshore mixing as a link between pre-competent and competent periods of development. American Naturalist **118**:16-26.

Jackson, G. A. and C. D. Winant. 1983. Effect of a kelp forest on coastal currents. Continental Shelf Research **2**:75-80.

Jones, G. P., G. R. Almany, G. R. Russ, P. F. Sale, R. S. Steneck, M. J. H. Oppen, and B. L. Willis. 2009. Larval retention and connectivity among populations of corals and reef fishes: history, advances and challenges. Coral Reefs **28**:307-325.

Jones, G. P., S. Planes, and S. R. Thorrold. 2005. Coral reef fish larvae settle close to home. Current Biology **15**:1314-1318.

Kaplan, D. M. and J. L. Largier. 2006. HF radar-derived origin and destination of surface waters off Bodega Bay, California. Deep-Sea Research II **53**:2906-2930.

Kirincich, A. R. and J. A. Barth. 2009. Alongshelf variability of inner-shelf circulation along the Central Oregon coast during summer. Journal of Physical Oceanography **39**:1380-1398.

Large, W. G. and S. Pond. 1981. Open ocean momentum flux measurements in moderate to strong winds. Journal of Physical Oceanography **11**:324-336.

Largier, J. L. 2002. Linking oceanography and nearshore ecology: perspectives and

challenges. Pages 207-239 *in* J. C. Castilla and J. L. Largier, editors. The oceanography and ecology of the nearshore and bays in Chile. Universidad Catolica de Chile, Chile.

Largier, J. L. 2003. Considerations in estimating larval dispersal distances from oceanographic data. Ecological Applications **13**:S71-S89.

Leis, J. M. 2006. Are larvae of demersal fishes plankton or nekton? Advances in Marine Biology **51**:57-141.

Lentz, S. 1994. Current dynamics over the northern California inner shelf. Journal of Physical Oceanography **24**:2461-2478.

Lentz, S., R. T. Guza, S. Elgar, F. Feddersen, and T. H. C. Herbers. 1999. Momentum balances on the North Carolina inner shelf. Journal of Geophysical Research-Oceans **104**:18205-18226.

Lentz, S. J. and M. Fewings. 2012. The wind- and wave-driven inner-shelf circulation. Annual Review of Marine Science **4**:317-343.

Lentz, S. J. and C. D. Winant. 1986. Subinertial currents on the Southern California shelf. Journal of Physical Oceanography **16**:1737-1750.

Levin, L. A. 2006. Recent progress in understanding larval dispersal: new directions and digressions. Integrative and Comparative Biology **46**:282-297.

Lewin, R. 1986. Supply-side ecology. Science **234**:25-27.

List, E. J., G. Gartrell, and C. D. Winant. 1990. Diffusion and dispersion in coastal

waters. Journal of Hydraulic Engineering **116**:1158-1179.

MacMahan, J., J. Brown, J. Brown, E. Thornton, A. Reniers, T. Stanton, M. Henriquez, E. Gallagher, J. Morrison, M. J. Austin, T. M. Scott, and N. Senechal. 2010. Mean Lagrangian flow behavior on an open coast rip-channeled beach: A new perspective. Marine Geology **268**:1-15.

Marliave, J. B. 1986. Lack of planktonic dispersal of rocky intertidal fish larvae. Transactions of the American Fisheries Society **115**:149-154.

Mitarai, S., D. A. Siegel, J. R. Watson, C. Dong, and J. C. McWilliams. 2009. Quantifying connectivity in the coastal ocean with application to the Southern California Bight. Journal of Geophysical Research-Oceans **114**:C10026.

Morgan, S. and J. Fisher. 2010. Larval behavior regulates nearshore retention and offshore migration in an upwelling shadow and along the open coast. Marine Ecology Progress Series **404**:109-126.

Morgan, S. G., J. L. Fisher, S. H. Miller, S. T. McAfee, and J. L. Largier. 2009. Nearshore larval retention in a region of strong upwelling and recruitment limitation. Ecology **90**:3489-3502.

Noble, M. A. and J. Xu. 2004. Huntington Beach shoreline contamination investigation, Phase III, final report: Coastal circulation and transport patterns: the likelihood of OCSD's plume impacting Huntington Beach shoreline. USGS Open File Rep. 2004-1019.

Ohlmann, J. C. and S. Mitarai. 2010. Lagrangian assessment of simulated surface current

dispersion in the coastal ocean. Geophysical Research Letters **37**:L17602.

Okubo, A. 1971. Oceanic diffusion diagrams. Deep-Sea Research **18**:789-802.

Paduan, J. D. and L. Rosenfeld. 1996. Remotely sensed surface currents in Monterey Bay from shore-based HF radar (Coastal Ocean Dynamics Application Radar). Journal of Geophysical Research-Oceans **101**:20669-20686.

Palumbi, S. R. 2004. Marine reserves and ocean neighborhoods: The spatial scale of marine populations and their management. Annual Review of Environment and Resources **29**:31-68.

Paris, C. B., L. M. Cherubin, and R. K. Cowen. 2007. Surfing, spinning, or diving from reef to reef: effects on population connectivity. Marine Ecology Progress Series **347**:285-300.

Pineda, J. S., J. A. Hare, and S. Sponaugle. 2007. Larval transport and dispersal in the coastal ocean and consequences for population connectivity. Oceanography **20**:22-39.

Rasmussen, L. L., B. D. Cornuelle, L. A. Levin, J. L. Largier, and E. Di Lorenzo. 2009. Effects of small-scale features and local wind forcing on tracer dispersion and estimates of population connectivity in a regional scale circulation model. Journal of Geophysical Research **114**:C01012.

Rosenfeld, L. 1983. CODE-2: Moored array and large-scale data report. WHOI Technical Report 85-35:1-242.

Rosman, J. H., J. R. Koseff, S. G. Monismith, and J. Grover. 2007. A field investigation

into the effects of a kelp fores (*Macrocystis pyrifera*) on coastal hydrodynamics and transport. Journal of Geophysical Research-Oceans **112**:C02016.

Roughgarden, J., S. Gaines, and H. Possingham. 1988. Recruitment dynamics in complex life-cycles. Science **241**:1460-1466.

Schlicting, H. 1979. Boundary-layer theory. McGraw-Hill, New York, NY.

Shanks, A. L. 2009. Pelagic larval duration and dispersal distance revisited. Biological Bulletin **216**:373-385.

Shanks, A. L. and R. K. Shearman. 2009. Paradigm lost? Cross-shelf distributions of intertidal invertebrate larvae are unaffected by upwelling or downwelling. Marine Ecology Progress Series **385**:189-204.

Siegel, D., B. Kinlan, B. Gaylord, and S. Gaines. 2003. Lagrangian descriptions of marine larval dispersion. Marine Ecology Progress Series **260**:83-96.

Siegel, D. A., S. Mitarai, C. J. Costello, S. D. Gaines, B. E. Kendall, R. R. Warner, and K. B. Winters. 2008. The stochastic nature of larval connectivity among nearshore marine populations. Proceedings of the National Academy of Sciences (USA) **105**:8974-8979.

Sponaugle, S., R. K. Cowen, A. L. Shanks, S. G. Morgan, J. M. Leis, J. S. Pineda, G. W. Boehlert, M. J. Kingsford, K. C. Lindeman, C. Grimes, and J. L. Munro. 2002. Predicting self-recruitment in marine populations: Biophysical correlates and mechanisms. Bulletin Of Marine Science **70**:341-375.

Spydell, M., F. Feddersen, and R. Guza. 2009. Observations of drifter dispersion in the

surfzone: The effect of sheared alongshore currents. Journal of Geophysical Research **114**:1-17.

Stommel, H. 1949. Horizontal diffusion due to oceanic turbulence. Journal of Marine Research **8**:199-225.

Swearer, S., J. S. Shima, M. Hellberg, S. Thorrold, G. Jones, D. Robertson, S. Morgan, K. Selkoe, G. Ruiz, and R. Warner. 2002. Evidence of self-recruitment in demersal marine populations. Bulletin Of Marine Science **70**:251-271.

Swearer, S. E., J. Caselle, D. W. Lea, and R. R. Warner. 1999. Larval retention and recruitment in an island population of a coral-reef fish. Nature **402**:799-802.

Thorrold, S., D. C. Zacherl, and L. A. Levin. 2007. Population connectivity and larval dispersal using geochemical signatures in calcified structures. Oceanography **20**:80-89.

Thorson, G. 1946. Reproduction and larval development of Danish marine bottom invertebrates. Meddelelser fra Kommissionen for Hovundersoegelser Serie Plankton **4**:1-523.

Watson, J., S. Mitarai, D. A. Siegel, J. Caselle, C. Dong, and J. Mcwilliams. 2010. Realized and potential larval connectivity in the Southern California Bight. Marine Ecology Progress Series **401**:31-48.

Weersing, K. and R. Toonen. 2009. Population genetics, larval dispersal, and connectivity in marine systems. Marine Ecology Progress Series **393**:1-12.

Werner, F. E., R. K. Cowen, and C. B. Paris. 2007. Coupled biological and physical

models: Present capabilities and necessary developments for future studies of population connectivity. Oceanography **20**:54-69.

White, J., L. W. Botsford, A. Hastings, and J. L. Largier. 2010. Population persistence in marine reserve networks: incorporating spatial heterogeneities in larval dispersal. Marine Ecology Progress Series **398**:49-67.

White, J. W., K. J. Nickols, L. Clarke, and J. L. Largier. 2010. Larval entrainment in cooling water intakes: spatially explicit models reveal effects on benthic metapopulations and shortcomings of traditional assessments. Canadian Journal of Fisheries and Aquatic Sciences **67**:2014-2031.

Wiberg, P. L., D. E. Drake, and D. A. Cacchione. 1994. Sediment resuspension and bed armoring during high bottom stress events on the Northern California inner continental shelf: measurements and predictions. Continental Shelf Research **14**:1191-1219.

Winant, C. D. and C. E. Dorman. 1997. Seasonal patterns of surface wind stress and heat flux over the Southern California Bight. Journal of Geophysical Research **102**:5641-5653.

Wing, S., J. Largier, L. Botsford, and J. Quinn. 1995. Settlement and transport of benthic invertebrates in an intermittent upwelling region. Limnology and Oceanography **40**:316-329.

Wolanski, E. 1992. Hydrodynamics of mangrove swamps and their coastal waters Hydrobiologia **247**:141-161.

Site	Slope	Orientation	Deployment start date	Deployment end date	Analysis start date	Analysis end date
Terrace Point	0.023	286°	1 Jul 2008	23 Jul 2008	3 Jul 2008	10 Jul 2008
Hopkins	0.044	142°	29 May 2008	19 Jun 2008	29 May 2008	5 Jun 2008
Pajaro	0.011	344°	30 Aug 2007	23 Oct 2007	31 Aug 2007	7 Sep 2007
Mohawk	0.033	278°	8 Jun 2007	14 Jun 2007	9 Jun 2007	14 Jun 2007
Huntington Beach	0.006	301°	19 Jul 2001	12 Oct 2001	19 Jul 2001	26 Jul 2001

Table 1.1. Shoreline characteristics, deployment timelines, and analysis time periods for all sites. Slope is measured as depth increment per horizontal distance traversed. Orientation is measured as compass heading (degrees clockwise from North).

Symbol	SI Unit	Definition
a	-	Coefficient of horizontal eddy viscosity profile
b	-	Intercept from regression of the natural logarithm of distance from shore against alongshore velocity
c	-	Slope from regression of depth-averaged velocity to bottom velocity
C_D	-	Neutral drag coefficient
d	-	Exponent of horizontal eddy viscosity profile
D	N m^{-2}	Integration constant in lateral stress profile equation
h	m	Water depth
K_y	m^2 s^{-1}	Horizontal eddy viscosity
K_z	m^2 s^{-1}	Vertical eddy viscosity
m	-	Slope from regression of the natural logarithm of distance from shore against alongshore velocity
P	N m^{-2}	Pressure
r	m s^{-1}	Linear drag coefficient
u	m s^{-1}	Depth-specific alongshore velocity
U	m s^{-1}	Depth-averaged alongshore velocity
u_*	m s^{-1}	Friction velocity based on bottom shear
U_{*CBL}	m s^{-1}	CBL-scale friction velocity
u'	m s^{-1}	Depth-averaged alongshore velocity residual
U_{calc}	m s^{-1}	Depth-averaged alongshore velocity calculated from vertical integration of the law of the wall
u_w	m s^{-1}	Alongshore wind velocity
V	m s^{-1}	Depth-averaged cross-shore velocity
v'	m s^{-1}	Depth-averaged cross-shore velocity residual
x	m	Alongshore position
y	m	Distance from shore (cross-shore position)
y_0	m	CBL-scale horizontal roughness parameter
z	m	Vertical distance from seafloor
z_0	m	Vertical roughness height
α	-	Bathymetric slope
κ	-	von Karman's constant
ρ	kg m^{-3}	Mass density of fluid
τ_0	N m^{-2}	Wall shear stress (bottom stress)
τ_b	N m^{-2}	Bottom stress
τ_{lat}	N m^{-2}	Lateral stress
τ_s	N m^{-2}	Surface wind stress

Table 1.2. List of symbols used in Chapter 1.

Site	Distance (depth)	Mean		STD		Site	Distance (depth)	Mean		STD	
		U	*V*	*U*	*V*			*U*	*V*	*U*	*V*
Mohawk	215 (7)	0.0295	0.0019	0.0084	0.0042	Hopkins	195 (10)	0.0012	0.0089	0.0036	0.0033
Mohawk	325 (11)	0.0737	0.0068	0.0351	0.0021	Hopkins	340 (15)	0.0062	0.0038	0.0072	0.0018
Mohawk	475 (15)	0.1053	0.005	0.0233	0.0038	Hopkins	415 (20)	0.0145	0.0017	0.0162	0.0029
Mohawk	610 (20)	0.1260	0.0087	0.0265	0.0037	Hopkins	470 (23)	0.0301	0.0026	0.0234	0.004
Pajaro	325 (5)	0.0163	0.0130	0.0234	0.0068	Hopkins	570 (25)	0.0427	0.0016	0.0308	0.0056
Pajaro	385 (7)	0.0220	0.0081	0.0453	0.0053	Terrace Point	300 (10)	0.0133	0.0029	0.0047	0.0058
Pajaro	540 (10)	0.0565	0.0017	0.0152	0.0027	Terrace Point	560 (15)	0.0489	0.0007	0.0167	0.0028
Pajaro	1870 (20)	0.0774	0.0020	0.0282	0.0052	Terrace Point	910 (18)	0.0782	0.0016	0.0326	0.0060
Huntington Beach	835 (10)	0.0332	0.0037	0.0305	0.0036	Terrace Point	930 (22)	0.0791	0.0005	0.0318	0.0051
Huntington Beach	1755 (15)	0.0847	0.0047	0.0615	0.0073	Terrace Point	1100 (25)	0.0745	0.0022	0.0358	0.0045
Huntington Beach	3605 (25)	0.1529	0.0118	0.0626	0.0151						
Huntington Beach	5790 (35)	0.1625	0.0329	0.0158	0.0195						

Table 1.3. Means and standard deviations of depth-averaged alongshore (*U*) and cross-shore (*V*) velocity magnitudes recorded over a one-week period. Units are in m s^{-1}. Stations within a site are listed by distance from shore and depth in m.

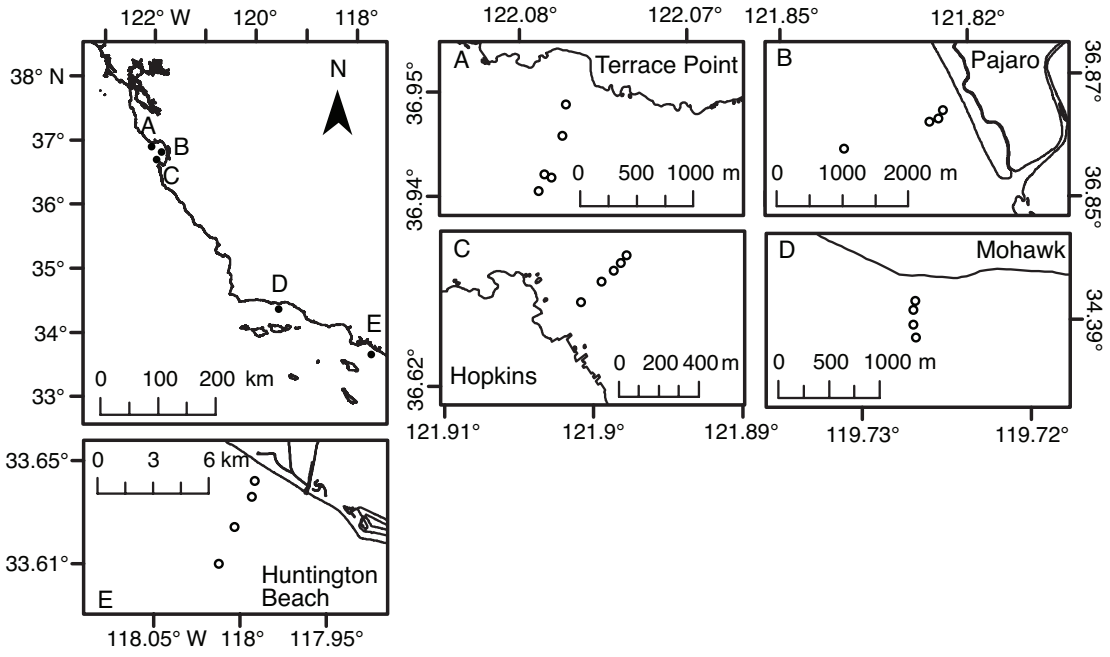

Figure 1.1. Study area (top left) and individual site maps (A-E). Open circles in A-E indicate instrument locations.

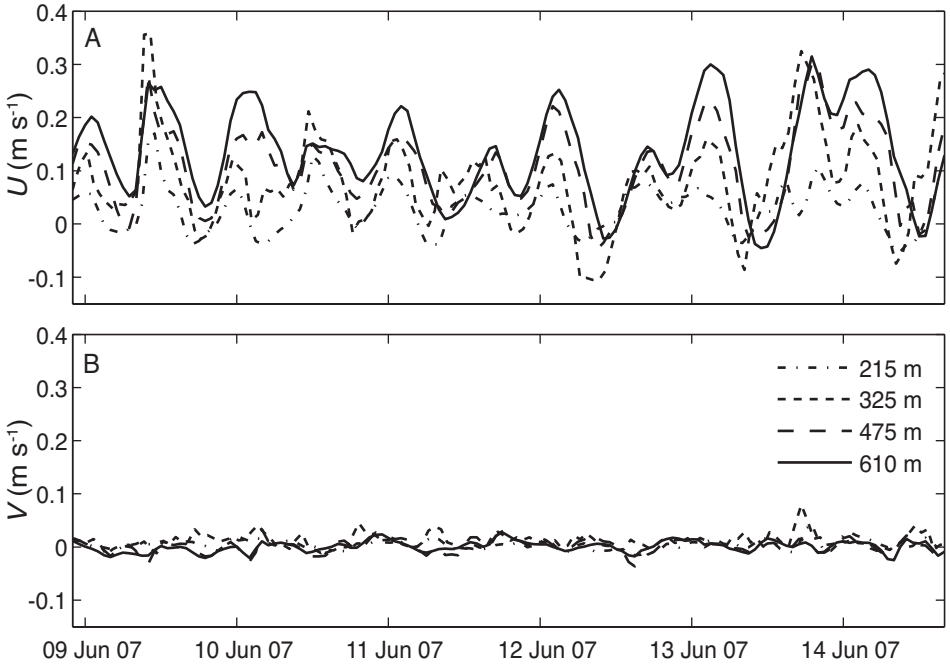

Figure 1.2. Unfiltered time series of depth-averaged (A) alongshore, *U*, and (B) cross-shore, *V*, velocity recorded at Mohawk, at several distances from shore. Patterns of polarized flow in the alongshore direction and decreased velocity magnitude and oscillation with decreased distance from shore were common amongst sites.

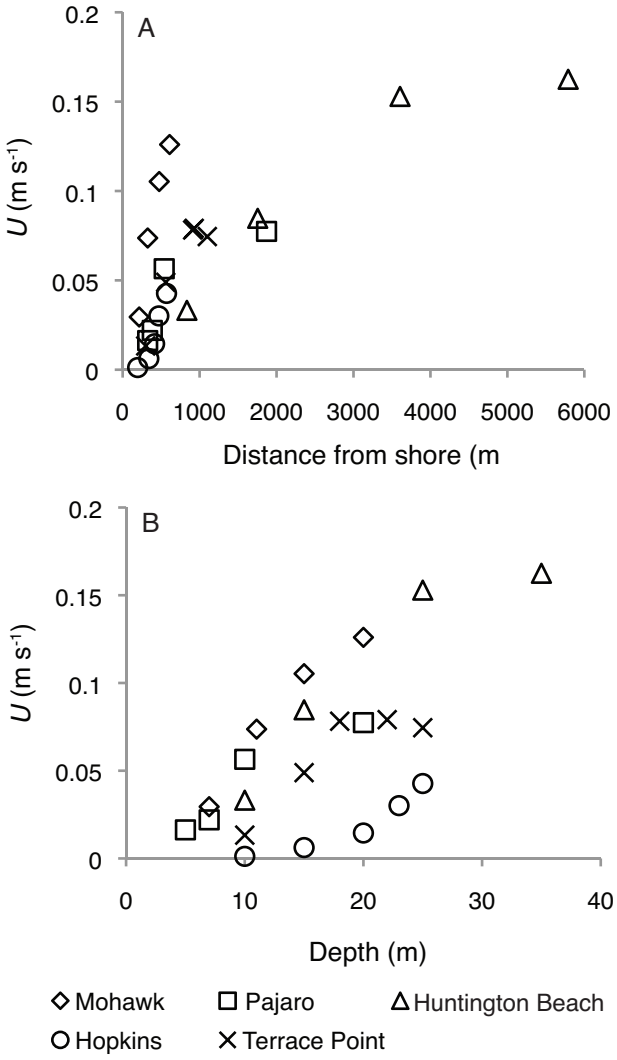

Figure 1.3. Week- and depth-averaged alongshore velocity, *U*, for all sites plotted against (A) distance from shore, and (B) depth.

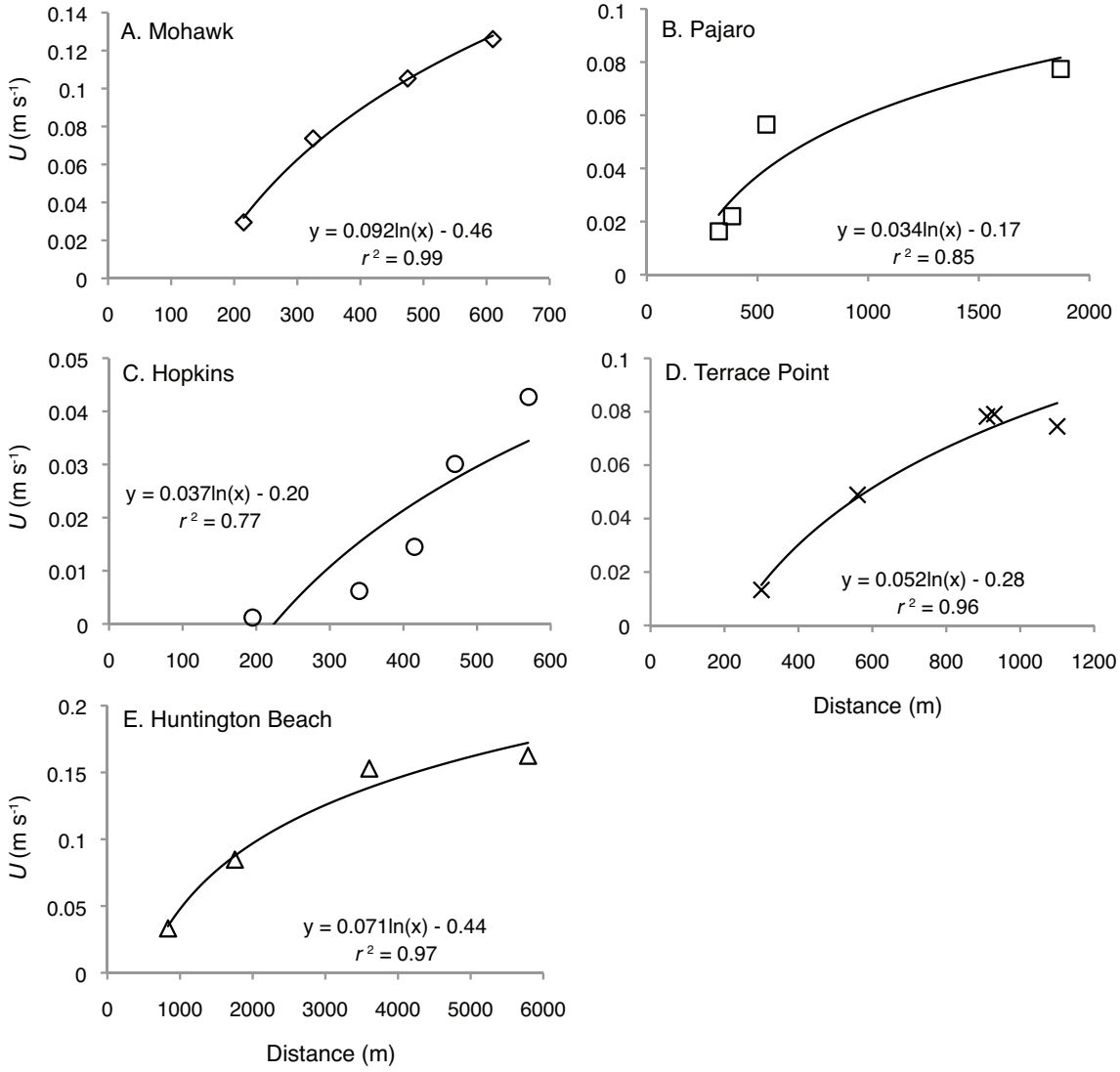

Figure 1.4. Depth- and time-averaged alongshore velocity profiles for each site (A-E) as a function of distance from shore. Solid lines show the associated best-fit logarithmic relationships for each site.

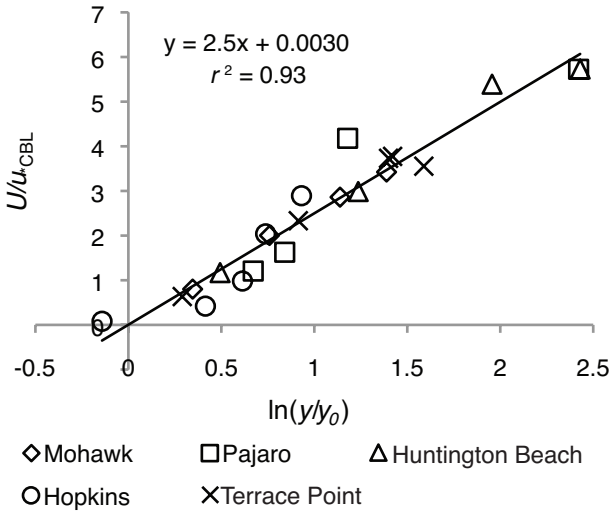

Figure 1.5. The law of the wall applied to coastal boundary layers. Note the collapse of all data to a single straight relationship when graphed as a semi-log plot. On the abscissa, distance from shore y is normalized by a CBL-scale horizontal roughness parameter, y_0. On the ordinate, depth-averaged alongshore velocity, U, is normalized by a CBL-scale friction velocity, U_{*CBL}. These two parameters were determined using Eq. 1.2.

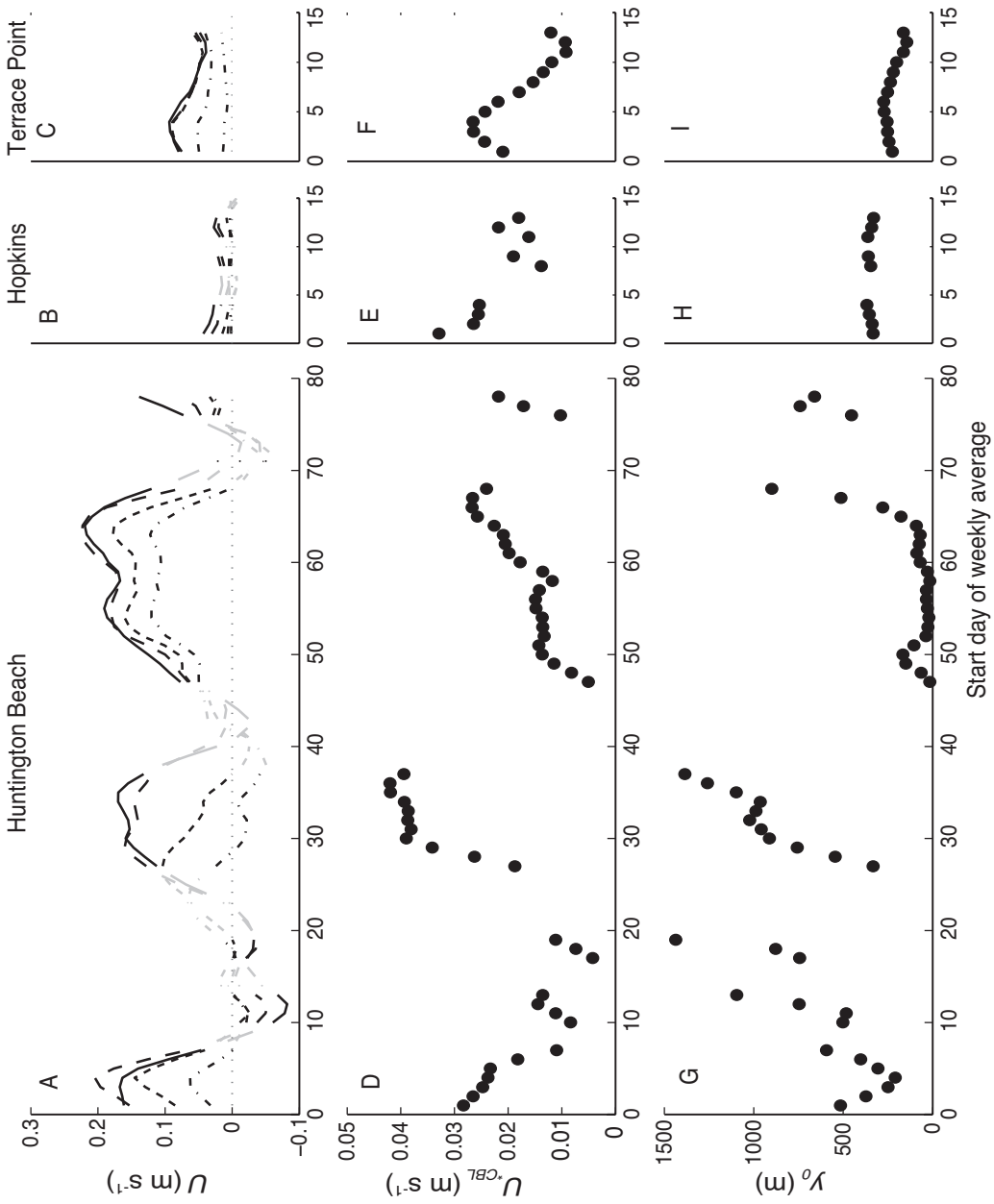
Huntington Beach
Hopkins
Terrace Point
A
B
C
D
E
F
G
H
I
U (m s-1)
U*CBL (m s-1)
y0 (m)
Start day of weekly average

Figure 1.6. Week-long means of depth-averaged alongshore velocity, U, at each cross-shore station for (A) Huntington Beach, (B) Hopkins, and (C) Terrace Point with corresponding values for U_{*CBL} (D-F) and y_0 (G-I) calculated from logarithmic cross-shore profiles. Successive estimates of the weeklong mean are advanced in one-day steps, and individual points are removed in A-C for clarity. Offshore stations in the upper panels are solid, and dashed lines of decreasing dash-length indicate increasingly inshore stations; gray values indicate periods when the cross-shore velocity profiles were not logarithmic. Zero velocity in A-C is indicated for reference using a dotted line.

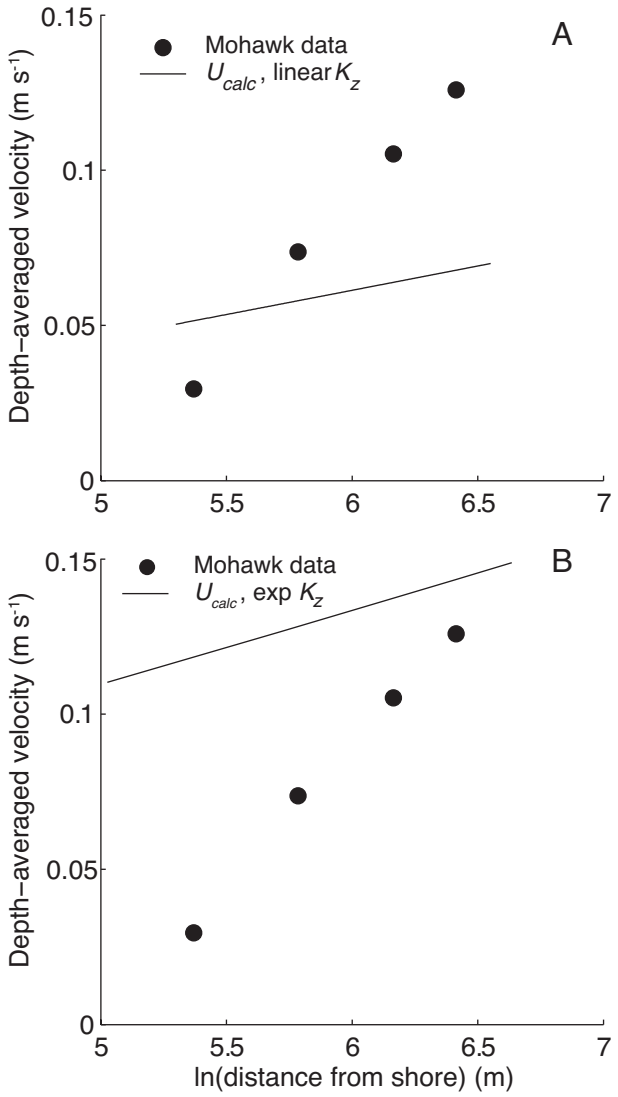

Figure 1.7. Mismatch between field-measured, depth-averaged velocity (U, solid circles) and modeled depth-averaged velocity based on a simple vertical integration of a benthic boundary layer. (A) Mismatch resulting from the use of realistic values of u_* and z_0 to compute U_{calc} assuming a linear vertical eddy viscosity profile (solid line). (B) Mismatch present after incorporating an exponential vertical eddy viscosity profile (solid line). Results are for Mohawk, but are consistent across sites.

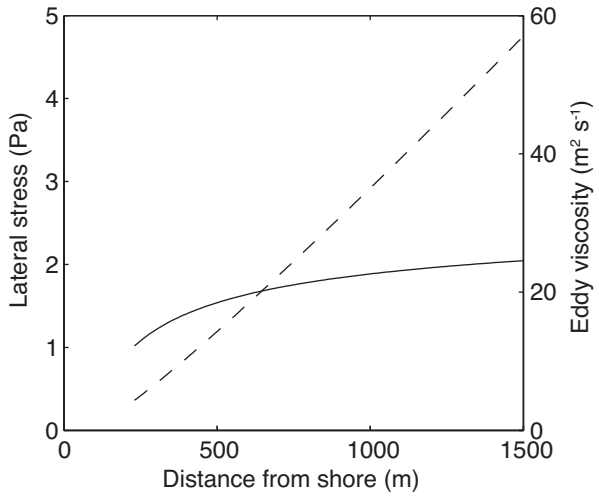

Figure 1.8. Profiles of lateral stress (left axis; solid line) and eddy viscosity (right axis; dashed line) as a function of distance from shore at Terrace Point based on a rudimentary scaling analysis from the alongshore momentum balance in the CBL.

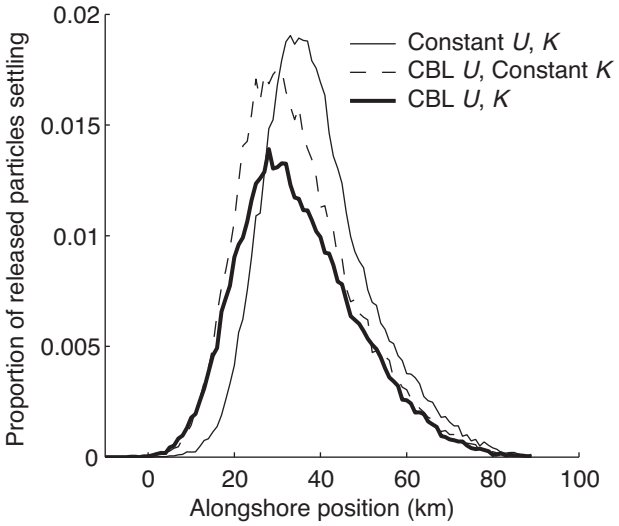

Figure 1.9. Dispersal kernels generated from a 2-dimensional random walk model with different assumptions about the existence and/or properties of the CBL. Case 1 (solid light line) incorporates a constant alongshore velocity, U, (0.075 m s^{-1}) and a constant horizontal eddy diffusivity, K_y, (40 m^2 s^{-1}). Case 2 (dashed line) incorporates a logarithmic velocity profile similar to that at Terrace Point but retains the constant eddy diffusivity. Case 3 (solid dark line) incorporates a full CBL, with both a logarithmic velocity gradient and linearly increasing eddy diffusivity, using parameter values similar to those observed at Terrace Point. Lines are fits through histograms partitioned into 1 km bins.

APPENDIX A1

Depth-averaged velocity derivation via the "law of the wall"

The depth-averaged velocity, U_{calc}, at a cross-shore location, y, is equal to the integral of velocity via the law of the wall (Eq. 1.1), divided by depth, h:

$$U_{calc}(y) = \frac{1}{h}\int_{z_0}^{h} \frac{u_*}{\kappa}\ln\left(\frac{z}{z_0}\right)dz \tag{A1.1}$$

This equation is rearranged to consider depth-averaged velocity as a function of distance from shore, rather than depth, by setting $h = y\tan\alpha$:

$$U_{calc}(y) = \frac{1}{y\tan\alpha}\int_{z_0}^{y\tan\alpha} \frac{u_*}{\kappa}\ln\left(\frac{z}{z_0}\right)dz \tag{A1.2}$$

where α is the bathymetric slope.

Separating the quantity $\ln\left(\frac{z}{z_0}\right)$ yields:

$$U_{calc}(y) = \frac{1}{y\tan\alpha}\int_{z_0}^{y\tan\alpha} \frac{u_*}{\kappa}\ln z\,dz \quad - \quad \frac{1}{y\tan\alpha}\int_{z_0}^{y\tan\alpha} \frac{u_*}{\kappa}\ln z_0\,dz \tag{A1.3}$$

$$U_{calc}(y) = \frac{u_*}{\kappa y\tan\alpha}\left(\int_{z_0}^{y\tan\alpha} \ln z\,dz \quad - \quad \int_{z_0}^{y\tan\alpha} \ln z_0\,dz\right) \tag{A1.4}$$

Integrating leads to:

$$U_{calc}(y) = \frac{u_*}{\kappa y\tan\alpha}\left(z\ln z - z\Big|_{z_0}^{y\tan\alpha} \quad - \quad z\ln z_0\Big|_{z_0}^{y\tan\alpha}\right) \tag{A1.5}$$

$$U_{calc}(y) = \frac{u_*}{\kappa y\tan\alpha}\left[\left(y\tan\alpha\left[\ln y\tan\alpha\right] - y\tan\alpha - \left[z_0\ln z_0 - z_0\right]\right) - \left(y\tan\alpha\ln z_0 - z_0\ln z_0\right)\right] \tag{A1.6}$$

$$U_{calc}(y) = \frac{u_*}{\kappa y \tan\alpha}\left[y\tan\alpha(\ln y\tan\alpha - 1) - z_0 \ln z_0 + z_0 - y\tan\alpha \ln z_0 + z_0 \ln z_0\right] \quad \text{(A1.7)}$$

$$U_{calc}(y) = \frac{u_*}{\kappa y \tan\alpha}\left[y\tan\alpha(\ln y\tan\alpha - 1 - \ln z_0)\right] + \frac{u_* z_0}{\kappa y \tan\alpha} \quad \text{(A1.8)}$$

$$U_{calc}(y) = \frac{u_*}{\kappa}(\ln y\tan\alpha - \ln z_0 - 1) + \frac{u_* z_0}{\kappa y \tan\alpha} \quad \text{(A1.9)}$$

$$U_{calc}(y) = \frac{u_*}{\kappa}\left[\ln\left(\frac{y\tan\alpha}{z_0}\right) - 1\right] + \frac{u_* z_0}{\kappa y \tan\alpha} \quad \text{(A1.10)}$$

APPENDIX B1

Solution for lateral stress and eddy viscosity profiles from an alongshore momentum balance

The alongshore momentum balance within the coastal boundary layer is represented by the sum of the alongshore pressure gradient ($\frac{\partial P}{\partial x}$), surface wind stress ($\tau_s$), bottom stress ($\tau_b$), and lateral stress divergence ($\frac{\partial \overline{u'v'}}{\partial y}$), with h = depth, y = cross-shore distance, and ρ is density:

$$\frac{1}{\rho}\frac{\partial P}{\partial x} + \frac{\tau_s}{\rho h} + \frac{\tau_b}{\rho h} + \frac{\partial \overline{u'v'}}{\partial y} = 0 \tag{B1.1}$$

Solving for the lateral stress divergence yields:

$$-\frac{\partial \overline{u'v'}}{\partial y} = \frac{1}{\rho}\frac{\partial P}{\partial x} + \frac{\tau_s}{\rho h} + \frac{\tau_b}{\rho h} \tag{B1.2}$$

This equation is rearranged to consider stress divergence as a function of distance from shore, rather than depth, by setting $h = y \tan\alpha$:

$$-\frac{\partial \overline{u'v'}}{\partial y} = \frac{1}{\rho}\frac{\partial P}{\partial x} + \frac{\tau_s}{\rho y \tan\alpha} + \frac{\tau_b}{\rho y \tan\alpha} \tag{B1.3}$$

where α is the bathymetric slope.

Multiplying both sides of Eq. B1.3 by ρ gives:

$$-\frac{\partial \rho\overline{u'v'}}{\partial y} = \frac{\partial P}{\partial x} + \frac{\tau_s}{y \tan\alpha} + \frac{\tau_b}{y \tan\alpha} \tag{B1.4}$$

Lateral stress, τ_{lat}, is equal to $-\rho\overline{u'v'}$:

$$\frac{\partial \tau_{lat}}{\partial y} = \frac{\partial P}{\partial x} + \frac{\tau_s}{y \tan\alpha} + \frac{\tau_b}{y \tan\alpha} \tag{B1.5}$$

Bottom stress is estimated following a linear drag law:

$$\tau_b = \rho r c U \tag{B1.6}$$

where r is a linear drag coefficient, U is depth-averaged velocity, and c is a conversion factor between depth-averaged and bottom velocity, determined from a linear regression of depth-averaged velocity against bottom velocity from velocity records.

In the coastal boundary layer, velocity increases logarithmically with distance from shore:

$$\frac{U(y)}{U_{*CBL}} = \frac{1}{\kappa}\ln\left(\frac{y}{y_0}\right) \tag{B1.7}$$

Substituting Eq. B1.7 into Eq. B1.6 yields:

$$\tau_b(y) = \rho r c \frac{U_{*CBL}}{\kappa}\ln\left(\frac{y}{y_{0CBL}}\right) \tag{B1.8}$$

Eq. B1.5 then becomes:

$$\frac{\partial \tau_{lat}}{\partial y} = \frac{\partial P}{\partial x} + \frac{\tau_s}{y\tan\alpha} + \frac{\rho r c U_{*CBL}}{\kappa y \tan\alpha}\ln\left(\frac{y}{y_{0CBL}}\right) \tag{B1.9}$$

The alongshore pressure gradient and wind stress remain constant with distance from shore.

Integrating Eq. B1.9 gives the function for lateral stress as a function of distance from shore:

$$\tau_{lat}(y) = \frac{\partial P}{\partial x}y + \frac{\tau_s \ln y}{\tan\alpha} + \frac{\rho r c U_{*CBL}}{2\kappa\tan\alpha}\left[\ln\left(\frac{y}{y_{0CBL}}\right)\right]^2 + D \tag{B1.10}$$

where D is an integration constant.

Lateral stress is related to eddy viscosity, K_y, by the following expression:

$$\tau_{lat} = \rho K_y \frac{dU}{dy} \tag{B1.11}$$

Rearranging to solve for K_y yields:

$$K_y = \frac{\tau_{lat}}{\rho}\left(\frac{dU}{dy}\right)^{-1} \tag{B1.12}$$

The velocity gradient, $\frac{dU}{dy}$, is equal to the derivative of the depth-averaged velocity profile, Eq. B1.7.

$$\frac{dU}{dy} = \frac{U_{*CBL}}{\kappa}\frac{1}{y} \tag{B1.13}$$

Substituting Eqs. B1.10 and B1.13 into Eq. B1.12 gives the function for eddy viscosity as a function of distance from shore:

$$K_y(y) = \frac{\kappa}{\rho U_{*CBL}} y\left[\frac{\partial P}{\partial x} y + \frac{\tau_s}{\tan\alpha}\ln y + \frac{\rho r U_{*CBL} c}{2\kappa \tan\alpha}(\ln\frac{y}{y_{0CBL}})^2 + D\right] \tag{B1.14}$$

CHAPTER 2

Importance of nearshore oceanography for larval dispersal and self-replenishment of coastal populations[*]

[*] Co-authors J.Wilson White, Brian Gaylord, and John L. Largier

ABSTRACT

Dispersal is a critical process in metapopulation dynamics. For systems in which physical processes heavily influence dispersal, such as through fluid motion, an understanding of the underlying physics is crucial to predictions of dispersal and population dynamics. In marine systems, population models are often underpinned by simple representations of ocean currents that allow focused studies on processes driving dynamics. However, as our knowledge of flow fields has developed, it may be time to revise our representations. The coastal boundary layer (CBL) is a region of lowered velocities near the shoreline that is prevalent across time and space and may alter predictions of dispersal in marine environments. We incorporated parameterizations of the CBL into a Lagrangian particle-tracking model to explore the potential importance of the CBL on mean and long distance dispersal, the shape of dispersal kernels, and self-retention across sites and life histories. Incorporating CBLs decreased mean dispersal distances up to 56% and was most profound for low pelagic larval durations (PLDs) and gentle bathymetric slopes associated with broader CBLs, where time spent in the CBL is comparable with the PLD. Maximum dispersal distances were also reduced by up to 30%. The presence of a CBL increased self-retention by three orders of magnitude, and led to measurable amounts of self-retention for sites and PLDs that were immeasurable under a uniform flow field. This work further demonstrates that successfully settling larvae are typically those that remain close to shore, and that ignoring the reduced velocities in CBLs may overestimate population connectivity. The CBL is a more detailed, yet still generalizable, representation of fluid motion that affects dispersal and population dynamics.

INTRODUCTION

For populations distributed among discrete habitat patches, dispersal is critical to connectivity of patches and metapopulation dynamics (Levin 1974, Roughgarden and Iwasa 1986, Hanski and Gilpin 1991). The representation of these dynamics is essential to predictions of species' responses to habitat destruction, extraction, and climate change, which has led to increased interest in spatially explicit population models (Hanski 1998, Sale et al. 2006). In systems where dispersal is primarily driven by fluid motion (e.g., wind [Greene and Johnson 1989, Vanschoenwinkel et al. 2008], rivers [Fonseca and Hart 2001, Pachepsky et al. 2005], and ocean currents [Scheltema 1986, Botsford et al. 1994]) dispersal can be affected more by physical forcing than behavior. For benthic marine organisms, dispersal is often obligate, as the larval phase is pelagic and requires entry into the water column, where many or perhaps most larvae are swept away from their natal site. Predicting metapopulation dynamics therefore requires an understanding of fluid dynamics, especially as inclusion of details of fluid motion – such as asymmetric dispersal patterns – in metapopulation models can lead to drastic changes in predictions of persistence and connectivity (Bode et al. 2008, Vuilleumier et al. 2010, White et al. 2010b).

The question is, how complex does the representation of fluid motion need to be to accurately predict dispersal relevant to metapopulation dynamics? All models must strike a balance between complexity and generality (Levins 1966, Caswell 1988). The problem of how many parameters and how much detail to include is a ubiquitous issue for ecological modelers. Complex models can produce results that are difficult to interpret, while more general models may be unrealistic (Van Nes and Scheffer 2005). In

the realm of seed dispersal, models range from phenomenological to mechanistic with a range of complexity in the representation of fluid (wind) dynamics (reviewed in Levin et al. 2003, Nathan et al. 2005). Similarly, for marine metapopulation models, the model continuum has generally extended from generic, strategic models with two-parameter flow (discussed below, e.g., Roughgarden et al. 1988, Kaplan 2006) to tactical, location-specific models with highly detailed flow representations (e.g., based on the Regional Ocean Modeling System: Cowen et al. 2006, Watson et al. 2010). While the tactical models offer realism lacking in strategic models, they are restricted by spatial resolution and results apply only to the modeled region (Watson et al. 2010, Drake et al. 2011). For most strategic models, an accurate representation of circulation was not the primary goal, and the intent was to capture key elements of fluid motion with as few parameters as possible in order to understand population dynamics. However, different scales of population dynamics may be associated with different parameters. For example, mechanistic models of seed dispersal parameterized by the mean and variance of wind velocity capture mean dispersal distance (Greene and Johnson 1989, Okubo and Levin 1989) but fail to capture long distance dispersal characterized by more complex fluid dynamics (Bullock and Clarke 2000, Katul et al. 2005).

Prior studies exploring how fluid flow should affect population dynamics in coastal marine metapopulations have used models primarily rooted in a two-parameter framework that describes the fluid environment in terms of the mean and variance of flow (e.g., Largier 2003). The use of this simple framework has allowed for focused investigations on how persistence (Hill 1990, Possingham and Roughgarden 1990, Hill 1991, Gaylord and Gaines 2000, White et al. 2010b), invasion speed (Byers and Pringle

2006), and genetic connectivity (Siegel et al. 2003, Pringle and Wares 2007, White et al. 2010a) depend on characteristics of oceanographic currents. Those theoretical results have also underpinned conservation planning decisions, notably choices about the proper size and spacing of no-take marine reserves (Moffitt et al. 2011, Saarman et al. unpublished manuscript), and in estimates of the effects of climate change on larval dispersal (O'Connor et al. 2007).

Much of the theory fundamental to our understanding of marine population dynamics is based on the two-parameter model, but this approach may overlook important complexities in dispersal. Flow along a straight coastline may be well approximated by two parameters, however, more complicated flow features are common and accounting for them can substantially alter dispersal predictions. Gaylord and Gaines (2000) modeled coastal invertebrate populations under uniform flow conditions (i.e., a two-parameter approach), as well as with more complicated flow conditions including a recirculation zone, or eddy, and demonstrated that inclusion of an eddy promoted persistence of populations that were predicted to go extinct under uniform flow conditions. Similarly, White et al. (2010b) revealed that marine reserves containing retention zones were more likely to be self-persistent than reserves exposed to mean flow conditions. Retentive flows may be produced by topographic (i.e. headlands and bays) or offshore features and often occur in predictable locations. These special features may be incorporated into models without necessitating a highly detailed tactical approach. There may also be unaccounted flow features present across a range of locations and topographies not represented by the two-parameter approach that may change predictions of dispersal appreciably.

One potentially important feature not included in the two-parameter framework is the coastal boundary layer (CBL), located outside of the surf zone to a few kilometers offshore. As with any fluid boundary, net flow at the coastal margin is zero, with zero variability. However, there is strong, variable flow offshore. The CBL is the region of the coastal ocean where velocities (and variations in velocity) transition from zero near the shore to free-stream conditions found offshore. The CBL has just recently been quantified at several sites along the California coast (Lentz et al. 1999, Nickols et al. in revision). Within the CBL, average alongshore velocity is an order of magnitude larger than cross-shore velocity (Lentz et al. 1999, Gaylord et al. 2007), and alongshore velocity increases logarithmically to the offshore values as a function of distance from shore (Nickols et al. in revision). The concept of the CBL, with decreased velocity toward a boundary, is analogous to traditional boundary layers studied in smaller scale fluid mechanics (Schlicting 1979). With decreased velocities adjacent to the coast, the CBL is a potential mechanism for reducing scales of dispersal of populations that spawn near the shoreline (Nickols et al. in revision).

In order to successfully recruit to a population, dispersed propagules from intertidal and shallow subtidal habitats – regardless of how long they spend in the plankton – must return to suitable habitat close to shore, traversing the CBL. Studies of larval community composition and abundance indicate that the majority of larvae of both fish and invertebrates stay within 3 km from shore throughout their larval period (Borges et al. 2007, Morgan et al. 2009, Shanks and Shearman 2009), indicating that many larvae may never leave the CBL. Reduced velocities found within the CBL are therefore potentially important to dispersal, and a prominent feature in a larva's lifetime.

If larvae are able to remain within the slow-moving waters of the CBL, they could greatly reduce their dispersal distance. However, due to the historical locations of oceanographic instrumentation, most marine metapopulation models used estimates of flow and variability from further offshore. Many parameterizations of flow velocity in larval dispersal models were taken from observations from the 30 m isobath or more and did not include observations near the shore, within the CBL (Largier 2003, Siegel et al. 2003, Byers and Pringle 2006). The simplicity of two-parameter models with limited flow information is a strength, as is their ability to make predictions over different combinations of velocity mean and variance, particularly over large spatial scales (Roughgarden et al. 1988). However, if the mean and variance of the flow field used in models were not derived from locations where larvae are concentrated, we may not be adequately describing larval dispersal. The few models that have incorporated reductions in velocity nearshore have shown that the strength and structure of the alongshore flow field can substantially alter dispersal predictions, although the nearshore velocity structure of these models was not explicitly linked to observations (Possingham and Roughgarden 1990, White et al. 2010c).

We take a nondimensional scaling approach that affords a general and broadly applicable solution to this problem. We model the CBL explicitly based on recent measurements unusually close to shore (Nickols et al. in revision) that allow us to assess how the default assumption used in dispersal modeling of uniform velocity and variability (no CBL) compares to predictions based on observations made within the CBL. We address the following questions: 1) What effect does accounting for the CBL have on predictions of dispersal distance and retention? 2) How does the importance of

the CBL depend on life history (e.g., pelagic larval duration)? 3) Does the importance of the CBL to coastal populations vary among locations (e.g., due to the differences in the slope of the coastline or velocity profile)? By addressing these questions, we reveal under what conditions it can be important to account for extreme nearshore processes when representing the population dynamics of coastal organisms.

METHODS

Modeling approach: dispersal kernels

To link physical dispersal processes to their effects on population dynamics, many authors have relied on the calculation of dispersal kernels, probability density functions that describe the probability of settlement at discrete spatial locations for propagules released from a single point. Attributes of these kernels are important in determining how fluid dispersal affects marine populations, specifically descriptions of mean dispersal distance, long distance dispersal distance, and self-retention (Fig. 2.1). For models that include net advection, such as through coastal currents, the mean dispersal distance is usually defined as the average distance settling propagules travel away from their natal site, the mean displacement of the dispersal kernel (e.g., Kaplan 2006). Mean dispersal distance is particularly important for estimating population persistence and determining whether or not shoreline populations are connected (Kinlan and Gaines 2003, Kaplan et al. 2009). The potential for long distance dispersal can be quantified from the tails of the dispersal kernel, such as the number of settlers that disperse a certain distance from their natal site, and the distances which extreme dispersers travel. Metrics of long distance dispersal are used to estimate invasion speed (Lester et al. 2007) and genetic connectivity

(Kinlan and Gaines 2003). An additional piece of information gleaned from dispersal kernels is self-retention (or local retention e.g., Botsford et al. 2009), which describes the proportion of larvae released at a location that settle near the release location in a region of finite width. The degree of self-retention within a given population informs whether a population can be self-persistent, or if its persistence depends on propagule input from other populations (i.e., network persistence; Hastings and Botsford 2006)).

Particle simulation and dispersal kernel calculation

We modeled a benthic population that occupies habitat in nearshore, shallow, subtidal waters. We used a Lagrangian particle-tracking model to calculate the dispersal kernel, the probability of larval dispersal from release (spawning) to settlement at locations along a linear coastline of length 750 km, composed of identical cells extending 1 km alongshore. We released 10^4 propagules from within a single 1 km cell at randomly selected locations uniformly distributed between the 5 and 10 m isobaths. Propagules were transported through the coastal ocean during a specified precompetency window, representing the time period after release when most marine species are developmentally unable to settle. Once this window passed, propagules entered a competency window, during which propagules could settle if near suitable habitat. Precompetency windows were set equal to competency windows, as propagules spending longer times in the plankton tend to have longer competency windows (Jackson and Strathmann 1981). Propagules were counted as "settled" if they were found inshore of the 10 m isobath at any point during their competency window. This rule assumes that larvae close to shore would either immediately settle, continue towards the coastline, or swim towards

settlement habitat once inside the 10 m isobath. We simulated dispersal kernels for several different flow scenarios, detailed below, over a range of values for precompetency and competency windows: 2-20 d (2 d intervals), corresponding to pelagic larval durations (PLDs) of 3-30 d (3 d intervals). We did not include larval mortality in this model.

We simulated propagule transport with a 2-dimensional Lagrangian random-walk particle-tracking model. This approach was chosen over the random flight approach of Siegel et al. (2003) due to the nature of the CBL. The random flight model includes a parameter – the decorrelation time scale – that describes the time scale after which propagule movements are independent of each other. Because we do not know how this parameter might change with distance from shore, we opted for a random walk approach, the details of which are provided in White et al. (2010c). At each model time step (Δt = 30 s; see Table 2.1 for list of symbols used in paper) particle positions were updated according to advective and diffusive displacements. Deviations from White et al,'s (2010c) modeling approach arise in the alongshore velocity and diffusivity profiles, which here were parameterized from measurements of alongshore velocity within the CBL at five sites along the California coast (Nickols et al. in revision). At all sites, alongshore velocity decreased logarithmically toward shore, following the expression:

$$\frac{U(y)}{U_{*CBL}} = \frac{1}{\kappa}\ln\left(\frac{y}{y_0}\right) \tag{2.1}$$

where κ is von Karman's constant, set to 0.4 (Schlicting 1979), U is the depth- and time-averaged alongshore component of velocity, y is distance from shore, and U_{*CBL} and y_0 represent CBL-scale friction velocity and roughness parameters, respectively. These latter two parameters were calculated for each site from the slope (m) and intercept (b) of

the linear regression of depth- and time-averaged alongshore velocity (U) versus the natural logarithm of distance from shore (y):

$$U_{*CBL} = \kappa m$$
$$y_0 = e^{\left(\frac{-b}{m}\right)} \quad (2.2)$$

This approach is analogous to traditional fluid mechanical boundary layers (e.g., Schlicting 1979). Velocity profiles from all five sites approximate a logarithmic pattern, revealing a remarkably general relationship between alongshore velocity and cross-shore distance (Fig. 2.2A). Velocity in the cross-shore direction, V, was assumed to be zero, as coastal velocity measurements were polarized in the alongshore direction and approached zero in the cross-shore direction over the time periods we were interested in, days to weeks (Nickols et al. in revision).

We approximated horizontal turbulent mixing using eddy diffusivity (Taylor 1922, Okubo 1971). We assumed that eddy diffusivity, K, increased linearly with distance from shore due to the effects of the CBL (Nickols et al. in revision):

$$K = \kappa U_{*CBL} L \quad (2.3)$$

(Fig. 2.2B). Here, L is a length scale, equal to x in the alongshore dimension, and y in the cross-shore dimension, with isotropic mixing in the cross- and along-shore directions (similar to the isotropic assumption used by Okubo 1971). Owing to its derivation from the slope of the regression between distance and alongshore velocity, the parameter U_{*CBL} is related to the velocity gradient at a given site. Together, the profiles of U and K at each of the sites provided 5 different physical settings with which to test the effects of the CBL on dispersal.

Field measurements from which these profiles were derived did not extend far enough in the cross-shore dimension to determine the offshore edge of the CBL. Previous studies indicate that the edge of the CBL, within which the shore and bottom friction influence flow, is generally near the 30 m isobath (Murthy and Csanady 1981, Rao and Murthy 2001). Therefore, we extended our alongshore velocity profiles to the 30 m isobath, at which point velocities were assumed to have reached free-stream values; offshore of this point velocity and diffusivity remained constant. For our 5 sites the 30 m isobath corresponded to 700-5555 m from shore, depending on the bathymetric slope of each site, with U between 0.0419 and 0.169 m s^{-1} and K between 4.13 and 63 m^2 s^{-1} (Table 2.2). These values of K are consistent with other published values of K near the 30 m isobath in coastal California, which range from 10-60 m^2 s^{-1} (Davis 1985, List et al. 1990, Drake and Edwards 2009). The inshore edge of the CBL is equal to y_0, the CBL-scale roughness parameter, and $U = 0$ for $y < y_0$. One may interpret y_0 as the cross-shore scale of the wave-dominated surf zone. Although alongshore velocities may be quite rapid within the surf zone, they may also be in the opposite direction of the mean alongshore flow within the CBL, which would potentially reduce dispersal distances of waterborne materials and enhance retention (K.J. Nickols and J.L. Largier unpublished data). Although $U = 0$ at $y = y_0$, diffusivity profiles extend to the coastal wall with $K = 0$ at $y = 0$ following Eq. 2.2.

Model analysis

Dispersal models used to quantify population dynamics in coastal marine systems following the two-parameter approach must choose a value for velocity representative of

the coastal ocean. These choices are often based on velocity measurements from current meters (e.g., Gaines et al. 2003, Largier 2003). Due to operational constraints, these instruments are generally found on or near the 30 m isobath, coinciding with the estimated offshore edge of the CBL. Therefore, our null dispersal model without a CBL contains a uniform flow field parameterized by the velocity and diffusivity found at the offshore end of the CBL, on the 30 m isobath. We compare the kernels from the null model with those resulting from a model that includes the CBL, with attenuated alongshore velocities and diffusivities inshore of the 30 m isobath.

For each model case we calculated the mean alongshore dispersal distance (the alongshore distance from point of origin of the larval particles to the center of the settlement distribution), the 95th percentile alongshore dispersal distance (the alongshore distance below which 95% of particles settle), the standard deviation of the dispersal kernel, and self-retention (the proportion of released particles that settle within 10 km of the release point). To further explore the relationship between site-specific characteristics of the CBL and dispersal outcomes, we compared these spatial statistics to the temporal scale of the CBL through a scaling analysis. We were primarily interested in the consequences of not including a CBL in a model flow field when making predictions about nearshore dispersal. We interpreted these results in terms of two time scales: the pelagic larval duration, T_{PLD}, and the timescale of the CBL, T_{CBL}. By definition, eddy diffusivity, K, is proportional to L^2/t, where L is a length scale and t is time (Largier 2003). Thus the time scale associated with a given diffusivity is proportional to L^2/K. We used that relationship to define a lower bound on the time scale of residence in the CBL, based on the maximum value of K at the offshore edge of the CBL, K_{max}:

$$T_{CBL} = \frac{L_{CBL}^2}{K_{\max}} \quad (2.4)$$

where L_{CBL} is the width of the CBL. The time scale of the CBL is a conservative estimate of the time scale for diffusive loss of larvae from the CBL. Since cross-shore velocity is set to zero in this model, all cross-shore displacements result from turbulent diffusion; T_{CBL} then represents the lower bound on the average time it takes to diffuse through the CBL.

Given that T_{CBL} is based on $K_{\max}$, a flow field that includes a CBL would increase the actual time larvae spend in the CBL, as lower diffusivities found nearshore would increase the duration of time spent in the CBL. This discrepancy should matter most when the time a larva spends in the plankton is comparable to the time spent in the CBL. For larvae with $T_{PLD} >> T_{CBL}$ the time of development within the CBL is a small fraction of the total time spent in the plankton, and inclusion of a CBL in the model will likely only affect a small fraction of the dispersal trajectory. For the case where $T_{PLD} < T_{CBL}$, lower velocities and diffusivities found nearshore will be prevalent throughout the larval lifespan. The ratio of T_{PLD} to T_{CBL} is a metric that compares the pelagic larval duration to the lower bound on the average time it would take for a larva to diffuse cross-shore through the CBL.

RESULTS

Dispersal trajectories and kernels

Model larvae subjected to a flow field with a CBL spent more time nearshore than larvae dispersing in a flow field lacking a CBL. This effect was evident for all sites regardless of the width of the CBL (Fig. 2.3). Larvae in both flow scenarios were

advected downstream from the release location; however, lower velocities near the coast with a CBL decreased transport of larvae away from their release location. These larvae also experienced lower cross-shore diffusive impulses, requiring more time for larvae to spread in either the cross- or along-shore direction than required under higher diffusivities. Therefore, it took larvae in a flow field with a CBL longer to 'escape' past the 30 m isobath, than those larvae in a flow field with constant velocity and diffusivity (Fig. 2.3).

On average, larvae dispersed shorter distances from their release site in the model case with a CBL. Dispersal kernels were centered closer to the release location when flow fields included CBLs (Fig. 2.4). These kernels were also broader, with a higher standard deviation than kernels resulting from model runs without a CBL, which were narrow and with less spread. Kernels resulting from either model scenario were non-Gaussian (Fig. 2.4, see Gaussian distribution with same mean and standard deviation as the no-CBL kernel). Peaks in the kernels, particularly for the no-CBL case, resulted from the precompetency window – larvae were advected downstream until they were developmentally competent, after which all larvae near suitable habitat settled. After the competency window opened, larvae were mixed farther downstream and offshore, resulting in lower probabilities of settlement seen in the tails of the distributions. These results were consistent across sites, although the degree of reduction of mean dispersal distance and increase of the standard deviation with a CBL varied by site according to the details of the CBL profiles enumerated below.

Spatial statistics

The ratio of spatial statistics (e.g., mean dispersal distance and standard deviation) with a CBL to without a CBL provided a metric for determining the degree to which inclusion of the CBL changed dispersal predictions. Comparisons of this ratio to the ratio of T_{PLD} to T_{CBL} afforded an evaluation of what conditions (e.g., pelagic larval duration, CBL width, and velocity gradients) corresponded to these changes.

For all sites and PLDs, the CBL reduced mean dispersal distance (Fig 2.5A). This reduction was greatest at Huntington Beach, with ratios of dispersal distance with to without a CBL ranging from 0.44-0.78 (decreased dispersal distance of 22-56%). The least reduction in mean dispersal distance was seen at Mohawk, with ratios of mean dispersal distance from 0.70-0.91 (decreased dispersal distance of 9-30%). Shorter PLD timescales led to larger deviations from the no-CBL assumption. As the PLD increased dispersal distances with a CBL began to converge toward the mean dispersal distance without a CBL, evidenced by the asymptote in Fig. 2.5A. However, the ratio of this statistic never equaled one. A ratio of T_{PLD} to T_{CBL} of 15 was required before all sites had a displacement ratio > 0.8. Even for the maximum ratio of time scales used in the study, when T_{PLD} was over 40 times greater than T_{CBL} (Fig. 2.5A: Mohawk, diamonds) the displacement ratio was still less than 0.95, with a reduction in mean dispersal distance of 9%. When $T_{PLD} \sim T_{CBL}$ mean dispersal distance was reduced by ~ 50%.

Inclusion of a CBL also decreased the 95th percentile dispersal distance for all sites and PLDs, although this result was less pronounced than the decrease in mean dispersal distance (Fig. 2.5B). For low ratios of T_{PLD} to T_{CBL} long distance dispersal distance was reduced by < 30%. As T_{PLD} increased this reduction decreased to < 5% at Mohawk, the site where long distance dispersal was the least affected (Fig. 2.5B

diamonds). All sites exhibited a displacement ratio > 0.9 by a ratio of T_{PLD} to T_{CBL} of 10, corresponding to differences in 95th percentile dispersal distance < 10%. Although reductions were still important for low ratios of T_{PLD} to T_{CBL}, the effect of the CBL on 95th percentile dispersal distance showed somewhat reduced importance compared to the effect of the CBL on mean displacement.

The standard deviation of kernels was higher for dispersal scenarios with CBLs for all sites and PLDs, with all ratios of standard deviation with a CBL to standard deviation without a CBL above one (Fig. 2.6A). The presence of a CBL added more variability to the kernels, with a greater variance in dispersal distance: standard deviations with a CBL ranged from 9% to 47% higher than standard deviations without CBLs. The standard deviation of kernels with CBLs was highest for situations where T_{PLD} was comparable to about 2 times greater than T_{CBL}. The difference in standard deviations between scenarios decreased as the timescales became less similar.

The increase in standard deviation with a CBL was due to the combined effects of cross-shore gradients in velocity and diffusivity. Velocity gradients acted to smear distributions of larvae in the alongshore direction, a process known as “shear dispersion” (Bowden 1965). Diffusivity gradients increased the standard deviation because lower diffusivities near the coast required more time steps for larvae to settle than that required with higher diffusivities of the no-CBL case; these delays in settlement added additional spread to the settlement distribution. To determine the relative contribution of shear dispersion to the increase in standard deviation, we conducted model runs with CBL velocity gradients and constant diffusivity (equal to the diffusivity used in the no-CBL case). Shear dispersion led to increases in the standard deviation of dispersal kernels of 6-

36%. The addition of a diffusivity gradient led to an additional increase up to 20% of the no-CBL standard deviation (data not shown). During the precompetency window, larvae were advected downstream from the release point. For the no-CBL case the advection velocity was the same for all particles, and any differences in particle positions were due to random impulses in the model. At the end of the precompetency window when particles began to settle, their initial distribution was narrow, with little spread around the mean displacement. When a velocity gradient was introduced, larvae were now advected at different rates downstream depending on their cross-shore position. At the end of the precompetency window, this initial distribution of competent larvae exhibited more spread than the no-CBL case, with a higher standard deviation due to shear dispersion.

The CBL and no-CBL kernels (Fig. 2.4) differed not just in standard deviation (the 2nd central moment of the distribution) but also in skew (the 3rd standardized moment). Dispersal kernels from model runs without a CBL were up to 60% more skewed than kernels from model runs with a CBL (Fig. 2.6B). The skewed nature of the no-CBL kernels indicated that dispersal was asymmetric, with the frequency of dispersal distances weighted to the left of the mean (positive skewness). The lower values of skewness in the kernels with a CBL indicated a more symmetric and even distribution, with a higher standard deviation than the asymmetric peaked kernels resulting from a flow field without a CBL.

Settlement and self-retention

Including the CBL in a modeling framework had consequences for the predictions of the number of settlers in addition to affecting the spatial distribution of settlers. Model

runs including the CBL resulted in 8% less settlement for all sites and PLDs (Fig. 2.7). This result was attributed to the representation of eddy diffusivity in the two model scenarios. The no-CBL case – with a constant value of diffusivity representative of more offshore conditions – had more turbulent mixing close to shore, which translated into greater cross-shore jumps in a given timestep. Lower diffusivities close to shore represented in the model runs with a CBL produced smaller cross-shore movements for each particle at a given timestep, which amounted to a larger number of timesteps needed to come back to shore than for a scenario with a larger, constant velocity that did not incorporate the CBL. This effect was most pronounced as the PLD increased at sites with broad CBLs, and across PLDs at sites with narrow CBLs. As T_{CBL} decreased under these conditions, it became more likely that larvae would leave the CBL and need to return. For sites with broad CBLs (Pajaro and Huntington), model runs for low pelagic larval durations resulted in similar settler numbers with or without a CBL (Fig. 2.7, data points near 1:1 line). Decreasing the model timestep did not affect these results.

Despite a reduction in the total number of settling larvae, the CBL drastically increased self-retention, the proportion of released larvae that settled within 10 km of their release site during the competency window. At least one released larva must settle within 10 km of the release site to detect self-retention in our model, resulting in a minimum detectable self-retention rate of 10^{-4}. Without including a CBL, only two sites (Pajaro and Hopkins) reached detectable levels of self-retention, and solely for the lowest PLDs (3 and 6 d; Fig. 2.8). Including a CBL in the dispersal model increased self-retention up to 3 orders of magnitude, and led to predictions of measurable self-retention for all sites. Hopkins had the highest amount of self-retention (53% and 27% for PLDs of

3 and 6 d), with measurable self-retention for PLDs up to 21 d when a CBL was represented in the model.

DISCUSSION

Descriptions of dispersal are paramount to our understanding of metapopulation dynamics. Ocean currents have the potential to disperse larvae of nearshore marine species great distances from their site of origin; however, there is limited information available regarding details of fluid motion close to shore where most larvae are concentrated. This means that many metapopulation models could be parameterized with flow data collected offshore of the CBL, and thus beyond the zone where most larvae are found. We have explored the effects of modeling increased resolution of fluid processes on predictions of dispersal of nearshore marine organisms. Accounting for lower velocities observed nearshore in the coastal boundary layer decreased mean dispersal distance and 95th percentile dispersal distance, and substantially increased self-retention. The shapes of settlement distributions also changed when CBLs were included in the modeling framework, owing to the representation of shear dispersion and mixing. These results were consistent across a range of life histories (modeled by different pelagic larval durations) and coastal locations (represented by different sites), with the largest affects of the CBL seen for short PLDs and sites with broad CBLs. By not accounting for extreme nearshore processes such as the CBL in dispersal models using a two-parameter framework, we may be overestimating population connectivity, and underestimating local retention. As discussed below, the CBL is a prominent feature over time and space in a

larva's lifetime, and although the CBL adds additional complexity to models, it may change our predictions of population dynamics.

The prevalence of the CBL

Owing to the need for larvae released near the shoreline to return to shallow habitat to settle, the CBL may be a prominent feature of the larval period. Our findings suggest that the CBL strongly affects dispersal when T_{CBL} (the time scale of diffusive loss from the CBL) is greater than one fifth of the pelagic larval duration (PLD). Taking L_{CBL} (the width of the CBL) to be 2 km, an average of the CBL widths used in this study, and employing a rough K_y estimate of 10 m^2 s^{-1}, one obtains T_{CBL} ~ 5 d. Given that a successful recruit that moves out of the CBL must move back through it to recruit to adult habitat, larvae with PLDs on the order of 10 d may spend their entire pelagic period in the CBL and larvae with PLD up to 25 d will have substantially reduced dispersal. These propagules will move much shorter alongshore distances than expected from estimates based on a flow field with uniform flow.

Given the dramatic effects including a CBL in the dispersal model had on spatial statistics of the dispersal distribution and self-retention, can we predict the effect CBLs will have on dispersal for sites beyond California? The degree of velocity attenuation within the CBL will determine the extent to which lower velocities dominate the inner portion of the CBL and decrease alongshore transport. The width of the CBL also establishes the spatial extent of gradients in velocity and diffusivity. The velocity gradient ($\frac{dU}{dy}$) combines both the degree of velocity attenuation and the width of the CBL into one parameter. At our study sites, the velocity gradient was inversely related to

the timescale of the CBL (T_{CBL}) and this relationship was nonlinear (Fig. 2.9). The site with the highest velocity gradient, Mohawk, had a narrow CBL with high velocities at the offshore edge, with $T_{CBL} < 1$ d. This site showed the least reduction in mean dispersal distance from inclusion of the CBL (Fig. 2.5A) and the least amount of self-retention (Fig. 2.8). The sites used in this study spanned a marked inflection in the relationship between the velocity gradient and T_{CBL} around a velocity gradient of 5×10^{-5} s^{-1}. For sites with velocity gradients below this value, Huntington Beach and Pajaro, T_{CBL} increased rapidly. These sites exhibited the greatest reduction in mean dispersal distance from including the CBL (Fig. 2.5A). Pajaro, with the lowest velocity gradient and highest T_{CBL} of the five sites, saw the greatest increase in predicted self-retention from including a CBL in the model (Fig. 2.8). The effects of the CBL (decreased mean and long distance dispersal distance, increased standard deviation of the larval dispersal kernel, and increased self retention) manifested across sites with different physical characteristics (e.g., velocity gradients, bathymetry, topography). Assuming that velocity approaches zero at the coast, knowledge of offshore current speed and bathymetry together provide a rough estimate of the velocity gradient, and should allow for predictions of T_{CBL} and an estimate of how the CBL affects dispersal kernels.

Distributions of larvae in the coastal ocean

While the model results presented here illustrate the importance of the nearshore zone to dispersing larvae, are these results consistent with empirical measurements of larval distributions? Plankton tows conducted at stations along cross-shore transects spanning 30 kilometers in both Oregon (Shanks and Shearman 2009) and California

(Morgan et al. 2009) revealed that the greatest numbers and diversity of larvae were consistently found close to shore (within 1 to 3 km from shore), and that this pattern was found across sampling days under a variety of offshore conditions. Dispersal trajectories shown here indicate that in the presence of a CBL, larvae spend more time nearshore than under uniform flow conditions (Fig. 2.3). The CBL is a nearshore flow feature that can be present across various offshore conditions, as the CBL-associated velocity and mixing gradients result from the increasing importance of bottom and horizontal drag as the water column becomes shallow (Nickols et al. in revision). We recognize that larval behavior also plays a large role in patterns of nearshore abundance for some species (Morgan and Fisher 2010). In that respect, larvae may exhibit behaviors that keep them within the CBL in slower-magnitude alongshore flows. This may be a particularly important strategy for those species with longer PLDs to decrease potential dispersal distance. In addition, larvae demonstrate a wide range of behaviors, yet most are found close to shore. The CBL provides a physical mechanism for staying nearshore and close to natal sites that applies across taxa.

Decreased transport within the CBL may be a mechanism contributing to the mismatch between predicted and empirical measurements of dispersal distances among marine organisms with a pelagic life stage. There has been much interest in comparing dispersal distances calculated based on a specie's PLD and assumptions about the flow field during the larval period, and other more biological metrics of dispersal distance such as genetic markers, natural tags, and observations of dispersal (Kinlan and Gaines 2003, Siegel et al. 2003, Lester and Ruttenberg 2005, Lester et al. 2007, Botsford et al. 2009, Shanks 2009, Selkoe and Toonen 2011). There are often large discrepancies between the

results produced by these techniques: dispersal distance calculated from a known PLD is often much larger than biological metrics of dispersal distance (Shanks 2009, Selkoe and Toonen 2011). The explanation typically offered for this discrepancy is that larvae do not behave as passive particles as assumed in these analyses (i.e., they can swim). Our model does not include larval swimming behavior, but it does offer an additional and complementary explanation for the discrepancy between observed and predicted dispersal distances: larvae do not spend their entire lives in the free-stream flow, and so analyses based on PLD and free-stream flow conditions should overestimate dispersal distances. This provides further evidence that consideration of the PLD in a uniform flow field provides merely an upper bound on dispersal distance.

A surprising result of this study was decreased settlement under CBL conditions. With a CBL, larvae are swept offshore less frequently than without a CBL, but if they do move offshore, it is much more difficult for them to return to the nearshore environment due to turbulent mixing. Gradients in mixing found in the ocean may be an unrecognized source of larval wastage. Additionally, while not included in this model, as diffusivity increases the time to return to the coast, there should be a concomitant increase in larval exposure to other sources of mortality (Possingham and Roughgarden 1990).

The CBL and population dynamics

With reductions in mean dispersal distance of over 50% and increases in self-retention by orders of magnitude, the CBL can have a substantial effect on propagule dispersal, and it may be necessary to reconsider representations for physical transport of larvae that operate over uniform conditions within the coastal ocean. While such simple

models have facilitated our understanding of specific drivers of population dynamics, the importance of these drivers may be altered by background flow conditions, such as the CBL. For example, by not including the CBL in the generation of dispersal kernels, we may be over-estimating the spatial scale of population connectivity of nearshore organisms. The consequences of including the CBL in models would be predictions of slower invasions, more self-persistence, and more genetic structure than previously expected. Although, genetic connectivity should be less affected by the CBL than demographic connectivity, as changes in predictions of long distance dispersal with a CBL were not as great as changes in mean dispersal distance.

For decades, ecologists have explored the evidence and consequences for open versus closed populations, and the role of the physical environment in the degree of population connectivity (Caley et al. 1996, Levin 2006). In recent years, there has been an increase in reports of "higher than expected" self-recruitment of benthic marine organisms (Swearer et al. 2002, Cowen and Sponaugle 2009). The CBL is a physical mechanism within the continuum of processes that lead to more "open" or "closed" populations. For sites with low velocity gradients and broad CBL widths similar to Pajaro, we might expect more closed populations as local retention is increased under these conditions. For locations with steep velocity gradients and narrow CBL widths, such as Mohawk, retention is lower, and these populations may be propagule sources for other sites, and be more 'open.' These populations would be expected to have minimal self-retention, relying on propagules from other populations within a network to persist (White et al. 2010b). The condition of population persistence relies on replacement: if enough larvae spawned at one location return to replace the adults in that population, it is

self-persistent. If there are shortfalls in return relative to reproductive output, that population must rely on larval input from elsewhere, and display network persistence (Hastings and Botsford 2006). Given the expected distribution of larval dispersal distances, network persistence should be more common than self-persistence for populations in an advective environment (White et al. 2010b). Populations whose larvae spend a minimal amount of their pelagic duration within the CBL likely rely on network persistence, and self-persistence should be highest for populations where the timescale of the CBL is equal to or greater than the PLD. Understanding the general scaling of the nearshore environment in relation to life history parameters of coastal species provides a rough estimation of the characteristics of more or less retentive coastal habitats.

Incorporating CBLs into models may lead to persistence in populations located in highly advective environments where the expectation is for all propagules to be swept downstream. Population models with constant advection have demonstrated that above certain velocities population persistence is not possible (Possingham and Roughgarden 1990, Hill 1991, Byers and Pringle 2006). For example, Hill (1990) found that populations of the Norway lobster, *Nephrops norvegicus*, could not retain sufficient numbers of larvae to persist with mean flows above 0.04 m s^{-1} (note that this value corresponds to the lowest offshore velocity measured amongst our five sites). However, the observed persistence of this species in the field implies that populations can overcome such advective loss. Increased supply may counteract advective loss of propagules, however, in the face of highly advective uniform flow fields, populations cannot be rescued by increased fecundity (Hill 1991). The presence of velocity gradients within the CBL, resulting in alongshore shear dispersion and decreased velocities nearshore,

decreases the overall advection speed of larvae, and is a possible mechanism for population persistence in advective environments. Possingham and Roughgarden (1990) modeled the effects of alongshore flow fields on population persistence and included both uniform flow fields and the addition of a coastal boundary layer, both with uniform diffusivity. The flow fields with a CBL led to persistent populations for offshore velocities that were not persistent with a uniform flow field. Wider CBLs increased retention and persistence, although it was unclear how the width of the boundary in the model related to locations in the natural world, as the parameterization of the CBL was phenomenological, and not directly based on a set of observations. Nonetheless, velocity gradients at the coast clearly have an impact on predictions of population dynamics, and it is surprising that more models have not incorporated this finding.

Predictions of population persistence and spread can also be affected by the shape of the dispersal kernel. Determining what kernel shape is appropriate for different populations and environmental settings is still an important issue for both terrestrial and marine systems (Bullock and Clarke 2000). For species that disperse in a fluid medium, the fluid dynamics of an environment can inform the shape of the dispersal kernel, and are incorporated in mechanistic descriptions of kernels (Greene and Johnson 1989, Okubo and Levin 1989, Gaylord et al. 2006). Leptokurtic distributions are often assumed for long distance dispersers in both marine and terrestrial systems and have been observed in nature (Kot et al. 1996, Lockwood et al. 2002), although both Gaussian and leptokurtic distributions are calculated from oceanographic simulations of dispersal kernels (Siegel et al. 2003, Aiken et al. 2007). The representation of dispersal by either a Gaussian or leptokurtic form can result in substantially different predictions. Leptokurtic

distributions, with higher concentrations of dispersers near the mean and tails than a Gaussian distribution with similar mean and variance, lead to higher estimates of population spread than Gaussian distributions (Kot et al. 1996). The results of our study support the idea that dispersal in nearshore marine systems is non-Gaussian (Fig. 2.4 red versus black line). However, our results suggest that the leptokurtic distribution often assumed for marine species requires caution. Shear dispersion acts to spread the settlement distribution, and kernels generated from model runs with a CBL resulted in less skewness and kurtosis than the leptokurtic kernels which resulted from assuming a uniform flow field (Fig. 2.4 red line versus blue line). Discrepancies between kernel shapes could be particularly important in the application of dispersal models to management decisions. Descriptions of the tails of dispersal distributions are particularly important for describing persistence of populations in a uni-directional advective environment (Lutscher et al. 2010) as well as predictions of population responses to climate change and invasive species dynamics, as the tails indicate population spread (Kot et al. 1996, Clark et al. 1999, Lockwood et al. 2002). If inclusion of more realistic features of the fluid environment substantially changes the shape of dispersal kernels, it warrants consideration in subsequent models of population dynamics.

Model complexity

The model presented here was designed to illustrate the potential effects a generalizable flow feature has on predictions of dispersal distributions. The approach was to demonstrate where, when, and for who resolution of the nearshore environment, in the form of the CBL, would substantially alter dispersal kernels and subsequent estimates of

population dynamics and metapopulation connectivity. This brings us back to our opening question: how complex does the representation of fluid motion need to be to accurately predict dispersal relevant to metapopulation dynamics? Our study implies that the CBL should be considered in future models exploring the dynamics of coastal species, particularly in the context of self-retention.

Incorporating the CBL adds complexity to the two-parameter approach; however, the functional form of the CBL (logarithmic velocity profile and linear mixing profile) can easily be incorporated into models. Including a CBL in a two-parameter modeling framework is still less complicated than developing and validating a large-scale oceanographic circulation model. It is also important to note that even in the case of models with highly detailed flow representations (e.g., based on the Regional Ocean Modeling System: Cowen et al. 2006; Watson et al. 2010), their spatial resolution is largely restricted to scales of 1 kilometer or more, and may not resolve fluid motion important to descriptions of dispersal, such as the CBL (Watson et al. 2010, Drake et al. 2011). Therefore, the model details presented here may be helpful not only to the expansion of simple models, but also to the advancement of large-scale models.

The field of metapopulation ecology has benefited substantially from our growing knowledge of dispersal processes. For example, inclusion of adult dispersal in the form of home range size, in addition to juvenile dispersal, has substantially changed predictions of metapopulation dynamics and informed management decisions (Moffitt et al. 2009, White et al. in review). Asymmetric dispersal is apparent in many contexts, from topographic dispersal barriers to advective fluid flow, and analyzing its effects have advanced our understanding of metapopulation persistence (Bode et al. 2008, Vuilleumier

et al. 2010). These more realistic scenarios increase our ability to accurately model dynamics, while still encapsulating some generality. While the CBL is an example of increased realism particular to marine systems, its commonality across time and space and the simplicity of its functional form warrant attention, especially given its potential for far-reaching demographic consequences.

ACKNOWLEDGMENTS

We thank L.W. Botsford for computing resources and helpful feedback on the manuscript. This work was funded by NSF grants OCE-927255 and OCE-1065990, and by the University of California Marine Council Coastal Environmental Quality Initiative grants 04-T-CEQI-08-0048 and 07-T-CEQI-10-0060. K.J. Nickols was supported by a Bodega Marine Laboratory Graduate Student Fellowship.

LITERATURE CITED

Aiken, C. M., S. A. Navarrete, M. I. Castillo, and J. C. Castilla. 2007. Along-shore larval dispersal kernels in a numerical ocean model of the central Chilean coast. Marine Ecology Progress Series **339**:13-24.

Bode, M., K. Burrage, and H. P. Possingham. 2008. Using complex network metrics to predict the persistence of metapopulations with asymmetric connectivity patterns. Ecological Modeling **214**:201-209.

Borges, R., R. Ben-Hamadou, M. A. Chicharo, P. Re, and E. J. Goncalves. 2007. Horizontal spatial and temporal distribution patterns of nearshore larval fish assemblages at a temperate rocky shore. Estuarine, Coastal and Shelf Science **71**:412-428.

Botsford, L., C. Moloney, A. Hastings, J. L. Largier, T. Powell, K. Higgins, and J. Quinn. 1994. The influence of spatially and temporally varying oceanographic conditions on meroplankton metapopulations. Deep-Sea Research II **41**:107-145.

Botsford, L. W., J. W. White, M. A. Coffroth, C. B. Paris, S. Planes, T. L. Shearer, S. R. Thorrold, and G. P. Jones. 2009. Connectivity and resilience of coral reef metapopulations in marine protected areas: matching empirical efforts to predictive needs. Coral Reefs **28**:327-337.

Bullock, J. and R. Clarke. 2000. Long distance seed dispersal by wind: measuring and modelling the tail of the curve. Oecologia **124**:506-521.

Byers, J. E. and J. M. Pringle. 2006. Going against the flow: retention, range limits and invasions in advective environments. Marine Ecology Progress Series **313**:27-41.

Caley, M., M. Carr, M. Hixon, T. Hughes, G. Jones, and B. Menge. 1996. Recruitment and the local dynamics of open marine populations. Annual Review of Ecology and Systematics **27**:477-500.

Caswell, H. 1988. Theory and models in ecology: A different perspective. Ecological Modeling **43**:33-44.

Clark, J., M. Silman, R. Kern, E. Macklin, and J. HilleRisLambers. 1999. Seed dispersal near and far: patterns across temperate and tropical forests. Ecology **80**:1475-1494.

Cowen, R., C. Paris, and A. Srinivasan. 2006. Scaling of connectivity in marine populations. Science **311**:522-527.

Cowen, R. K. and S. Sponaugle. 2009. Larval dispersal and marine population connectivity. Annual Review of Marine Science **1**:443-466.

Davis, R. 1985. Drifter observations of coastal surface currents during CODE - the statisitical and dynamical views Journal of Geophysical Research-Oceans **90**:4756-4772.

Drake, P., C. Edwards, and J. Barth. 2011. Dispersion and connectivity estimates along the U.S. west coast from a realistic numerical model. Journal of Marine Research **69**:1-37.

Drake, P. T. and C. Edwards. 2009. A linear diffusivity model of near-surface, cross-shore particle dispersion from a numberical simulation of central California's coastal ocean. Journal of Marine Research **67**:385-409.

Fonseca, D. and D. Hart. 2001. Colonization history masks habitat preferences in local distributions of stream insects. Ecology **82**:2897-2910.

Gaines, S., B. Gaylord, and J. Largier. 2003. Avoiding current oversights in marine reserve design. Ecological Applications **13**:S32-S46.

Gaylord, B. and S. Gaines. 2000. Temperature or transport? Range limits in marine species mediated solely by flow. American Naturalist **155**:769-789.

Gaylord, B., D. Reed, P. T. Raimondi, and L. Washburn. 2006. Macroalgal spore dispersal in coastal environments: mechanistic insights revealed by theory and experiment. Ecological Monographs **76**:481-502.

Gaylord, B., J. H. Rosman, D. C. Reed, J. R. Koseff, J. Fram, S. MacIntyre, K. Arkema, C. McDonald, M. A. Brzezinski, J. L. Largier, S. G. Monismith, P. T. Raimondi, and B. Mardian. 2007. Spatial patterns of flow and their modification within and around a giant kelp forest. Limnology and Oceanography **52**:1838-1852.

Greene, D. and E. Johnson. 1989. A model of wind dispersal of winged or plumed seeds. Ecology **70**:339-347.

Hanski, I. 1998. Metapopulation dynamics. Nature **396**:41-49.

Hanski, I. and M. Gilpin. 1991. Metapopulation dynamics: brief history and conceptual domain. Biological Journal of the Linnean Society **42**:3-16.

Hastings, A. and L. Botsford. 2006. Persistence of spatial populations depends on returning home. Proceedings of the National Academy of Sciences (USA) **103**:6067-6072.

Hill, A. 1990. Pelagic dispersal of Norway lobster *Nephrops norvegicus* larvae examined using an advection-diffusion-mortality model. Marine Ecology Progress Series **64**:217-226.

Hill, A. E. 1991. Advection-diffusion-mortality solutions for investigating pelagic larval dispersal. Marine Ecology Progress Series **70**:117-128.

Jackson, G. and R. Strathmann. 1981. Larval mortality from offshore mixing as a link between pre-competent and competent periods of development. American Naturalist **118**:16-26.

Kaplan, D. 2006. Alongshore advection and marine reserves: consequences for modeling and management. Marine Ecology Progress Series **309**:11-24.

Kaplan, D. M., L. W. Botsford, M. R. O'Farrell, S. D. Gaines, and S. Jorgensen. 2009. Model-based assessment of persistence in proposed marine protected area designs. Ecological Applications **19**:433-448.

Katul, G. G., A. Porporato, R. Nathan, M. Siqueira, M. B. Soons, D. Poggi, H. S. Horn, and S. A. Levin. 2005. Mechanistic analytical models for long-distance seed dispersal by wind. American Naturalist **166**:368-381.

Kinlan, B. and S. Gaines. 2003. Propagule dispersal in marine and terrestrial environments: A community perspective. Ecology **84**:2007-2020.

Kot, M., M. Lewis, and P. van den Driessche. 1996. Dispersal data and the spread of invading organisms. Ecology **77**:2027-2042.

Largier, J. 2003. Considerations in estimating larval dispersal distances from oceanographic data. Ecological Applications **13**:S71-S89.

Lentz, S., R. Guza, S. Elgar, F. Feddersen, and T. Herbers. 1999. Momentum balances on the North Carolina inner shelf. Journal of Geophysical Research-Oceans **104**:18205-18226.

Lester, S. E. and B. I. Ruttenberg. 2005. The relationship between pelagic larval duration and range size in tropical reef fishes: a synthetic analysis. Proccedings of the Royal Society B **272**:585-591.

Lester, S. E., B. I. Ruttenberg, S. D. Gaines, and B. P. Kinlan. 2007. The relationship between dispersal ability and geographic range size. Ecology Letters **10**:745-758.

Levin, L. 2006. Recent progress in understanding larval dispersal: new directions and digressions. Integrative and Comparative Biology **46**:282-297.

Levin, S. 1974. Dispersion and population interactions. American Naturalist **108**:207-228.

Levin, S. A., H. C. Muller-Landau, R. Nathan, and J. Chave. 2003. The ecology and evolution of seed dispersal: A theoretical perspective. Annual Review of Ecology, Evolution and Systematics **34**:575-604.

Levins, R. 1966. The strategy of model building in population biology. American Scientist **54**:421-431.

List, E., G. Gartrell, and C. Winant. 1990. Diffusion and dispersion in coastal waters. Journal of Hydraulic Engineering **116**:1158-1179.

Lockwood, D. R., A. Hastings, and L. W. Botsford. 2002. The effects of dispersal patterns on marine reserves: Does the tail wag the dog? Theoretical Population Biology **61**:297-309.

Lutscher, F., R. M. Nisbet, and E. Pachepsky. 2010. Population persistence in the face of advection. Theoretical Ecology **3**:271-284.

Moffitt, E. A., L. W. Botsford, D. M. Kaplan, and M. R. O'Farrell. 2009. Marine reserve networks for species that move within a home range. Ecological Applications **19**:1835-1847.

Moffitt, E. A., J. W. White, and L. W. Botsford. 2011. The utility and limitations of size and spacing guidelines for designing marine protected area (MPA) networks. Biological Conservation **144**:306-318.

Morgan, S. and J. Fisher. 2010. Larval behavior regulates nearshore retention and offshore migration in an upwelling shadow and along the open coast. Marine Ecology Progress Series **404**:109-126.

Morgan, S. G., J. L. Fisher, S. H. Miller, S. T. McAfee, and J. L. Largier. 2009. Nearshore larval retention in a region of strong upwelling and recruitment limitation. Ecology **90**:3489-3502.

Murthy, C. and G. Csanady. 1981. Frictional and inertial coastal boundary layers in the Great Lakes. Ocean Management **6**:237-237.

Nathan, R., N. Sapir, A. Trakhtenbrot, G. G. Katul, G. Bohrer, M. Otte, R. Avissar, M. B. Soons, H. S. Horn, M. Wikelski, and S. A. Levin. 2005. Long-distance biological transport processes through the air: can nature's complexity be unfolded *in silico*? Diversity and Distributions **11**:131-137.

Nickols, K. J., B. Gaylord, and J. L. Largier. in revision. The coastal boundary layer: predictable current structure decreases alongshore transport and alters scales of dispersal. Marine Ecology Progress Series.

O'Connor, M. I., J. F. Bruno, S. D. Gaines, B. S. Halpern, S. E. Lester, B. P. Kinlan, and J. M. Weiss. 2007. Temperature control of larval dispersal and the implications

for marine ecology, evolution, and conservation. Proceedings of the National Academy of Sciences (USA) **104**:1266-1271.

Okubo, A. 1971. Oceanic diffusion diagrams. Deep-Sea Research **18**:789-802.

Okubo, A. and S. A. Levin. 1989. A theoretical framework for data analysis of wind dispersal of seeds and pollen Ecology **70**:329-338.

Pachepsky, E., F. Lutscher, R. Nisbet, and M. Lewis. 2005. Persistence, spread and the drift paradox. Theoretical Population Biology **67**:61-73.

Possingham, H. and J. Roughgarden. 1990. Spatial population dynamics of a marine organism with a complex life cycle. Ecology **71**:973-985.

Pringle, J. M. and J. P. Wares. 2007. Going against the flow: maintenance of alongshore variation in allele frequency in a coastal ocean. Marine Ecology Progress Series **335**:69-84.

Rao, Y. and C. Murthy. 2001. Coastal boundary layer characteristics during summer stratification in Lake Ontario. Journal of Physical Oceanography **31**:1088-1104.

Roughgarden, J., S. Gaines, and H. Possingham. 1988. Recruitment dynamics in complex life-cycles. Science **241**:1460-1466.

Roughgarden, J. and Y. Iwasa. 1986. Dynamics of a metapopulation with space-limited subpopulations. Theoretical Population Biology **29**:235-261.

Saarman, E., J. W. White, and L. W. Botsford. unpublished manuscript.

Sale, P., I. Hanski, and J. Kritzer. 2006. The merging of metapopulation theory and marine ecology: establishing the historical context. Pages 3-30 *in* J. Kritzer and P. Sale, editors. Marine Metapopulations. Elsevier Academic Press, Burlington, MA.

Scheltema, R. 1986. On dispersal and planktonic larvae of benthic invertebrates - an eclectic overview and summary of problems. Bulletin of Marine Science **39**:290-322.

Schlicting, H. 1979. Boundary-layer theory. McGraw-Hill, New York, NY.

Selkoe, K. and R. Toonen. 2011. Marine connectivity: a new look at pelagic larval duration and genetic metrics of dispersal. Marine Ecology Progress Series **436**:291-305.

Shanks, A. L. 2009. Pelagic larval duration and dispersal distance revisited. Biological Bulletin **216**:373-385.

Shanks, A. L. and R. K. Shearman. 2009. Paradigm lost? Cross-shelf distributions of intertidal invertebrate larvae are unaffected by upwelling or downwelling. Marine Ecology Progress Series **385**:189-204.

Siegel, D., B. Kinlan, B. Gaylord, and S. Gaines. 2003. Lagrangian descriptions of marine larval dispersion. Marine Ecology Progress Series **260**:83-96.

Swearer, S., J. S. Shima, M. E. Hellberg, S. Thorrold, G. Jones, D. R. Robertson, S. G. Morgan, K. A. Selkoe, G. M. Ruiz, and R. R. Warner. 2002. Evidence of self-recruitment in demersal marine populations. Bulletin of Marine Science **70**:S251-S271.

Taylor, G. I. 1922. Diffusion by continuous movements. Proceedings of the London Mathematical Society **20**:196-212.

Van Nes, E. H. and M. Scheffer. 2005. A strategy to improve the contribution of complex simulation models to ecological theory. Ecological Modeling **185**:153-164.

Vanschoenwinkel, B., S. Gielen, H. Vandewaerde, M. Seaman, and L. Brendonck. 2008. Relative importance of different dispersal vectors for small aquatic invertebrates in a rock pool metacommunity. Ecography **31**:567-577.

Vuilleumier, S., B. M. Bolker, and O. Lévêque. 2010. Effects of colonization asymmetries on metapopulation persistence. Theoretical Population Biology **78**:225-238.

Watson, J., S. Mitarai, D. Siegel, J. Caselle, C. Dong, and J. Mcwilliams. 2010. Realized and potential larval connectivity in the Southern California Bight. Marine Ecology Progress Series **401**:31-48.

White, C., K. A. Selkoe, J. Watson, D. A. Siegel, D. C. Zacherl, and R. J. Toonen. 2010a. Ocean currents help explain population genetic structure. Proceedings of the Royal Society B **277**:1685-1694.

White, J., L. Botsford, A. Hastings, and J. Largier. 2010b. Population persistence in marine reserve networks: incorporating spatial heterogeneities in larval dispersal. Marine Ecology Progress Series **398**:49-67.

White, J. W., K. J. Nickols, L. Clarke, and J. L. Largier. 2010c. Larval entrainment in cooling water intakes: spatially explicit models reveal effects on benthic metapopulations and shortcomings of traditional assessments. Canadian Journal of Fisheries and Aquatic Sciences **67**:2014-2031.

Symbol	Definition
b	Intercept from regression of the natural logarithm of distance from shore against alongshore velocity
K	Eddy diffusivity
K_{max}	Eddy diffusivity at the offshore edge of the CBL
L	Length scale
L_{CBL}	Width of the CBL
m	Slope from regression of the natural logarithm of distance from shore against alongshore velocity
t	Time scale
T_{CBL}	Lower bound on average time to diffuse through CBL
T_{PLD}	Pelagic larval duration
U	Depth- and time-averaged alongshore velocity
U_{*CBL}	CBL-scale friction velocity
V	Depth- and time-averaged cross-shore velocity
Δt	Model time step
κ	von Karman's constant

Table 2.1. List of symbols used in Chapter 2.

Site	CBL width (m)	Maximum velocity U ($m\ s^{-1}$)	Maximum diffusivity K ($m^2\ s^{-1}$)
Mohawk	915	0.165	13.5
Pajaro	3335	0.101	18
Huntington Beach	5555	0.169	63
Hopkins	700	0.0419	4.13
Terrace Point	1595	0.103	13.4

Table 2.2. Flow parameters for each site. For flow scenarios with a CBL, maximum velocity and diffusivity values apply to the offshore edge of the CBL (y = CBL width). For the no-CBL flow scenario, these values apply to a uniform flow field (constant U and constant K).

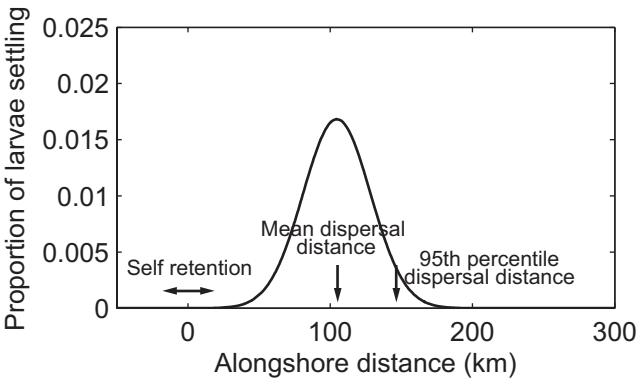

Figure 2.1. Schematic of a larval dispersal kernel, the probability distribution function of settlement along a coast, with depictions of important spatial statistics of the settlement distribution, including mean dispersal distance and the 95th percentile dispersal distance. Self retention is the total fraction of released larvae from a site that settle within 10 km of the spawning site.

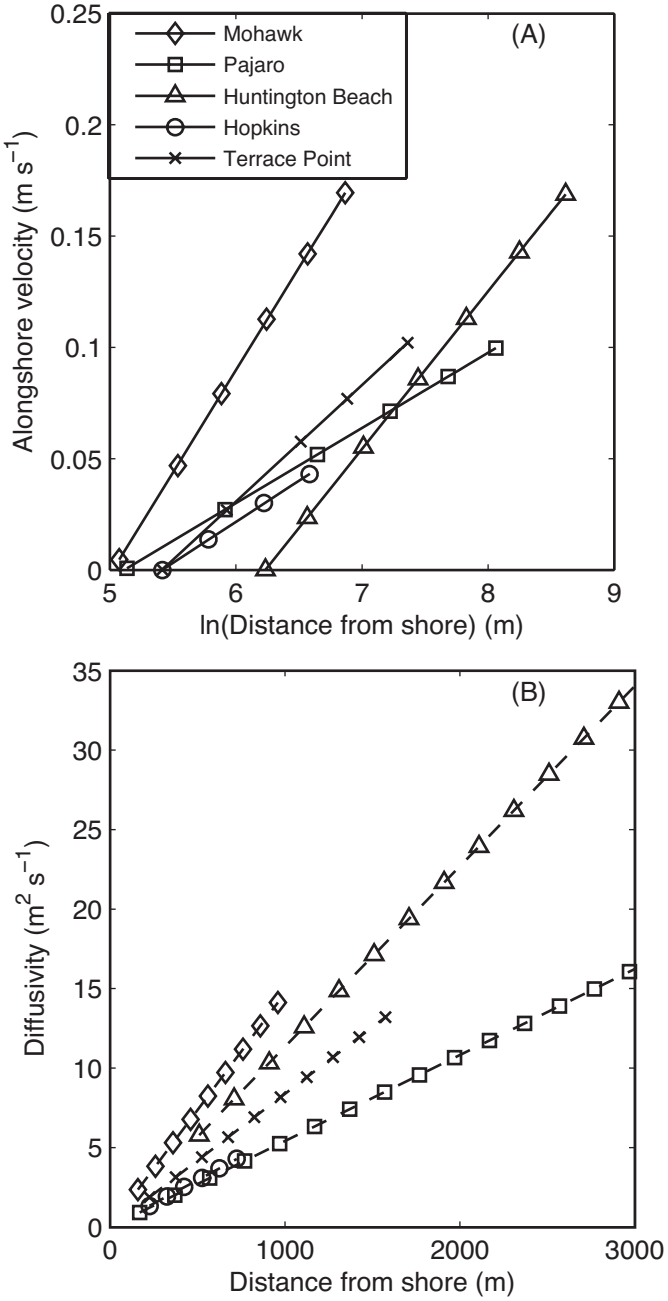

Figure 2.2. (A) Alongshore velocity profiles from five coastal sites. The natural logarithm of distance from shore is plotted against depth- and weekly averaged velocities. Data are from Nickols et al. (unpublished manuscript); (B) Eddy diffusivity profiles parameterized from velocity measurements in (A) plotted on a linear scale.

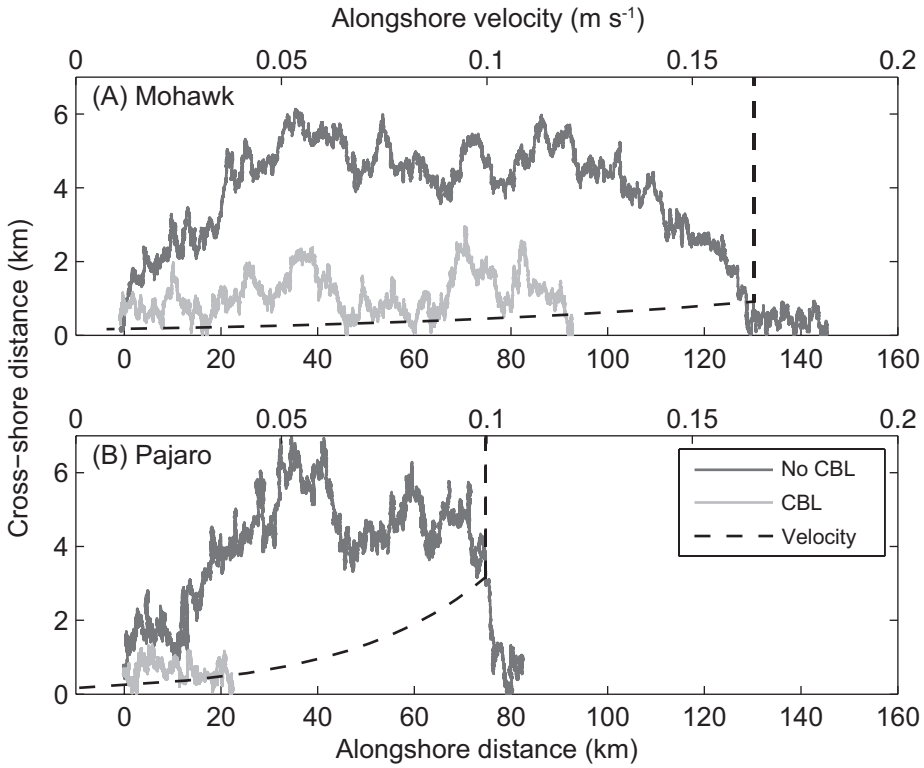

Figure 2.3. Sample dispersal trajectories for model larvae with and without a CBL for flow fields representing (A) Mohawk and (B) Pajaro, with the accompanying CBL velocity profiles for these sites (dashed line; top axis). Depicted trajectories are for a PLD of 15 d.

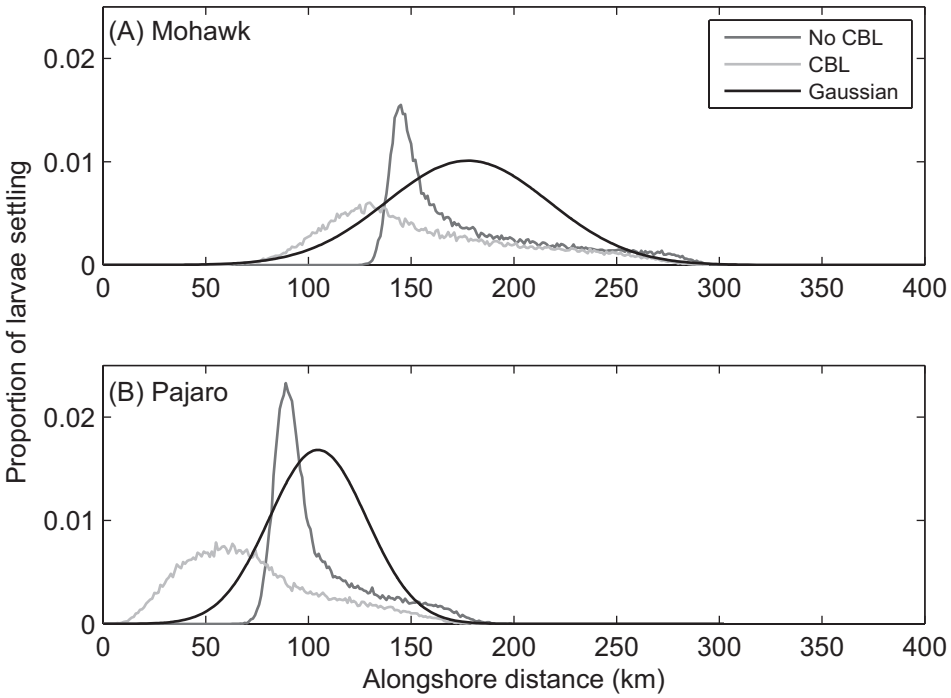

Figure 2.4. Larval dispersal kernels resulting from model runs with and without a CBL for flow fields representing (A) Mohawk and (B) Pajaro for a PLD of 15 d. A Gaussian kernel with mean and standard deviation equal to that calculated from the dispersal kernel without a CBL is shown in black for reference.

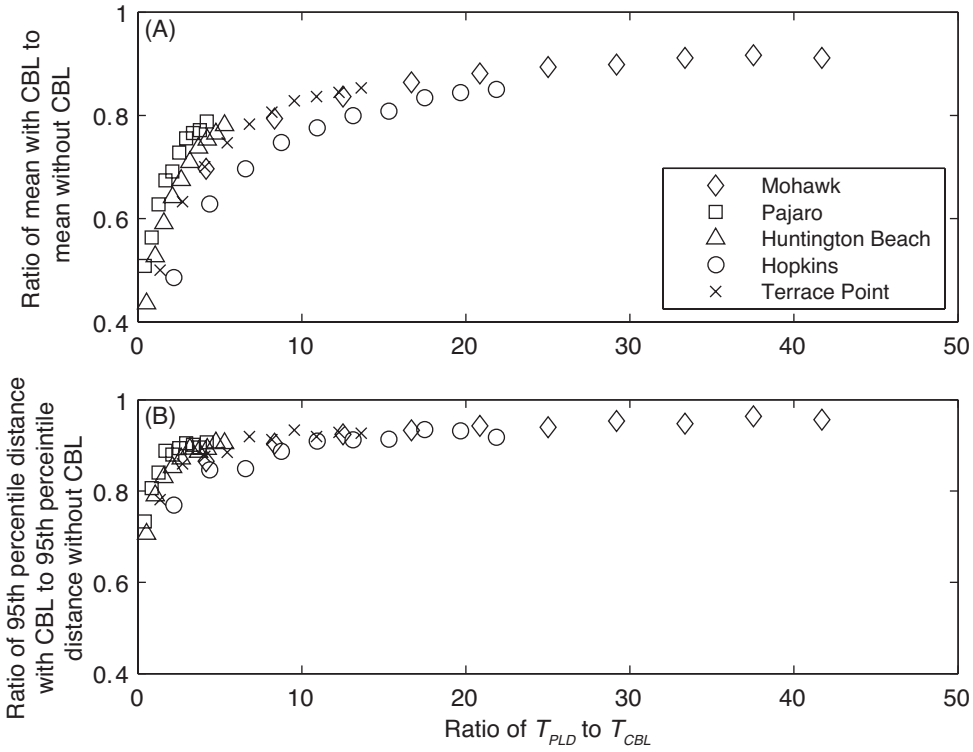

Figure 2.5. Ratio of PLD to the timescale of the CBL (T_{CBL}) plotted against the ratio of (A) mean dispersal distance and (B) 95th percentile dispersal distance, calculated from model runs with a CBL relative to no-CBL values. Model runs are for all sites and PLDs.

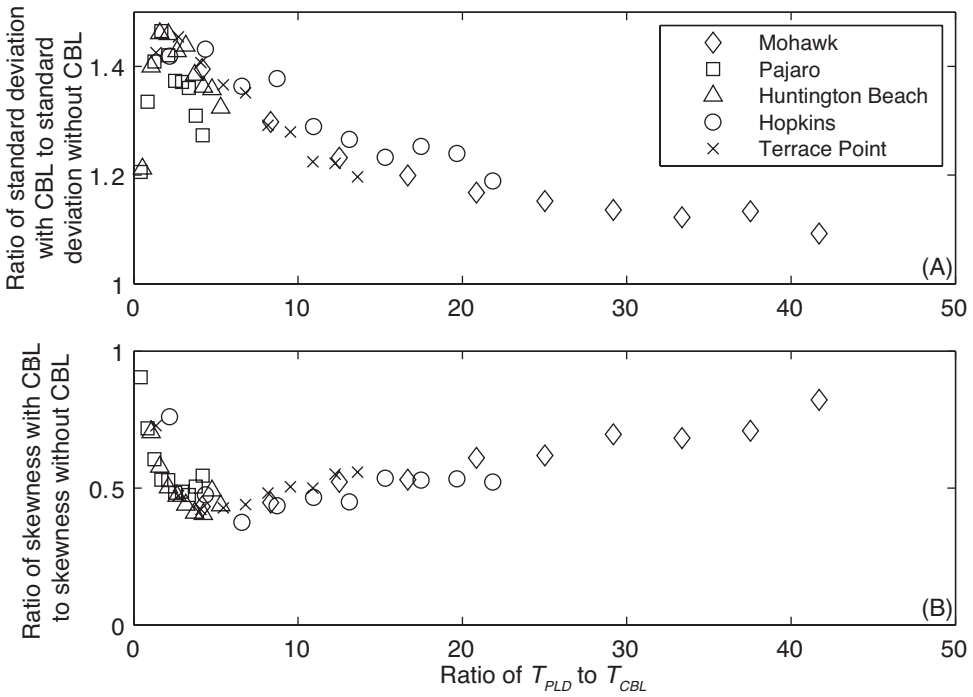

Figure 2.6. Ratio of PLD to the timescale of the CBL (T_{CBL}) plotted against the ratio of (A) standard deviation and (B) skewness, calculated from model runs with a CBL relative to no-CBL values. Model runs are for all sites and PLDs.

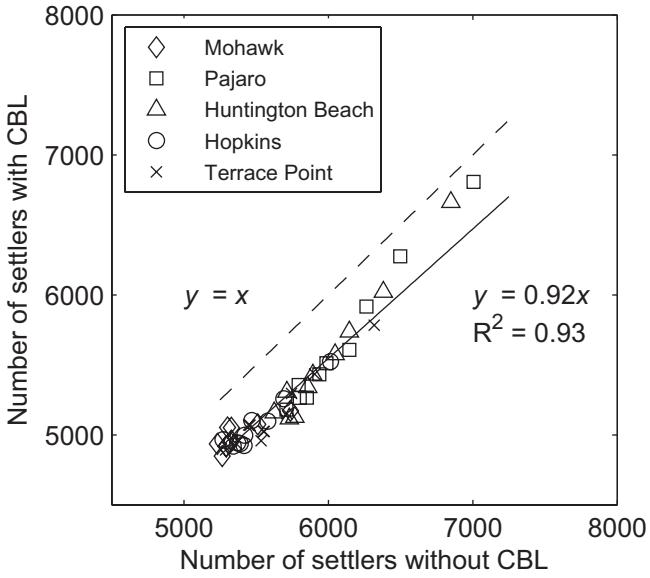

Figure 2.7. Total number of settling particles from model runs without a CBL plotted against total number of settlers resulting from model runs with a CBL, for all sites and PLDs. The 1:1 line is shown with a dashed line for reference.

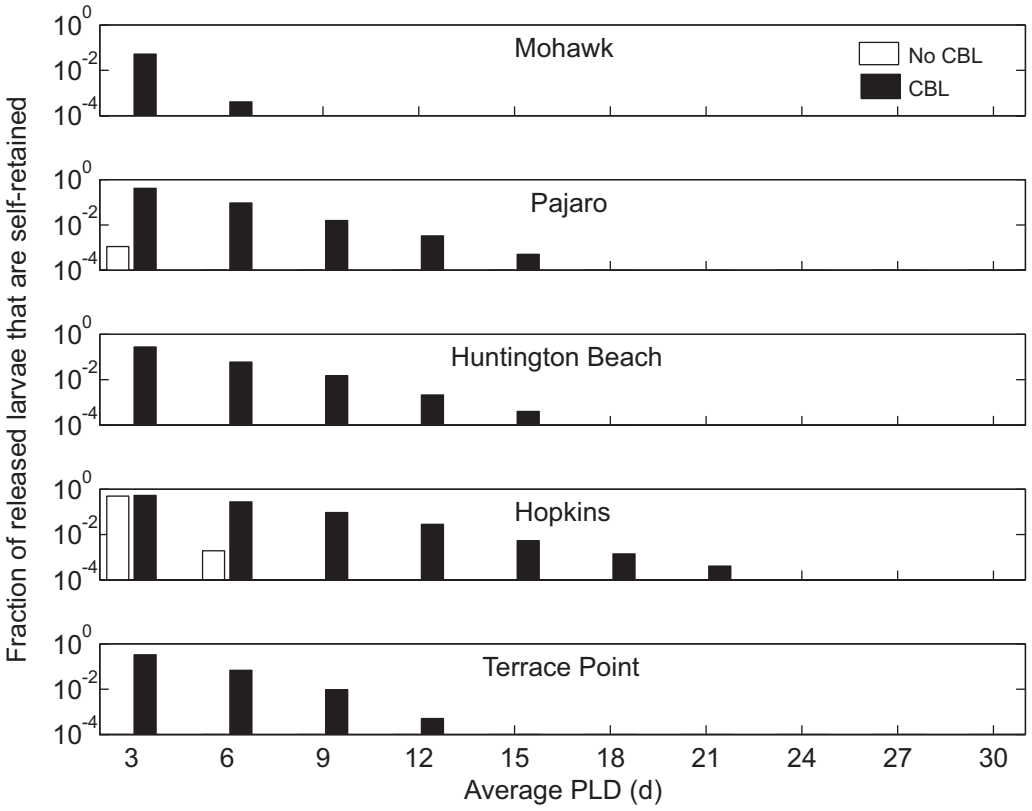

Figure 2.8. Fraction of released larvae that settled within 10 km of the release site (self-retention) in scenarios without a CBL (clear bars) and with a CBL (solid bars) for all sites and PLDs. The minimum self-retention measurable was 10^{-4}, as at least one settler out of 10^4 released larvae must return.

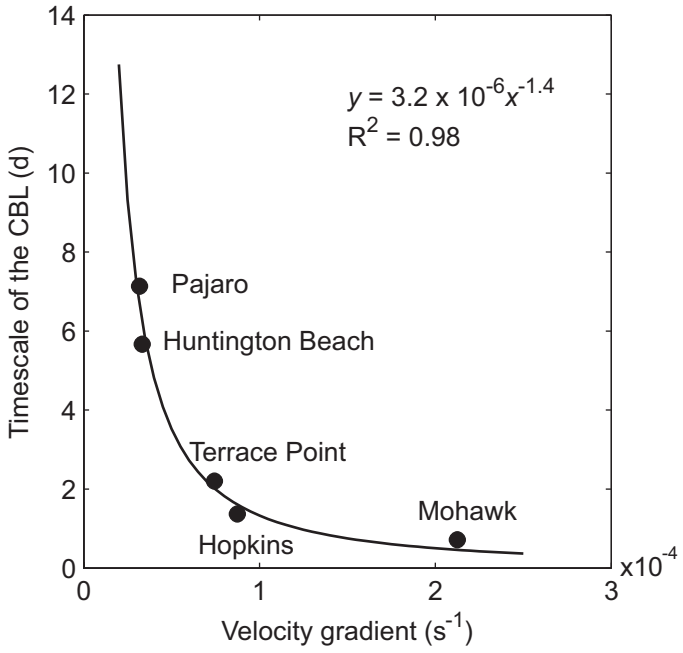

Figure 2.9. The velocity gradient, change in alongshore velocity over the width of the CBL, plotted against the timescale of the CBL, T_{CBL} for all five sites. An increase in the velocity gradient is associated with a decrease in T_{CBL}.

CHAPTER 3

Too close for comfort? Spatial differences in larval supply within the coastal boundary layer*

* Co-authors Seth H. Miller, Brian Gaylord, John L. Largier, and Steven G. Morgan

ABSTRACT

The dynamics of the very nearshore zone are a missing piece in understanding larval transport and delivery to suitable habitats, particularly for recruitment-limited populations. The distribution and abundance of larvae in the coastal ocean is variable in time and space, and depends on physical processes, such as circulation. Larvae also exhibit behaviors that can lead to biophysical interactions that increase larval retention nearshore and to natal sites. While recent evidence suggests that larvae are retained within 1-3 km of the shore, few studies continue these measurements inshore to assess supply adjacent to shoreline habitats. We measured cross-shore distributions of crustacean larvae between 250 and 1100 m from shore within the coastal boundary layer (CBL), a region of reduced alongshore flow, as well as physical factors that may influence larval distributions within the CBL. We found high larval abundance within the CBL, with a peak in abundance at 850 m from shore, which decreased in the very nearshore at the inner edge of the transect. We also found distinct larval communities between the CBL and the inshore edge of the CBL. These patterns persisted across sample dates, suggesting that the spatial structure of nearshore larval communities is robust to changes in physical conditions. While larval supply appears to be high within the CBL, the narrow band of water adjacent to the surf zone is largely unoccupied by larvae. Low larval supply adjacent to suitable habitats has important implications for the coupling of supply and recruitment and dynamics of shoreline populations.

INTRODUCTION

A central goal of ecology is to understand patterns of abundance and distribution of populations. Determining the key factors that drive population dynamics requires knowledge of population inputs (birth and immigration) and outputs (death and emigration). In marine systems, the process of larval dispersal adds additional complexity to quantifying population inputs as many marine organisms release dispersive larvae. While larval recruitment is a critical determinant of population structure (Gaines and Roughgarden 1985, Underwood and Fairweather 1989, Menge et al. 2004) and larval delivery has long been recognized for its role in driving population dynamics (Thorson 1946), larval transport pathways and connectivity are difficult to quantify due to the small size of larvae and the difficulty to track them (Levin 2006).

Larval recruitment to coastal populations relies not only on reproductive output of parent populations and post-settlement processes, but also on oceanographic processes that affect the dispersal and delivery of settlers. The concept of supply-side ecology (Lewin 1986) advanced our understanding of the influence oceanographic processes can have on larval recruitment and population dynamics (Cowen 1985, Gaines et al. 1985, Roughgarden et al. 1988, Morgan 2001, Underwood and Keough 2001), and studies of coastal populations suggested links between larval supply and settlement (Underwood et al. 1983, Connell 1985). If larval supply determines population inputs, we need to understand how larval supply varies over time and space and how physical factors, such as coastal circulation, affect supply.

There are relatively few studies that concurrently measure larval supply and settlement to explicitly link the two. Those that have measured both arrived at differing

conclusions regarding the coupling of supply and settlement: some found supply and settlement to be coupled (e.g., Gaines et al. 1985, Bertness et al. 1992, Gaines and Bertness 1992, Dudas et al. 2009) while others did not (e.g., Yoshioka 1982, McCulloch and Shanks 2003, Rilov et al. 2008). These differences may be due to the magnitude of recruitment, as larval supply can be a strong predictor of adult dynamics in regions where recruitment is limited (Connell 1985). Along the West Coast of North America there is a strong latitudinal gradient in recruitment, with much higher recruitment in Northern and Central Oregon than in Northern and Central California (Connolly et al. 2001). This gradient may be related to larval supply, and requires consideration of the distribution and abundance of larvae in the coastal ocean, as well as the physical drivers.

The recruitment-limited coast of California is a major upwelling region that may affect larval distributions. During times of strong equatorward winds, the predominant currents move equatorward and offshore, and can transport larvae in surface waters offshore. The potential for upwelling waters to move larvae offshore has been widely recognized (Yoshioka 1982, Roughgarden et al. 1988, Botsford et al. 1994), and is consistent with observations that larval settlement and supply in persistent upwelling regions is higher during relaxation events when wind speeds decrease or reverse directions (Farrell et al. 1991, Wing et al. 1995a, Wing et al. 1995b, Botsford 2001). Larvae also appear to be able to avoid offshore transport associated with upwelling through physical and behavioral mechanisms. Nearshore retention zones have been observed on mesoscales associated with topographic effects on coastal circulation (Graham and Largier 1997, Roughan et al. 2005), and are associated with higher larval abundances and settlement (Mace and Morgan 2006, Morgan et al. 2009a, Morgan et al.

2011). Avoidance of surface water by larvae favors retention and decreases offshore transport (Shanks and Brink 2005, Morgan et al. 2009b, Morgan et al. 2009c, Shanks and Shearman 2009, Morgan and Fisher 2010) and there is mounting evidence that larval concentrations are high close to shore, even in areas of strong upwelling that were thought to be recruitment-limited.

A number of recent studies measured larval abundance in cross-shore transects and found increases in abundance toward shore for a range of invertebrates and fishes (Borges et al. 2007, Tapia and Pineda 2007, Morgan et al. 2009b, Morgan et al. 2009c, Shanks and Shearman 2009). Morgan et al. (2009c) measured crustacean larval abundance from 1 km from shore out to the shelf break (30 km offshore) along the open coast of Northern California and found that the highest larval abundance was within 3 km from shore, suggesting that nearshore waters play an important role in larval ecology. The combination of larval behaviors (e.g., swimming and vertical migration) and nearshore processes may increase retention of larvae close to shore and to their natal site. Such retention is consistent with evidence across a range of species and systems that self-recruitment is higher and dispersal distances smaller than previously thought (Swearer et al. 2002, Levin 2006, Shanks 2009), and further emphasizes the importance of understanding the role of nearshore processes in larval supply and population dynamics.

Processes close to shore may reduce scales of dispersal in a number of ways. Adjacent to the shore within the surf zone, rip tides can create recirculation zones (MacMahan et al. 2010) and onshore wave transport can lead to accumulation of water-borne material (McPhee-Shaw et al. 2011). Outside of the surf zone conditions nearshore are still quite different from that farther offshore, in a region termed the coastal boundary

layer (CBL). As with any fluid boundary, net flow at the coastal margin is zero, with zero variability. However, there is strong, variable flow offshore. The CBL is the region of the coastal ocean where velocities transition from zero near the shore to free-stream conditions found offshore. The CBL has recently been quantified at several sites along the California coast (Nickols et al. in revision). Within the CBL, average alongshore velocity is an order of magnitude larger than cross-shore velocity (Lentz et al. 1999, Gaylord et al. 2007), and alongshore velocity increases as a function of distance from shore (Nickols et al. in revision). With decreased velocities adjacent to the coast, the CBL is a potential mechanism for reducing scales of dispersal in coastal populations (Nickols et al. in revision, Nickols et al. in prep). If a strategy of coastal larvae is to stay close to shore and to their natal site, benefits could accrue from remaining within the CBL. However, we currently lack knowledge regarding actual larval distributions within the CBL. Previous descriptions of larval distributions as a function of cross-shore distance stopped at the outer edge of the CBL (Morgan et al. 2009b, Morgan et al. 2009c), did not sample throughout the CBL (McQuaid and Phillips 2000, Shanks and Shearman 2009), or sampled over a small temporal scale (Tapia and Pineda 2007).

The goals of this study were to address the following questions: 1) Does larval abundance increase with distance from shore within the CBL? 2) Are there differences in larval communities close to shore, i.e. are different larvae found inshore versus offshore? and 3) what plays a bigger role in describing the variability in larval supply: time, potentially due to shifting physical processes transporting larvae, or space, potentially due to differences in physical processes with distance to shore? We recognize that we are unable to ascribe particular mechanisms to patterns observed within the CBL; rather, our

aim is to present the first descriptions of the distribution and variability in larval communities within the CBL. We hope that this study will also inform a methodological question of where supply should be measured when concerned with relationships between settlement and supply to ultimately address questions about marine population dynamics in regions of recruitment limitation.

METHODS

Study system

This study was conducted along the open coast in northern California, USA, near Bodega Head, California (Fig. 3.1), a region characterized by strong seasonal upwelling during spring and summer that drives the predominant currents equatorward and offshore (Winant et al. 1987, Largier et al. 1993). When the winds weaken (relax) or reverse directions, currents move poleward, often responding within a day or less in the nearshore (Send et al. 1987). These nearshore currents observed previously on the scale of kilometers are slower than currents farther offshore, have a higher tendency to move poleward (Kaplan et al. 2005), and are associated with increases in invertebrate settlement (Wing et al. 1995a, Wing et al. 1995b). Crustacean larvae are present during both relaxation and upwelling conditions within areas of topographic retention and along the open coast, and are retained nearshore (within 1-3 km) via a combination of physical and behavioral mechanisms (Morgan et al. 2009c, Morgan and Fisher 2010). The present study addresses waters between 1 km and hundreds of meters from shore.

Our study focused on larval crustaceans, which are the most well-studied meroplankton in this region, and data from other studies that sampled farther offshore were available for comparison. Larval crustacean abundance is at its highest during the spring and summer. Barnacle species from both subtidal (*Balanus crenatus*, *B. nubilus*) and intertidal (*B. glandula*, *Chthamalus* spp., and *Pollicipes polymerus*) habitats are common in this region (Morgan and Fisher 2010). Barnacles molt through 6 larval stages (nauplii) and a postlarval stage (cyprid) and spend about 2 to 4 wk in the water column (Strathmann 1987). Barnacle larval release generally begins in spring (Gaines et al. 1985, Strathmann 1987) and is continuous through the summer months (Shanks and Eckert 2005). Crab larvae in this region spend weeks to months in the plankton and peak recruitment for most species is during the spring and summer (Shanks and Eckert 2005, Mace and Morgan 2006). The most common taxa include members of the families Pinnotheridae, Porcellanidae, Cancridae, Majidae.

Larval samples

Cross-shore distributions of nearshore larvae were sampled during six daytime cruises using a 0.5 m diameter, 200 micron mesh net equipped with a mechanical flow meter (Model 2030, General Oceanics Inc., Miami, Florida). The net was modified with a sled to accommodate towing along the bottom. Cruise dates spanned three months during the upwelling season, from May through July 2010, occurring approximately every 10 days (Fig. 3.2), and under a variety of oceanographic conditions. We sampled four stations in a cross-shore transect along the 10, 15, 22, and 30 m isobaths, corresponding

to approximately 250, 425, 850, and 1100 m from shore (Fig. 3.1). We conducted a single 10 minute oblique tow at each station, which sampled from the bottom to the surface of the water column. Larvae were sorted and identified to species, or the lowest taxonomic group possible, and developmental stage. Larval abundances were calculated per m^3 to standardize across stations.

Physical data

To provide a physical context to the nearshore plankton distributions we measured currents, temperature, salinity, and winds. Current speed and direction were measured throughout the water column using moored acoustic Doppler current profilers (Workhorse Sentinel ADCP, 1200 kHz; Teledyne RD Instruments, Poway, California). Instruments were located on the 10, 15, and 22 m isobaths near the starting positions of plankton tows. The ADCPs collected 1 minute bursts of 0.75 Hz velocity data every two minutes in 1 m vertical bins that typically extended from ~1.5 m above the bottom to ~ 1.5 m below the surface. The velocity record at the 10 m station ended on 10 June 2012. To quantify general velocity patterns the raw velocity time series were depth-averaged, rotated onto their principal axes, and low-pass filtered with a 33-h cutoff to remove dominant tidal motions (Rosenfeld 1983). The major principal axes aligned parallel to shore along-isobath, corresponding to an angle of 300˚.

Bottom temperature was recorded at the ADCP mooring sites every minute over the duration of the study at the 10, 15, and 22 m stations, and temperatures at depths of 4, 7, 10, and 14 m were recorded at the 15 m station (SBE 37 and SBE 39, Sea-Bird

Electronics, Bellevue, Washington). During cruises, temperature, salinity, and fluorescence were profiled at each station throughout the water column using a conductivity, temperature, and depth profiler (SBE 19-Plus, Sea-Bird Electronics, Bellevue, Washington).

Wind data during this study were available from an anemometer located onshore at the Bodega Marine Laboratory at a height of 20 m (38° 19' 3.35" N, 123° 4' 17.20" W; RM Young 05103 Wind Monitor; data available online http://bml.ucdavis.edu/boon/).

Data analysis

To address whether or not larval abundance varies with distance from shore we plotted the mean cross-shore distributions of all larvae. We also examined patterns of cross-shore abundance for crab and barnacle larvae, as well as cross-shore patterns according to larval stage. Further, we assessed whether larval assemblages were structured by space and time. All statistical analyses were done using the multivariate statistical software package PRIMER (version 6.1.10). We determined whether larval assemblages changed with distance from shore and with sampling date using nonparameteric analysis of similarity (ANOSIM) and hierarchical cluster analysis and ordination. Data were fourth-root transformed to reduce the heterogeneity of variance among samples and assembled into a Bray-Curtis dissimilarity matrix with a dummy variable of 1. The resultant dendrogram was tested for group differences using a similarity profile test (SIMPROF), and the percentage contribution (SIMPER) of each species and stage to the significant clusters was assessed to classify species-stage

combinations by their cross-shore distributions and sampling date. We used nonmetric multidimensional scaling (NMDS) to examine separation of communities according to sample date and distance from shore. To assess if community composition was structured in space or time we repeated these analyses on untransformed data that were normalized by total sample abundance. For all analyses, when there was significant structure among samples we then determined which species and stages contributed to the patterns.

RESULTS

Physical conditions

During the study period we captured a variety of oceanographic conditions, including upwelling, relaxation, and post-relaxation circulations (Fig. 3.2; Table 3.1). However, our larval sampling dates generally occurred during low wind conditions due to logistical constraints. During sampling dates, alongshore wind speed ranged from -8 m s^{-1}, indicative of northwesterly winds, to 8 m s^{-1}, indicative of southeasterly winds (Fig. 3.2A) and depth-averaged alongshore currents were northward (Fig. 3.2B). In general, depth-averaged alongshore current velocities measured at inshore locations (10 and 15 m isobaths) were lower than velocities measured at the most offshore instrument on the 22 m isobath (Fig. 3.2B), characteristic of a coastal boundary layer. Exceptions occurred during times of sustained upwelling favorable winds (e.g., 6 June and 7 July) and flow reversals, when currents at the inshore stations were similar to or exceeded current velocities at the 22 m station. Bottom temperatures were less than 10°C and were similar across stations during the first five sampling dates, after which temperatures substantially

increased, reaching up to 14°C at the shallowest station (Fig. 3.2C). Stratification at the 15 m station was weak throughout most of the sampling dates, and became stronger in early to mid July (Fig. 3.2D).

Larval abundance

We found larvae of 21 crustacean species during our study. The most offshore station, at the 30 m isobath, had the highest number of species, with 10 species on average as compared to 6-7 species at the other stations. Throughout the study, larvae were most abundant along the 22 m isobath, 850 m from shore (Fig. 3.3A). This pattern was driven by high abundance of barnacle larvae at that station (Fig. 3.3B). Early, middle and late stage barnacle larvae were present at all stations with the highest abundance at the 22 m station (Fig. 3.4A). Barnacle post-larvae (cyprids) were found in similar abundance across stations. Crab larvae were most abundant near the 30 m isobath, 1100 m from shore (Fig. 3.3C). All larval crab stages had highest abundance at the two outer stations, although early stage crab larvae dominated the samples and abundance decreased with increasing stage (Fig. 3.4B). Very few crab larvae were found at the inner stations, and the majority of those were early stage larvae.

Larval communities

Larval assemblages within the CBL differed among stations (2-way ANOSIM $\rho_{av} = 0.322$, $p = 0.017$) and were similar among dates. Because larval assemblages were not

structured by date we performed a 1-way ANOSIM to detect differences among assemblages at the different stations. The innermost station drove differences between assemblages, and was significantly different from the two outer stations (1-way ANOSIM pairwise test 10 vs. 30: $R = 0.463$, $p < 0.01$; 10 vs. 22: $R = 0.609$, $p < 0.01$). These differences were echoed in the dendrogram from the cluster analysis and the nonmetric multidimensional scaling (NMDS) ordination, which both revealed spatial structure with two main clusters: an inshore cluster defined by low numbers of larvae, with samples primarily from inshore stations, and an offshore cluster defined by high numbers of larvae, with samples primarily from offshore stations (Fig. 3.5).

The patterns of the two main taxa we investigated, barnacles and crabs, differed. Crab larval assemblages by themselves did not differ by station or date, and barnacle larval assemblages differed by station and by sampling date (2-way ANOSIM station $\rho_{av} = 0.322$, $p = 0.02$; date $\rho_{av} = 0.35$, $p < 0.01$). The dendrogram from the cluster analysis and the NMDS ordination revealed two main clusters of barnacle samples: an early season, mostly offshore, cluster composed of samples from all stations during May and samples from the offshore stations during June and July, and an inshore late season cluster with primarily inshore samples, and samples from the late June through July (Fig. 3.6). Samples in the early season, offshore, assemblage had barnacle larval abundances as high as 7200 larvae m^{-3}, whereas the late season, inshore, assemblage had barnacle larval abundances of less than 500 larvae m^{-3}.

We also analyzed changes in community composition over time and space. We divided our larval counts (both species and stage) by the total larval number of larvae in each sample, providing a fraction of the total sample for each species and stage, to

normalize the data for differences in larval abundance across time. Larval community composition within the CBL differed mostly among stations, but also by date (2-way ANOSIM station $\rho_{av} = 0.394$, $p < 0.01$; date $\rho_{av} = 0.282$, $p = 0.026$). Although the effect of date was significant, this is largely due to one particular date evident in subsequent analyses. The dendrogram from the cluster analysis and the NMDS ordination showed three distinct communities (Fig. 3.7). There was a distinct community in the inshore samples (10 and 15 m stations) on 9 June that were 92% similar, and an additional inshore community primarily containing samples from the most inshore station that were 68% similar (Fig. 3.7). An offshore community contained nearly all the samples from the offshore stations, as well as the 15 m station, and these samples were 67% similar.

The barnacles *Balanus crenatus* and *Balanus nubilus* dominated larval community composition and drove the differences between community clusters. The community found at the inshore stations on 9 June (Fig. 3.7) was composed of > 75% *B. crenatus* cyprids. All other samples were composed of 30% or less *B. crenatus* cyprids. In addition, the 9 June inshore community contained < 16% *B. crenatus* nauplii (early, middle, and late stage), compared to the offshore community which was composed of 39-99% *B. crenatus* nauplii. The larger cluster of inshore communities also had low percentages of *B. crenatus* nauplii, ranging from 3-37%, as well as a high proportion of *B. nubilus* cyprids, which ranged from 11-74%, as opposed to the offshore community, which was composed of <1-10% *B. nubilus* cyprids. Crab larvae were found in nearly all samples, but did not generally makeup a large percentage of community composition, except in the larger inshore cluster which was composed of 21% crab larvae, compared to

an average of <0.1% crab larvae in the 9 June inshore community, and 4% crab larvae in the offshore community.

DISCUSSION

Spatial variability of larval supply within the CBL

Consistent with previous work in this study region (Morgan et al. 2009b, Morgan et al. 2009c, Morgan and Fisher 2010), we found high abundances of crustacean larvae nearshore across sampling days under different oceanographic conditions. However, we found a striking pattern of decreased larval abundance in the very nearshore (< 500 m from shore). While there were differences among taxa in cross-shore distributions, with barnacle abundance peaking at 850 m from shore and crab abundance highest 1100 m from shore, all crustaceans were at their lowest abundance at the inshore station in our transect. We are unable to assess whether larvae are being transported away from the inner portion of the nearshore or they are actively avoiding this region. However, the consistency of low larval abundance across sampling days and oceanographic conditions suggests that larvae are able to avoid the inner edge of the CBL regardless of background transport conditions. These patterns are similar to that measured in Southern California, a region of weak upwelling. Tapia and Pineda (2007) measured larval concentrations of *Balanus glandula* and *Chthamalus* spp. at three cross-shore stations within 1100 m from shore over a period of 7 d. While concentrations of most larval stages of *B. glandula* were not different among stations, concentrations of third through sixth stage *Chthamalus* nauplii were significantly lower at the innermost station, 300 m from shore (Tapia and

Pineda 2007). Even over a short temporal period barnacle concentrations showed spatial structure and potential avoidance of very nearshore waters by barnacle nauplii.

Larval retention within the CBL

Despite low concentrations of larvae at the inner edge of the CBL, the high concentrations of all larval stages of barnacles at the 15, 22, and 30 m stations suggest that many barnacle nauplii may be retained within the CBL and develop in nearshore waters. All larval stages of crabs were found at the outer two stations and could also complete development within the CBL. These findings are consistent with other studies in both weak and strong upwelling regions that found high abundances of all larval stages within a few kilometers from shore (Tapia and Pineda 2007, Morgan et al. 2009b, Morgan et al. 2009c, Shanks and Shearman 2009, Morgan and Fisher 2010). Crustacean larvae exhibit depth preferences that can aid nearshore retention. By remaining near the bottom larvae can take advantage of slower velocities in the bottom boundary layer (in both the along- and cross-shore directions), as well as avoid offshore transport in the surface Ekman layer (Shanks and Shearman 2009, Morgan and Fisher 2010). We could not test the hypothesis that larvae were actively staying within the CBL via depth preferences, as our samples were depth-integrated, and future studies of larvae within the CBL should address this question.

Inshore and offshore communities within the CBL

Larval communities in the very nearshore and the CBL were distinct. While some features of the communities changed with time, the predominant factor that explained the structure of these communities was space. In addition, not only was there spatial structure when considering larval abundance, but there was spatial structure in community composition as well. This spatial structure appears despite the lack of a clear difference in physical parameters between the innermost station and those further offshore (Fig. 3.2); although more data would be needed to fully address the physical differences between stations.

The spatial boundary between inshore and offshore communities within the CBL is dynamic. Larval assemblages on half of the sampling dates at the 15 m station were most similar to the 10 m station, and on the other half of sampling dates were more similar to the 22 m station. There is no clear physical difference between these groupings of days apparent from our data, as they spanned conditions. One possibility of a physical factor that may influence the demarcation of the inshore community is the width of the surf zone, which is itself a dynamic boundary, dependent on the significant wave height and tidal elevation (Lentz et al. 1999, Brown et al. 2009). Surf zone characteristics have recently been shown to impact shoreline settlement of invertebrates, with low settlement observed at reflective beaches, which are characterized by high beach slopes and standing waves, and are thought to have reduced cross-shore exchange (Shanks et al. 2010). Rocky shores are hypothesized to be similar to reflective beaches, and if so, the associated reduction in cross-shore exchange may explain low settlement at some locations, and potentially low abundances of larvae in the very nearshore (Shanks et al. 2010).

In addition to potential physical differences between the habitat of the inshore and offshore communities, there may be biological factors leading to the observed spatial structure. Within the narrow band of very nearshore water there may be higher predation than further offshore. Habitat along the 10 m isobath at our study site features rocky substrate with some areas supporting stands of the bull kelp, *Nereocystis luetkeana*. In Central California, larval abundances were found to be negatively correlated with kelp density, and decreased larval abundance on the inshore edge of kelp forests was attributed to predation (Gaines and Roughgarden 1987). While the kelp in this region was not nearly as dense as the giant kelp (*Macrocystis pyrifera*) beds in Central California, predation is still a possible explanation for decreased abundance at the most inshore station of our study.

Implications of cross-shelf larval structure within the CBL

Larvae are clearly spending time within the coastal boundary layer, and some may even complete their entire development within the CBL, which can impact estimates of population connectivity. During their time in the CBL, larvae are exposed to slower moving alongshore flows than further offshore, which will have an impact on overall dispersal distance (Nickols et al. in revision, Nickols et al. in prep). Although we did not have current velocity measurements beyond the 22 m isobath, we know that current velocities are faster further offshore from measurements of surface currents from high-frequency radar (data not shown). The radar domain begins 2 km offshore, and generally has high agreement with measurements from ADCPs (Kaplan et al. 2005). Estimates of

dispersal distance in this region should therefore consider current velocities within 1 km or less from shore, as this is where the majority of larvae appear to be concentrated. Such consideration may improve estimates of dispersal distance derived from pelagic larval durations, which are often larger than dispersal distances estimated from genetics, tagging, and natural tracers (Palumbi 2004, Jones et al. 2009, Shanks 2009). Refining our understanding of dispersal distances will improve our ability to accurately model population dynamics and assess population persistence (Botsford et al. 2009, White et al. 2010).

The coast of Northern California generally has lower recruitment than other regions along the west coast of North America (Connolly et al. 2001), and the outstanding question has been whether or not this pattern is linked to larval supply. There is evidence that larval supply is diminished because larvae are forced offshore due to persistent upwelling (e.g., Roughgarden et al. 1988), however, numerous studies now indicate that at least some larvae are retained nearshore, and that larvae are found nearshore in times of both upwelling and relaxation (Tapia and Pineda 2007, Morgan et al. 2009b, Morgan et al. 2009c, Shanks and Shearman 2009, Morgan and Fisher 2010). We also found high abundance of larvae close to shore in an area of persistent upwelling not previously viewed as a retentive zone.

The sum of the work addressing larval supply in a region of high upwelling reflects our evolving knowledge of coastal upwelling and larval ecology. Roughgarden et al.'s (1988) seminal work on this topic showed that the strength of the upwelling index was related to how far offshore larval barnacles were found. The larval data available for this study came from cross-shore transects of zooplankton that began at a distance of 5

miles from the coast, collected by the California Cooperative Oceanic Fisheries Investigation (CalCOFI) (Roughgarden et al. 1988). An important contribution of recent work has been to investigate gradients in larval abundance closer to shore. Our physical understanding of coastal upwelling has also advanced, largely due to the increase in studies of the inner shelf (Lentz 1994, Austin and Lentz 2002). Reductions in cross-shelf circulation within the inner shelf have been observed during upwelling, and waters within 3-6 km from shore, the region now associated with high larval abundance, may not be heavily influenced by wind-driven upwelling (Kirincich et al. 2005). Finally, there is now greater appreciation for the role that larval behavior may play in the distribution of coastal larvae. Through depth preferences, vertical migration, and swimming, larvae may interact with physical gradients, such as reduced flow in the CBL, to increase retention and reduce offshore transport (Leis 2006, Morgan and Fisher 2010).

Ultimately, although we found high larval abundance in the CBL, we did not see a similar larval pool in the very nearshore, adjacent to shoreline rocky habitat. Most studies that measured larval supply as a function of distance from shore did not continue measurements to the shore (Morgan et al. 2009b, Morgan et al. 2009c, Shanks and Shearman 2009). Ours is the first study to examine the spatial structure of larvae throughout the nearshore zone in a recruitment-limited area. While high abundances at the 22 m station by itself may suggest that larval supply is not limiting shoreline recruitment in this region, we consistently found low abundances of larvae at the innermost station, the station that should be supplying larvae to the shore. This mismatch raises important questions surrounding the mechanisms leading to lower abundances adjacent to the shore, while also highlighting methodological concerns of studies that

explore the potential link between supply and settlement. This nearshore zone will be essential to study as we continue to address recruitment limitation and population dynamics of coastal systems and try to understand where have all the larvae gone.

ACKNOWLEDGMENTS

We thank J. Demmer, R. Fontana, and N. Weidberg for assistance in the field as well as D. Dann, M. Robart, and J. Herum for help with deployments of oceanographic instrumentation. J. Fisher provided guidance and feedback. This work was funded by California Sea Grant (NA08AR4170669) and the National Science Foundation (OCE-0927196). K.J. Nickols was also supported by a Bodega Marine Laboratory Graduate Student Fellowship.

LITERATURE CITED

Austin, J. and S. Lentz. 2002. The inner shelf response to wind-driven upwelling and downwelling. Journal of Physical Oceanography **32**:2171-2193.

Bertness, M., S. Gaines, E. Stephens, and P. Yund. 1992. Components of recruitment in populations of the acorn barnacle *Semibalanus balanoides* (Linnaeus) Journal of Experimental Marine Biology and Ecology **156**:199-215.

Borges, R., R. Ben-Hamadou, M. A. Chicharo, P. Re, and E. J. Goncalves. 2007. Horizontal spatial and temporal distribution patterns of nearshore larval fish assemblages at a temperate rocky shore. Estuarine, Coastal and Shelf Science **71**:412-428.

Botsford, L. W., C. Moloney, A. Hastings, J. L. Largier, T. Powell, K. Higgins, and J. Quinn. 1994. The influence of spatially and temporally varying oceanographic conditions on meroplankton metapopulations. Deep-Sea Research II **41**:107-145.

Botsford, L. W. 2001. Physical influences on recruitment to California Current invertebrate populations on multiple scales. ICES Journal of Marine Science **58**:1081-1091.

Botsford, L. W., J. W. White, M. A. Coffroth, C. B. Paris, S. Planes, T. L. Shearer, S. R. Thorrold, and G. P. Jones. 2009. Connectivity and resilience of coral reef metapopulations in marine protected areas: matching empirical efforts to predictive needs. Coral Reefs **28**:327-337.

Brown, J., J. MacMahan, A. Reniers, and E. Thornton. 2009. Surf zone diffusivity on a rip-channeled beach. Journal of Geophysical Research **114**:C11015.

Connell, J. H. 1985. The consequences of variation in initial settlement vs. post-settlement mortality in rocky intertidal communities. Journal of Experimental Marine Biology and Ecology **93**:11-45.

Connolly, S. R., B. A. Menge, and J. Roughgarden. 2001. A latitudinal gradient in recruitment of intertidal invertebrates in the northeast Pacific Ocean. Ecology **82**:1799-1813.

Cowen, R. 1985. Large-scale pattern of recruitment by the labrid, *Semicossyphus pulcher*: Causes and implications Journal of Marine Research **43**:719-742.

Dudas, S. E., G. Rilov, J. Tyburczy, and B. A. Menge. 2009. Linking larval abundance, onshore supply and settlement using instantaneous versus integrated methods. Marine Ecology Progress Series **387**:81-95.

Farrell, T., D. Bracher, and J. Roughgarden. 1991. Cross-shelf transport causes recruitment to intertidal populations in central California Limnology and Oceanography **36**:279-288.

Gaines, S. and M. Bertness. 1992. Dispersal of juveniles and variable recruitment in sessile marine species. Nature **360**:579-580.

Gaines, S., S. Brown, and J. Roughgarden. 1985. Spatial variation in larval concentrations as a cause of spatial variation in settlement for the barnacle, *Balanus glandula*. Oecologia **67**:267-272.

Gaines, S. and J. Roughgarden. 1987. Fish in offshore kelp forests affect recruitment to intertidal barnacle populations. Science **235**:479-481.

Gaines, S. D. and J. Roughgarden. 1985. Larval settlement rate: A leading determinant of structure in an ecological community of the marine intertidal zone. Proceedings of the National Academy of Sciences (USA) **82**:3707-3711.

Gaylord, B., J. H. Rosman, D. C. Reed, J. R. Koseff, J. Fram, S. MacIntyre, K. Arkema, C. McDonald, M. A. Brzezinski, J. L. Largier, S. G. Monismith, P. T. Raimondi, and B. Mardian. 2007. Spatial patterns of flow and their modification within and around a giant kelp forest. Limnology and Oceanography **52**:1838-1852.

Graham, W. and J. Largier. 1997. Upwelling shadows as nearshore retention sites: The example of northern Monterey Bay. Continental Shelf Research **17**:509-532.

Jones, G. P., G. R. Almany, G. R. Russ, P. F. Sale, R. S. Steneck, M. J. H. Oppen, and B. L. Willis. 2009. Larval retention and connectivity among populations of corals and reef fishes: history, advances and challenges. Coral Reefs **28**:307-325.

Kaplan, D. M., J. Largier, and L. Botsford. 2005. HF radar observations of surface circulation off Bodega Bay (northern California, USA). Journal of Geophysical Research **110**:C10020.

Kirincich, A., J. Barth, B. Grantham, B. Menge, and J. Lubchenco. 2005. Wind-driven inner-shelf circulation off central Oregon during summer. Journal of Geophysical Research-Oceans **110**:C10S03.

Largier, J. L., B. A. Magnell, and C. D. Winant. 1993. Subtidal circulation over the Northern California shelf. Journal of Geophysical Research **98**:18147-18179.

Leis, J. M. 2006. Are larvae of demersal fishes plankton or nekton? Advances in Marine Biology **51**:57-141.

Lentz, S., R. Guza, S. Elgar, F. Feddersen, and T. Herbers. 1999. Momentum balances on the North Carolina inner shelf. Journal of Geophysical Research-Oceans **104**:18205-18226.

Lentz, S. J. 1994. Current dynamics over the northern California inner shelf. Journal of Physical Oceanography **24**:2461-2478.

Levin, L. 2006. Recent progress in understanding larval dispersal: new directions and digressions. Integrative and Comparative Biology **46**:282-297.

Lewin, R. 1986. Supply-side ecology Science **234**:25-27.

Mace, A. J. and S. G. Morgan. 2006. Larval accumulation in the lee of a small headland: implications for the design of marine reserves. Marine Ecology Progress Series **318**:19-29.

MacMahan, J., J. Brown, J. Brown, E. Thornton, A. Reniers, T. Stanton, M. Henriquez, E. Gallagher, J. Morrison, M. J. Austin, T. M. Scott, and N. Senechal. 2010. Mean Lagrangian flow behavior on an open coast rip-channeled beach: A new perspective. Marine Geology **268**:1-15.

McCulloch, A. and A. L. Shanks. 2003. Topographically generated fronts, very nearshore oceanography and the distribution and settlement of mussel larvae and barnacle cyprids. Journal of Plankton Research **25**:1427-1439.

McPhee-Shaw, E. E., K. J. Nielsen, J. L. Largier, and B. A. Menge. 2011. Nearshore chlorophyll-a events and wave-driven transport. Geophysical Research Letters **38**:1-5.

McQuaid, C. D. and T. E. Phillips. 2000. Limited wind-driven dispersal of intertidal mussel larvae: in situ evidence from the plankton and the spread of the invasive

species *Mytilus galloprovincialis* in South Africa. Marine Ecology Progress Series **201**:211-220.

Menge, B. A., C. Blanchette, P. Raimondi, T. Freidenburg, S. Gaines, J. Lubchenco, D. Lohse, G. Hudson, M. Foley, and J. Pamplin. 2004. Species interaction strength: Testing model predictions along an upwelling gradient. Ecological Monographs **74**:663-684.

Morgan, S. G. and J. L. Fisher. 2010. Larval behavior regulates nearshore retention and offshore migration in an upwelling shadow and along the open coast. Marine Ecology Progress Series **404**:109-126.

Morgan, S. G. 2001. The larval ecology of marine communities.*in* M. D. Bertness, S. D. Gaines, and M. E. Hay, editors. Marine Community Ecology. Sinauer, Sunderland, Massachusetts.

Morgan, S. G., J. L. Fisher, and J. L. Largier. 2011. Larval retention, entrainment and accumulation in the lee of a small headland: recruitment hotspots along windy coasts. Limnology and Oceanography **56**:161-178.

Morgan, S. G., J. L. Fisher, and A. Mace. 2009a. Larval recruitment in a region of strong, persistent upwelling and recruitment limitation. Marine Ecology Progress Series **394**:79-99.

Morgan, S. G., J. L. Fisher, A. Mace, L. Akins, A. M. Slaughter, and S. M. Bollens. 2009b. Cross-shelf distributions and recruitment of crab postlarvae in a region of strong upwelling. Marine Ecology Progress Series **380**:173-185.

Morgan, S. G., J. L. Fisher, S. H. Miller, S. T. McAfee, and J. L. Largier. 2009c. Nearshore larval retention in a region of strong upwelling and recruitment limitation. Ecology **90**:3489-3502.

Nickols, K. J., B. Gaylord, and J. L. Largier. *In revision*. The coastal boundary layer: Predictable current structure decreases alongshore transport and alters scales of dispersal. Marine Ecology Progress Series.

Nickols, K. J., J. W. White, J. L. Largier, and B. Gaylord. *In prep*. Importance of nearshore oceanography for larval dispersal and self-replenishment of coastal populations. American Naturalist.

Palumbi, S. R. 2004. Marine reserves and ocean neighborhoods: The spatial scale of marine populations and their management. Annual Review of Environmental Resources **29**:31-68.

Rilov, G., S. E. Dudas, B. A. Menge, B. A. Grantham, J. Lubchenco, and D. R. Schiel. 2008. The surf zone: a semi-permeable barrier to onshore recruitment of invertebrate larvae? Journal of Experimental Marine Biology and Ecology **361**:59-74.

Rosenfeld, L. 1983. CODE-2: Moored array and large-scale data report. WHOI Technical Report 85-35:1-242.

Roughan, M., A. Mace, J. L. Largier, S. G. Morgan, J. L. Fisher, and M. Carter. 2005. Subsurface recirculation and larval retention in the lee of a small headland: A variation on the upwelling shadow theme. Journal of Geophysical Research-Oceans **110**:C10027.

Roughgarden, J., S. Gaines, and H. Possingham. 1988. Recruitment dynamics in complex life-cycles. Science **241**:1460-1466.

Send, U., R. C. Beardsley, and C. D. Winant. 1987. Relaxation from upwelling in the Coastal Ocean Dynamics Experiment. Journal of Geophysical Research **92**:1683-1698.

Shanks, A. L. 2009. Pelagic larval duration and dispersal distance revisited. Biological Bulletin **216**:373-385.

Shanks, A. L. and L. Brink. 2005. Upwelling, downwelling, and cross-shelf transport of bivalve larvae: test of a hypothesis. Marine Ecology Progress Series **302**:1-12.

Shanks, A. L. and G. L. Eckert. 2005. Population persistence of California Current fishes and benthic crustaceans: A marine drift paradox. Ecological Monographs **75**:505-524.

Shanks, A. L., S. G. Morgan, J. MacMahan, and A. J. H. M. Reniers. 2010. Surf zone physical and morphological regime as determinants of temporal and spatial variation in larval recruitment. Journal of Experimental Marine Biology and Ecology **392**:140-150.

Shanks, A. L. and R. K. Shearman. 2009. Paradigm lost? Cross-shelf distributions of intertidal invertebrate larvae are unaffected by upwelling or downwelling. Marine Ecology Progress Series **385**:189-204.

Strathmann, M. F. 1987. Reproduction and development of marine invertebrates of the northern Pacific Coast. University of Washington Press, Seattle, WA.

Swearer, S., J. S. Shima, M. E. Hellberg, S. Thorrold, G. Jones, D. R. Robertson, S. G. Morgan, K. A. Selkoe, G. M. Ruiz, and R. R. Warner. 2002. Evidence of self-

recruitment in demersal marine populations. Bulletin of Marine Science **70**:S251-S271.

Tapia, F. J. and J. Pineda. 2007. Stage-specific distribution of barnacle larvae in nearshore waters: potential for limited dispersal and high mortality rates. Marine Ecology Progress Series **342**:177-190.

Thorson, G. 1946. Reproduction and larval development of Danish marine bottom invertebrates. Meddelelser fra Kommissionen for Hovundersoegelser Serie Plankton **4**:1-523.

Underwood, A. and P. Fairweather. 1989. Supply-side ecology and benthic marine assemblages. Trends in Ecology and Evolution **4**:16-20.

Underwood, A. J., E. J. Denley, and M. J. Moran. 1983. Experimental analyses of the structure an dynamics of mid-shore rocky intertidal communities in New South Wales. Oecologia **56**:202-219.

Underwood, A. J. and M. J. Keough. 2001. Supply-side ecology: the nature and consequences of variations in recruitment of intertidal organisms. *in* M. D. Bertness, S. D. Gaines, and M. E. Hay, editors. Marine community ecology. Sinauer, Sunderland, Massachusetts, USA.

White, J., L. Botsford, A. Hastings, and J. Largier. 2010. Population persistence in marine reserve networks: incorporating spatial heterogeneities in larval dispersal. Marine Ecology Progress Series **398**:49-67.

Winant, C. D., R. C. Beardsley, and R. E. Davis. 1987. Moored wind, temperature, and current observations made during Coastal Ocean Dynamics Experiments 1 and 2

over the Northern California continental shelf and upper slope. Journal of Geophysical Research **92**:1569-1604.

Wing, S., L. Botsford, J. L. Largier, and L. Morgan. 1995a. Spatial structure of relaxation events and crab settlement in the northern California upwelling system. Marine Ecology Progress Series **128**:199-211.

Wing, S., J. L. Largier, L. Botsford, and J. Quinn. 1995b. Settlement and transport of benthic invertebrates in an intermittent upwelling region. Limnology and Oceanography **40**:316-329.

Yoshioka, P. M. 1982. Role of planktonic and benthic factors in the population dynamics of the bryozoan *Membranipora membranacea*. Ecology **63**:457-468.

	5/17/10	5/27/10	6/9/10	6/25/10	7/4/10	7/14/10
Winds	Downwelling	Relaxation	Upwelling	Upwelling	Relaxation	Post-relaxation
Currents	Rapid Northward	Slow Northward	Current reversals	Slow Northward	Slow Northward	Slow Northward
Bottom temperature	Cold Similar across stations	Cold Similar across stations	Cold Similar across stations	Cold Similar across stations	Cold Similar across stations	Warm temperatures increased inshore
Stratification	-	No	No	No	No	Yes

Table 3.1. Summary of physical conditions on sampling days (Fig. 3.1), including wind conditions (upwelling, downwelling, relaxation, post-relaxation), current relative speed and direction, bottom temperature (cold <10°C, warm >10°C), and whether or not the water column on the 15 m isobath was stratified.

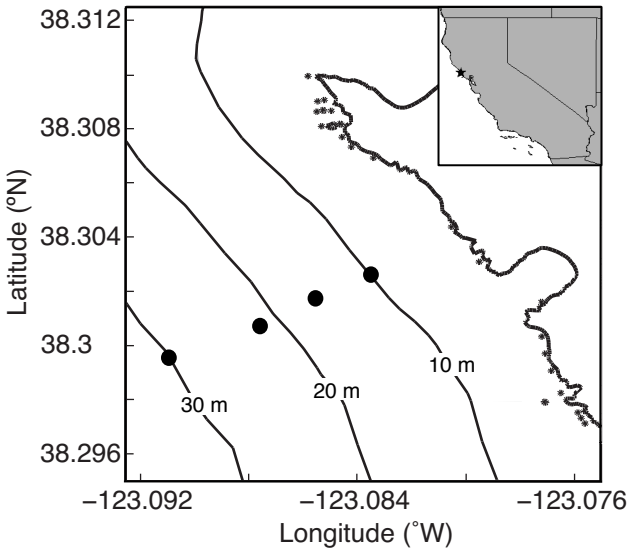

Figure 3.1. Map of the study region showing the cross-shelf transect located off Bodega Head in northern California, USA.

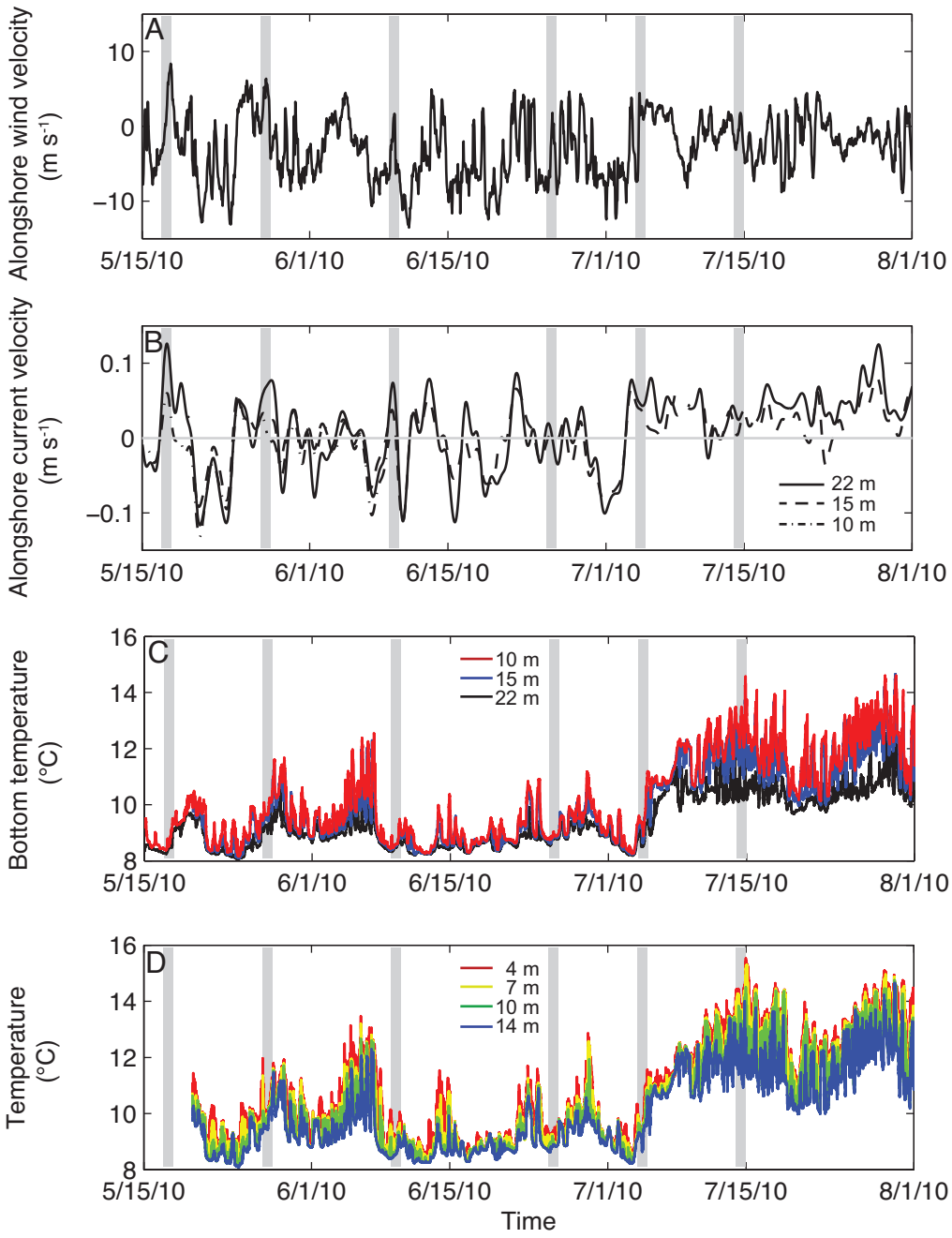

Figure 3.2. (A) Alongshore wind velocity measured onshore at the Bodega Marine Laboratory. (B) Alongshore depth-averaged and 33-h low-pass filtered current velocity measured by bottom-moored ADCPs at the 10, 15, and 22 m isobaths. Positive alongshore velocity is poleward and negative alongshore velocity is equatorward. (C)

Bottom temperature measured on the ADCP moorings at the 10, 15, and 22 m isobaths. (D) Temperature at depths of 4, 7, 10, and 14 m measured at the 15 m isobath.

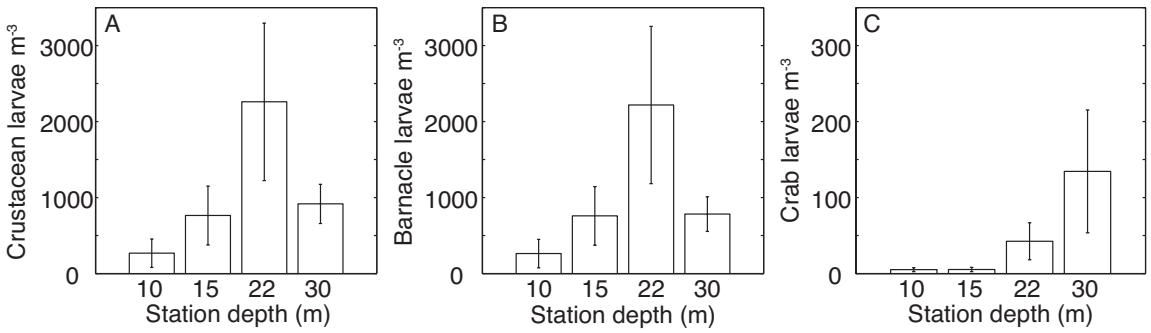

Figure 3.3. Average larval abundance across date by station for (A) all crustaceans, (B) barnacles, and (C) crabs. Note that y-axis of (C) is an order of magnitude smaller than (A) and (B).

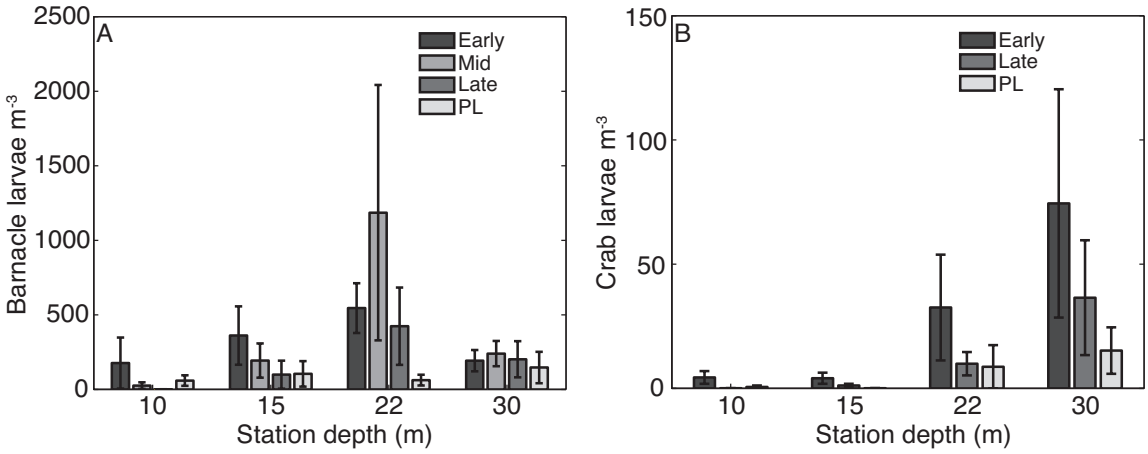

Figure 3.4. Average larval abundance across date by station for (A) barnacles according to early, mid, late, and post-larval stage and (B) crabs according to early, late, and post-larval stage.

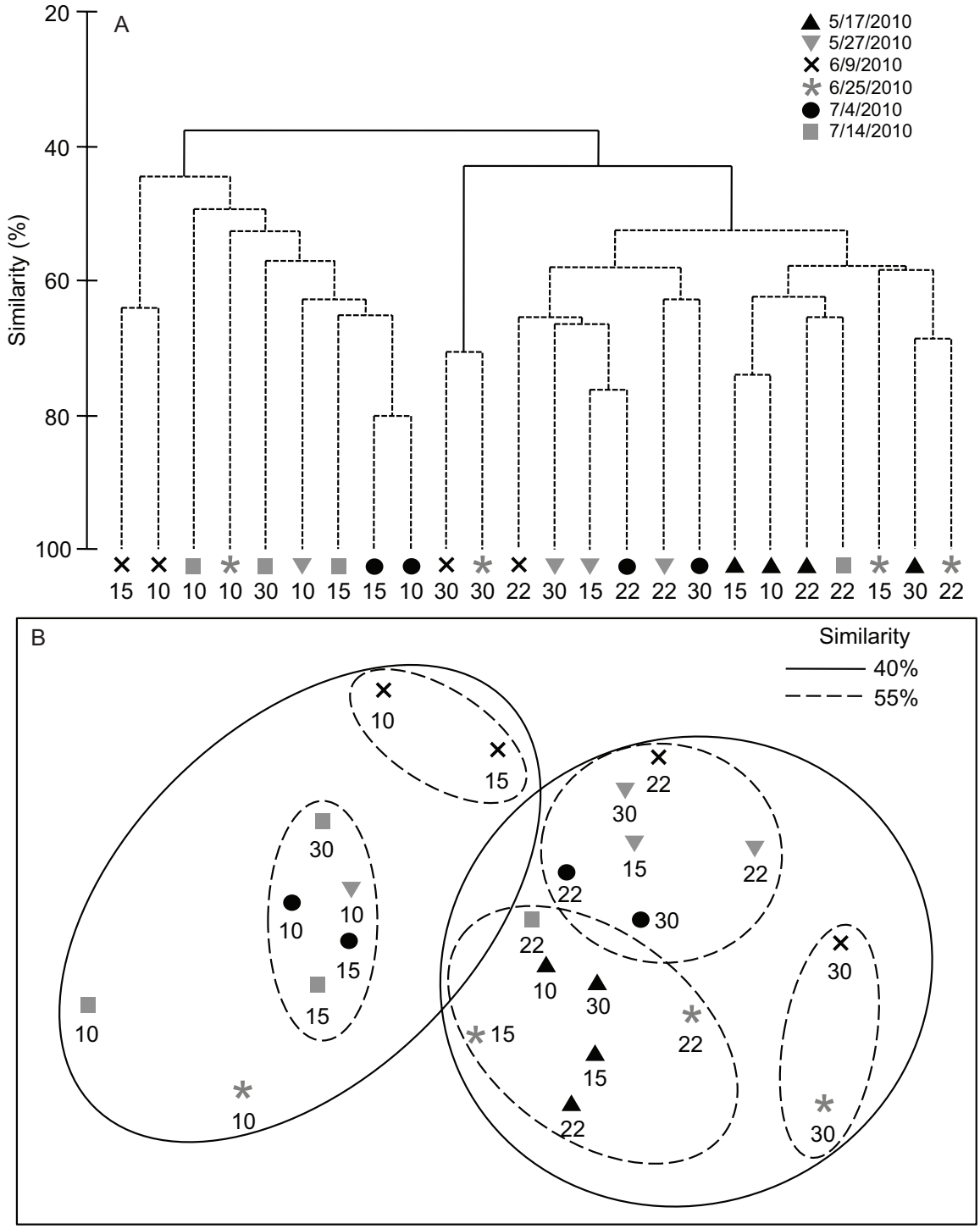

Figure 3.5. (A) Hierarchical clustering dendrogram (using group-average linking) of larval assemblages from 24 samples taken on six days at four sampling stations across the coastal boundary layer (along the 10, 15, 22, and 30 m isobaths). Solid black lines

indicate significant group structure at the 5% level. Dashed lines represent nonsignificant group structure >1%. Sample station isobaths are reported beneath each group. (B) Nonmetric multidimensional scaling plot (2-D stress, 0.15; 3-D stress, 0.09) from the 24 samples with superimposed significant clusters at similarity levels of 40% (solid lines) and 55% (dashed lines).

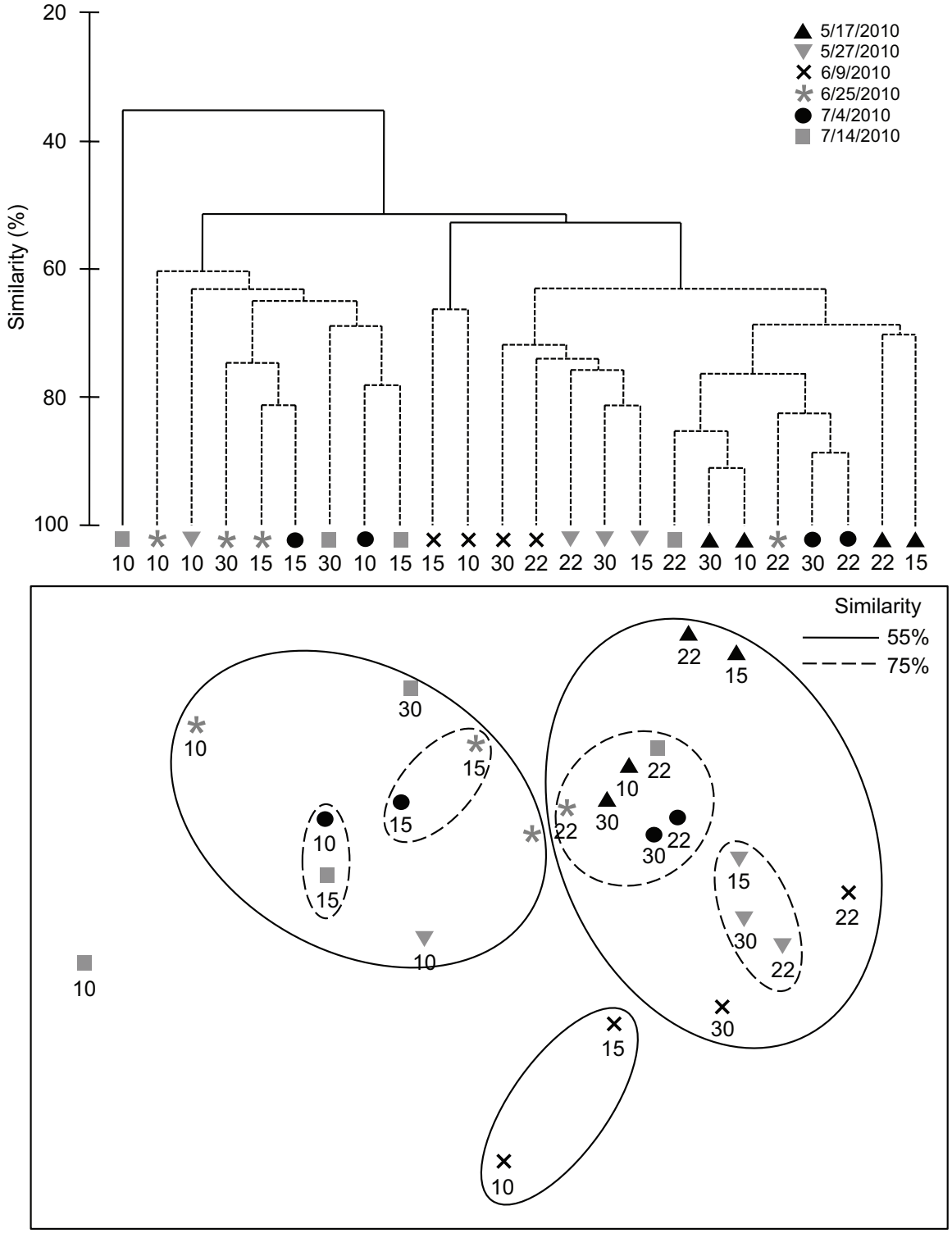

Figure 3.6. (A) Hierarchical clustering dendrogram (using group-average linking) of barnacle larval assemblages from 24 samples taken on six days at four sampling stations

across the coastal boundary layer (along the 10, 15, 22, and 30 m isobaths). Solid black lines indicate significant group structure at the 5% level. Dashed lines represent nonsignificant group structure >1%. Sample station isobaths are reported beneath each group. (B) Nonmetric multidimensional scaling plot (2-D stress, 0.12; 3-D stress, 0.07) from the 24 samples with superimposed significant clusters at similarity levels of 55% (solid lines) and 75% (dashed lines).

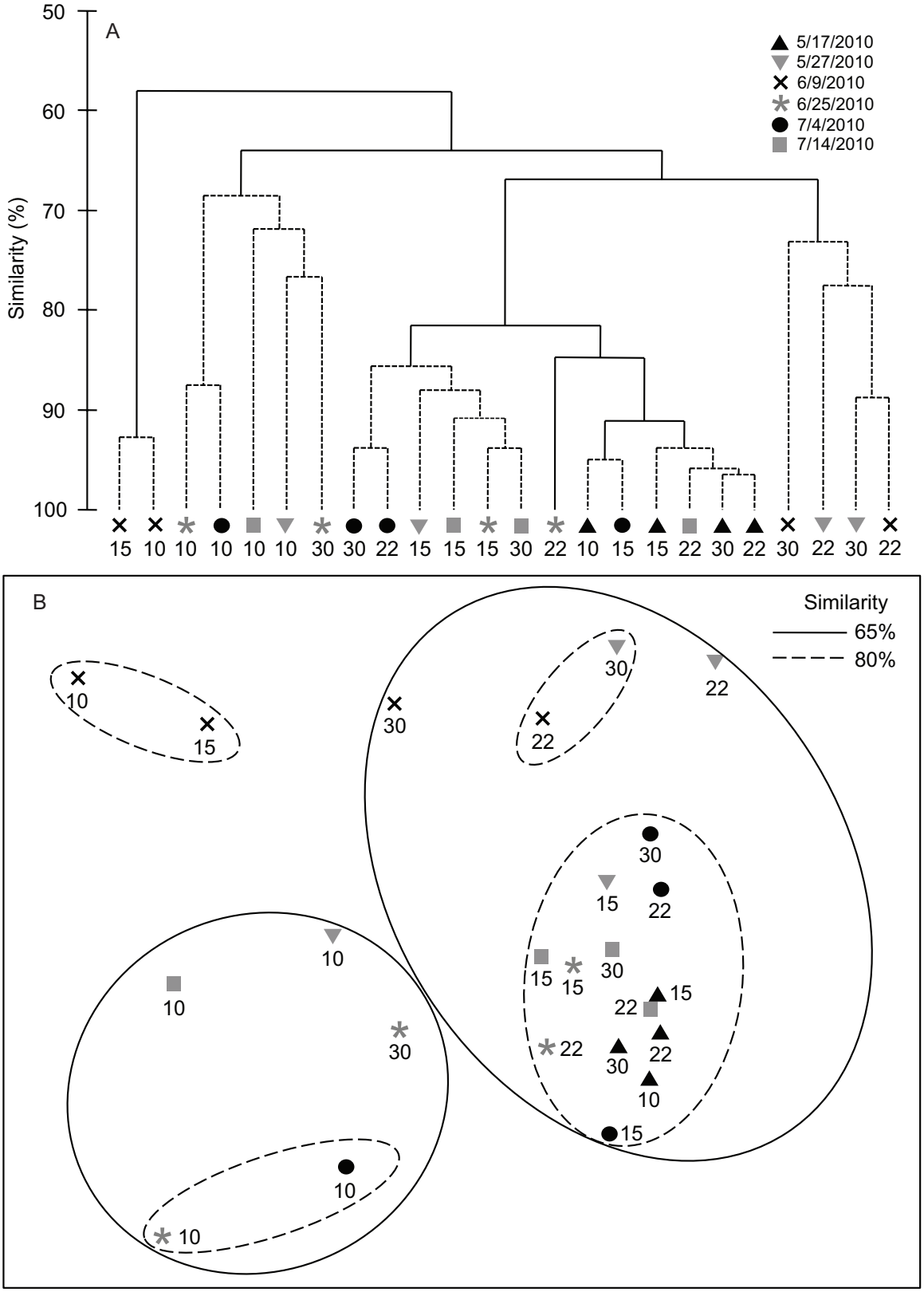
A
Similarity (%)
50
60
70
80
90
100
5/17/2010
5/27/2010
6/9/2010
6/25/2010
7/4/2010
7/14/2010
15 10 10 10 10 10 30 30 22 15 15 15 30 22 10 15 15 22 30 22 30 22 30 22
B
Similarity
65%
80%

Figure 3.7. (A) Hierarchical clustering dendrogram (using group-average linking) of community composition from 24 samples taken on six days at four sampling stations across the coastal boundary layer (along the 10, 15, 22, and 30 m isobaths). Solid black lines indicate significant group structure at the 5% level. Dashed lines represent nonsignificant group structure >1%. Sample station isobaths are reported beneath each group. (B) Nonmetric multidimensional scaling plot (2-D stress, 0.09; 3-D stress, 0.06) from the 24 samples with superimposed significant clusters at similarity levels of 65% (solid lines) and 80% (dashed lines).